Effect of plant structure modification and natural convection in solvent on the rate of supercritical extraction

Kristina Rochova

Université de La Rochelle
UFR de Sciences

&

Institute of Chemical Technology, Prague
Faculty of Chemical Engineering
Institute of Chemical Process Fundamentals, AV SC, v.v.i.

A thesis submitted for the degree of
DOCTOR
Field of study: Chemical Engineering

Effect of plant structure modification and natural convection in solvent on the rate of supercritical extraction

by

Kristina ROCHOVÁ

Supervised by Dr. Helena SOVOVÁ & Prof. Václav SOBOLÍK

The 11th December 2008, La Rochelle

JURY:

Prof. Karim ALLAF, Université de La Rochelle, France *(chairman)*
Prof. Václav SOBOLÍK, Université de La Rochelle, France *(supervisor)*
Dr. Helena SOVOVÁ, Institute of Chemical Process Fundamentals, AV SC, Czech Republic *(supervisor)*
Prof. Danielle BARTH, LSGC ENSIC, France *(opponent)*
Prof. Kamil WICHTERLE, Technical University of Ostrava, Czech Republic *(opponent)*
Assoc. Prof. Vladimír VÁCLAVEK, Institute of Chemical Technology, Prague, Czech Republic *(opponent)*

The thesis was realised in regime of joint supervision (French term is “cotutelle”) partially in France and in the Czech Republic. It is written in English, condensed reports in Czech and French are attached at the end of the work.

Titre de la thèse

Effet de la modification de structure des végétaux et de la convection naturelle dans le solvant sur l’extraction supercritique

Discipline: Génie des Procédés Industriels

Adresse:

Laboratoire d’Étude des Phénomènes de Transfert et de l’Instantanéité: Agro-industrie et Bâtiment (LEPTIAB)
Pôle Sciences et Technologie
Université de La Rochelle
Avenue Michel CREPEAU
17042 La Rochelle Cedex 01

Název práce

Vliv modifikace struktury rostlin a přirozené konvekce rozpouštědla na superkritickou extrakci.

Studijní program: Chemické a procesní inženýrství
Studijní obor: Chemické inženýrství

Kontaktní adresy:

Ústav chemických procesů, AV ČR, v.v.i.
Rozvojová 135
Praha 6 – Suchdol, 165 02

Vysoká škola chemicko-technologická v Praze
Fakulta chemicko-inženýrská
Technická 5
Praha 6 – Dejvice, 166 28

The thesis was worked out at the Institute of Chemical Process Fundamentals, Academy of Sciences of the Czech Republic, and in the laboratory LMTAI (LEPTIAB), University of La Rochelle, France, from September 2006 to September 2008.
The thesis consists of this main text and the CD support with Annexes.

I hereby declare that I have developed this thesis independently while noting all resources used, as well as all co-authors. I consent to the publication of this thesis under Act No. 111/1998, Coll., on universities, as amended by subsequent regulations. I have been informed of all duties and obligations applicable under Act No. 121/2000, Coll., the Copyright Act, as amended by subsequent regulations.

Prague, September 30, 2008

Signature

Foremost, I would like to thank Dr. Helena Sovová and Prof. Václav Sobolík for scientific leadership of my work, valuable discussions, encouragement and kind personal attitude.

I am grateful to Prof. Karim Allaf for accepting me kindly to his laboratory. I also thank all my colleagues from both Department of Separation Process and laboratory LMTAI who have helped me by their opinions, ideas and recommendations.

Many thanks belong to French government and CROUS for financial support and organization that enabled me to realize this thesis partially at University of La Rochelle.

Last, but not least, I am indebted to my mother for her patient support during the three years when I was migrating between Prague and La Rochelle.

ABSTRACT

Two problems related to the efficiency of supercritical CO_2 extraction were studied in this work. The first objective was to test the ability of the process of Instantaneous Controlled Pressure-Drop (DIC) applied as pretreatment technique to enhance the supercritical extraction by structure modification of extracted material. The second objective was to introduce the method of measurement of residence time distribution characteristics into the laboratory in order to follow the effect of flow direction on axial dispersion in a supercritical extractor.

Supercritical CO_2 extraction has received particular attention in the field of natural compounds separation, because it possesses several advantages over conventional techniques. However, the larger scale applications of the method are often inhibited by high investment costs. Thus, optimization of process parameters is necessary to reduce total costs of the method. Pretreatment of the material before extraction is one of the most important parameters, having effect on extraction rate and total yield. In this work, the process of Instantaneous Controlled Pressure-Drop (DIC) was tested as a pretreatment method. Amaranth seeds, soybeans and green coffee beans were treated by the DIC process and extracted by supercritical CO_2. Material structure was determined using scanning electron microscopy, mercury porosimetry and helium pycnometry. Model of broken and intact cells (BIC) and modified hot ball model were used to evaluate the extraction data. The most important effect of the treatment was observed in the case of soybeans. The porosity of soybeans was considerably increased by the DIC process and the internal mass transfer rate was enhanced six times. Structure of amaranth seeds and green coffee beans was not modified by the DIC process, and the extraction data shows no enhancement. Problem of caffeine extraction related to the presence of water in the coffee beans is discussed.

Supercritical fluids are more prone to natural convection because of their very low kinematic viscosity. Subsequently, the natural convection influences the extraction rate and yield. There are several studies concerning axial dispersion in supercritical extractor evaluated by means of tracer response technique. However, they deal with the system SCO_2-tracer and do not study the system during the extraction, which is just the case where the density differences may cause natural convection. In this work, a method of residence time distribution was introduced to the laboratory. Benzoic acid was used as tracer. Several solutes were tested; tetracosane was chosen for subcritical conditions (12 MPa, 25°C), trilaurin was applied at supercritical conditions (12 MPa, 40°C). Extraction was carried out under downflow and upflow mode. Preliminary results have shown a strong influence of flow direction during the extraction under supercritical conditions, on the other hand, no effect on the flow pattern was observed at subcritical conditions. Future studies will be oriented to verify the preliminary results of this part of the work.

SOUHRN

Disertační práce se týká dvou oblastí studia spojených se superkritickou extrakcí. Prvním cílem bylo studium vlivu modifikace struktury rostlinného materiálu na následnou extrakci superkritickým CO_2. Druhým úkolem bylo zavedení metody měření odezvy na stopovací látku pro potřeby laboratoře tak, aby tato metoda dále mohla být využívána ke studiu charakteru proudění v superkritickém extraktoru.

Zájem o extrakci superkritickým CO_2 v poslední době roste, protože tato metoda má mnohé výhody oproti klasickým extrakčním technikám. Její využití v průmyslovém měřítku je nicméně často brzděno vysokými investičními náklady na vysokotlaké zařízení. Snížení celkových nákladů procesu lze dosáhnout optimalizací jeho parametrů. Jedním z nejdůležitějších parametrů ovlivňujících průběh extrakce a její výtěžek je zpracování materiálu před extrakcí. Jako alternativní technika předzpracování byla v této práci testována metoda okamžité řízené expanze (proces DIC). Semena amarantu, sójové boby a zelené kávové boby byly zpracovány procesem DIC a následně extrahovány. Strukturní změny v materiálu byly studovány s využitím elektronového mikroskopu, rtuťové porozimetrie a heliové pyknometrie. K popisu experimentálních dat byl použit matematický model extrakce z celých a rozbitých buněk a upravený model difúze z koule. Nejvýraznější efekt úpravy procesem DIC byl pozorován u sójových bobů. Jejich porozita po úpravě výrazně stoupla a přestup hmoty v extrahovaných částicích se zvýšil šestkrát. Struktura semen amarantu a zelených kávových bobů nebyla procesem DIC nijak ovlivněna, a ani průběh extrakce se u takto upravených bobů nelišil od průběhu extrakce u nezpracovaného materiálu. V práci je zároveň diskutována role vlhkosti při extrakci kofeinu z kávových bobů.

Superkritické tekutiny jsou díky své velmi nízké kinematické viskozitě náchylné k přirozené konvekci, která ovlivňuje průběh a výtěžek extrakce. Axiální disperze v superkritickém extraktoru byla několikrát v literatuře studována metodou sledování odezvy na stopovací látku, data se však vždy vztahují na systém čistý SCO_2-stopovací látka, tedy nezahrnují v sobě současně probíhající extrakci, při které právě může vznikat přirozená konvekce vlivem změn hustoty roztoku. V této práci byla pro účely laboratoře vypracována metodika měření doby odezvy na stopovací látku. Jako stopovací látku jsme použili kyselinu benzoovou. Z několika testovaných látek pro extrakci byl vybrán tetrakosan pro pokusy v podkritických podmínkách (12 MPa, 25°C) a trilaurin pro supekritické podmínky (12 MPa, 40°C). Extrakce byla sledována při toku rozpouštědla ve směru a proti směru gravitace. Předběžné výsledky ukazují, že při supekritických podmínkách a probíhající extrakci se výrazně projevuje vliv směru toku na charakter proudění v extraktoru, zatímco u podkritických podmínek tento trend pozorován nebyl. Výsledky a hypotézy formulované v této části práce je potřeba ověřit dalším studiem.

RESUME COURT

La thèse présentée concerne l'étude de deux problématiques liées à l'extraction supercritique. Le premier objective a été de tester la capacité du procédé de la Détente Instantanée Contrôlée (DIC), appliquée en tant que technique de prétraitement, à l'efficacité de l'extraction par le CO_2 supercritique grâce à la modification de la structure du matériel extrait. Le deuxième objective a été d'élaborer une méthode de mesure de la distribution des temps de séjour afin d'observer l'effet de la direction du flux moyen sur la distribution des temps de séjour dans un extracteur supercritique.

L'extraction supercritique attire attention grâce aux avantages qu'elle possède en comparaison avec les méthodes d'extraction conventionnelles. Néanmoins, les applications de la technique à l'industrie sont souvent inhibées par les coûts d'investissement de l'installation de haute pression. Optimisation des paramètres de procédé peut baisser les coûts totaux. Le prétraitement du produit avant l'extraction est un des paramètres les plus importants qui influence la cinétique et le rendement de l'extraction. Dans cette étude, le procédé DIC a été testé en tant que technique de prétraitement. Les grains d'amarante, de soja et de café ont été traités par DIC et extraits par le CO_2 supercritique. La structure du matériel a été étudiée par la microscopie électronique à balayage, la porosimétrie à mercure et la pycnométrie à hélium. Les données expérimentales ont été décrites par deux modèles: le modèle BIC basé sur l'extraction des cellules cassées et intactes, et le modèle « hot ball » basé sur la diffusion dans une sphère. L'effet le plus remarquable a été observé pour les grains de soja. Leur porosité a augmenté considérablement après le traitement par DIC et la vitesse de transfert interne de masse a augmenté six fois. La structure des grains d'amarante et de café n'a pas été modifiée par le traitement par DIC, et les résultats de l'extraction ne montrent aucune amélioration. La problématique de l'extraction de la caféine par rapport à la présence de l'eau a été discutée.

Grâce à la viscosité cinématique basse, les fluides supercritiques inclinent plus à la convection naturelle, ce qui influence la cinétique et le rendement d'extraction. Plusieurs études sont accessibles concernant la dispersion axiale dans l'extracteur supercritique, évaluée à l'aide des mesures de la réponse à l'injection du traceur dans l'extracteur. Ces travaux étudient le système CO_2 pure-traceur, mais ils observent pas la réponse pendant l'extraction proprement dite, ce qui est justement le cas où la convection naturelle peut se développer à cause des différences de densité. Le but de cette étude a été d'élaborer une méthode de mesure de la réponse à l'injection du traceur. L'acide benzoïque a été utilisé comme traceur. Plusieurs solutés ont été testés; le tetracosane a été choisi pour les expériences sous conditions subcritiques (12 MPa, 25ºC), la trilaurine pour les expériences supercritiques (12 MPa, 40ºC). L'extraction a été réalisée avec le solvant passant dans le sens de la pesanteur et aussi dans la direction opposite. Les résultats préliminaires montrent un effet significatif de la direction de flux de solvant sous conditions supercritiques. Par contre, cet effet n'a pas été observé sous conditions subcritiques. Les résultats obtenus doivent être encore vérifiés par une étude suivante.

CONTENTS

INTRODUCTION

Plant extracts have been used since centuries for preparation of drugs, cosmetics, as colorants, spices or food additives. Although nowadays the most of valuable compounds present naturally in plants can be synthesised chemically, natural extracts are still highly important especially in medicine and pharmaceutical industry. Traditional methods of extraction are distillation, cold pressing or solvent extraction. Quality of extract is closely related to the choice of solvent; conventional solvents, however, possess several disadvantages, such as low selectivity and destruction of thermally unstable compounds. Therefore, new extraction techniques are being developed to eliminate these disadvantages.

One of these modern techniques is extraction with supercritical CO_2. In comparison with conventional extraction solvents, supercritical CO_2 is environmentally and health friendly, cheap and can be easily completely separated from the extract. Moreover, by changing extraction pressure and temperature, its selectivity can be partially changed. Thus, supercritical CO_2 extraction has received particular attention in the field of natural compounds separation; the attention is even intensified by the fact, that rules for the use of chemical agents have become strict recently. Decaffeination of coffee and extraction of bitter compounds from hops for beer production are the most important applications of supercritical extraction.

Naturally, there are disadvantages of this technique as well. The main drawback is represented by high investment costs of the high pressure installation, which often makes the supercritical extraction more expensive than conventional techniques, though operating costs are not that high. Investment costs can be hardly reduced, but total costs of the process can be decreased by optimization of process parameters.

Pretreatment of the material before extraction is one of the most important parameters, having effect on extraction rate and total yield. Beside standard mechanical disintegration (milling, flaking, chopping), alternative techniques of pretreatment are used in specific cases, such as moisturizing or enzymatic hydrolysis. In this work, the process of Instantaneous Controlled Pressure-Drop (DIC) will be presented and tested as a pretreatment method. The process is based on the thermomechanical processing induced by subjecting a substance partially humid to high pressure steam followed by a rapid expansion to vacuum. The rapid pressure drop causes a bursting evaporation of a part of the moisture from the bulk of the material, which blows and breaks the walls of cavities. The objective of this work is to determine the extent of structural changes caused by DIC in vegetable matrix, and to study the effect of these changes on the rate supercritical extraction.

Another factor that can influence the extraction rate and yield is the presence of natural convection in supercritical extractor. Systems with flowing supercritical fluids are more prone to natural convection, as their kinematic viscosity is very low, of about two orders of magnitude lower that for liquids. Researchers coincide that at the gravity-assisted flow (downflow) the extraction is faster, while under

gravity-opposed flow (upflow), slowing down of extraction was observed. This is caused by density difference between pure CO_2 and solute-laden CO_2, resulting in a mixing in the vessel. The phenomenon has been studied by several authors; to determine flow pattern in extractor, the method of tracer response and evaluation of axial dispersion was used. However, those studies concerned systems of pure CO_2 passing through inert support in the extractor, so the real behaviour during extraction has not been described yet, even though this information is interesting from the scientific point of view and important for design and optimization of when large scale supercritical extractors. Therefore, the second part of this work concerns the flow pattern in laboratory extractor, specifically the introduction of tracer response method to the laboratory and preliminary experiments to test the method in order to study flow pattern.

This work is based on collaboration of two institutions – Institute of Chemical Process Fundamentals of Academy of Science of the Czech Republic (ICPF AS CR) and laboratory LMTAI (presently LEPTIAB) at University of La Rochelle.

GOALS OF THE THESIS

Two problems related to the efficiency of supercritical CO_2 extraction are studied in this work.
The first one deals with the pretreatment of extracted material. The objective is to test the ability of the process of Instantaneous Controlled Pressure-Drop (DIC) applied as pretreatment technique to enhance the supercritical extraction by structure modification of extracted material. Specific steps are

- to study the effect of the DIC pretreatment of model material (soybeans, green coffee beans, amaranth seeds) on its structure and on the rate of supercritical extraction;
- to describe extraction curves for non-treated and DIC-treated material with a mathematical model and compared mass transfer parameters of the extraction;
- to determine the impact of various DIC conditions on the extraction rate.

The second problem deals with flow pattern in supercritical extractor. The objective is to introduce the method of measurement of RTD characteristic into the laboratory in order to follow the effect of flow direction on flow pattern in a supercritical extractor. Specific steps are

- to assemble the apparatus for RTD measurements and to develop a methodology;
- to find and appropriate extraction system (natural matrix or solute deposited on inert support);
- to test the method in preliminary RTD measurements.

1. LITERATURE REVIEW

1.1 Properties of supercritical fluids

A pure component is considered to be in supercritical state if its temperature and its pressure are higher than the critical values. The critical temperature is the highest temperature at which a gas can be converted to a liquid by an increase of pressure; the critical pressure is the highest pressure at which a liquid can be converted to a gas by an increase in a liquid temperature. In the supercritical region, there is only one phase possessing some of the properties of both gas and liquid (Figure 1.1).

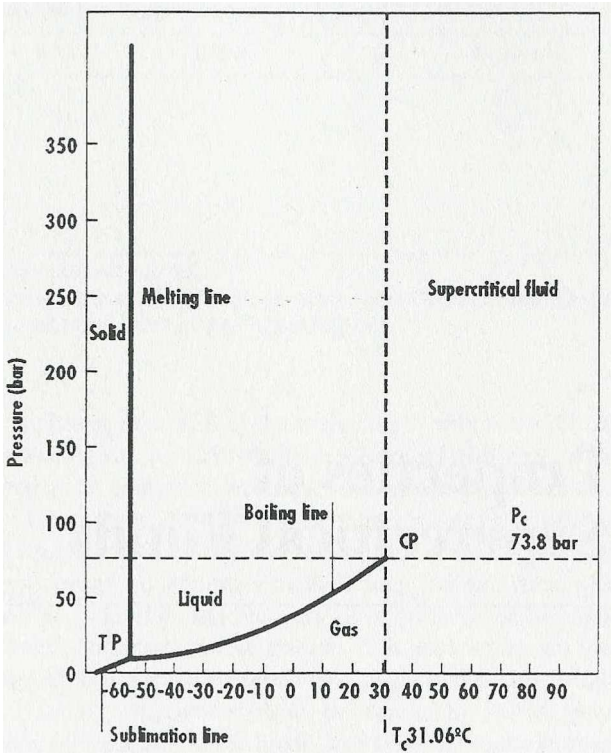

Figure 1.1. Phase diagram of CO_2. TP – triple point, CP – critical point, P_C – critical pressure, T_C – critical temperature [1].

A mixture of components is considered to be supercritical with respect to pressure, temperature or composition if conditions of state (*p*, *T*, composition) are beyond the critical point of the mixture (Figure 1.2). With respect to pressure, the critical point of a mixture is always on the top of the two-phase area at constant temperature and composition of the mixture. The critical temperature, on the contrary, does not limit the two-phase region with respect to temperature. Similarly, at constant pressure and temperature, the critical point in general is not at the maximum value of the two-phase region with respect to the concentration of one of compounds [2]. In this theoretical review, only pure components will be treated.

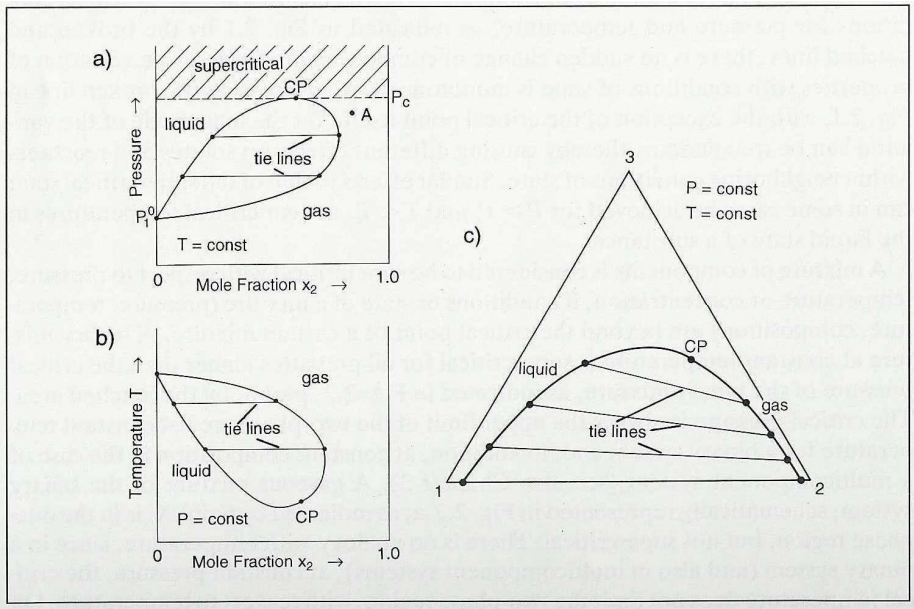

Figure 1.2. Critical points in binary and ternary mixtures. P_1^0 vapour pressure of component 1 [2].

1.1.1 Thermodynamic properties – PVT behaviour

In contrast to liquids, properties of supercritical fluids (SCF) vary strongly with conditions of state and these variations are the basis for many applications. When the critical point is approached, predictions and even correlation curves are very difficult because of the non-classical behaviour in this region. The models used to predict equilibrium in the supercritical fluids can be divided into the following groups [3]:

- the Van der Waals family of cubic equations of state (E.O.S.);
- the virial family of E.O.S.;
- the group contribution E.O.S.;
- E.O.S. for associating and polar fluids;
- E.O.S. from theory and computer simulation.

The common feature of equations of state is that they are constructed by combining separate contributions resulting from repulsive and attractive interactions. If the classification of different E.O.S. is based on the degree of the volume-expansion equation, the equations of state can be simply divided into cubic (semi-empirical) and non-cubic.

Cubic equations of state are using the repulsive term (Z^{+rep}) proposed by Van der Waals (Table 1.1). Various attractive terms (Z^{-att}) have been proposed in the literature. Peng-Robinson and Soave-Redlich-Kwong equations are widely used since they require little computer time and little input information (only critical properties and an acentric factor) to calculate the generalized parameters. However, these equations do not predict well liquid densities, the generalized expressions are not accurate for non-hydrocarbons and long-chain molecules, and they are not accurate in the critical region. The greatest use of cubic E.O.S. is for phase equilibrium calculations involving mixtures.

Mixtures' parameters *a* and *b* are used in equations for pure fluids; they are most commonly obtained using the Van der Waals one-fluid mixing rules to find *a*, *b*, and combining rules to find a_{ij}, b_{ij}.

Table 1.1. Repulsive and attractive terms used in E.O.S.: η - reduced volume ($\eta = b/4V$; V – molar volume (m^3/mol)), α – non-sphericity parameter [4]

Equation	$\mathbf{Z^{+rep}}$, $\mathbf{Z^{-att}}$
repulsive terms	
Van der Waals	$\frac{1}{1-4\eta}$
Carnahan-Starling	$\frac{1+\eta+\eta^2-\eta^3}{(1-\eta)^3}$
Hard Convex Body (HCB)	$\frac{1+(3\alpha-2)\eta+(3\alpha^2-3\alpha+1)\eta^2-\alpha^2\eta^3}{(1-\eta)^3}$
attractive terms	
Van der Waals	$\frac{a}{RTV}$
Redlich-Kwong	$\frac{a}{(V+b)RT^{1,5}}$
Soave	$\frac{a(T)}{(V+b)RT}$
Peng-Robinson	$\frac{Va(T)}{[V(V+b)+b(V-b)]RT}$

Cubic equations of state embody a corresponding state theory, which assumes similarity of molecular size and force constant. Therefore, they are forced to describe a situation for which they are not developed, because supercritical fluid solutions are highly asymmetric in force constant and size.

The non-cubic equations of state have more theoretical basis because there is a contribution of statistical mechanics and computer simulations; however, the gain of replacement of cubic E.O.S. by non-cubic one is often only marginal. Non-cubic equations are characterized by the use of a repulsive term that is based on the Carnahan-Starling or on the HCB expressions (Table 1.1); attractive term is generally based on a term derived from the perturbed hard chain theory or from the statistical associating fluid theory [4]. More detailed description of thermodynamic properties and phase equilibrium at high pressures can be found in [2], [4].

Diagram in Figure 1.3 represents the temperature-pressure-density relationship in terms of reduced variables (e.g. $P/P_C = P_R$), applicable to all substances. The supercritical region lies just above T_R=1.0, P_R=1.0. At subcritical temperatures, the volume of a gas decreases (i.e. its density increases) with an increasing pressure until the phase boundary line is reached and crossed with formation of liquid

phase. As long as the total density of the mixture lies in the two-phase region, gas phase and liquid phase coexist at constant pressure. When all gas is liquefied, further reduction in volume would lead to a rapid increase in pressure due to low compressibility of liquids. On the other hand, at supercritical temperatures, a gas can be compressed to liquid-like volume without visible changes of phase. The critical isotherm T_C has a horizontal tangent at the critical point and isotherms in its vicinity ($T>T_C$) are flat. Therefore, a very small increase in pressure near critical point, at T_R=1.0-1.2, results in a dramatic increase in density towards liquid-like values. The same increase in pressure at T_R>1.5 hardly changes the fluid density. This fact is useful when performing SCF fractionation. The density of a supercritical fluid practically never exceeds the density of comparable liquid, regardless of the pressure.

Based on many solubility measurements, it can be stated that solvent power of a supercritical fluid increases with density at given temperature, and with temperature at given density. The increase in density enhances solute-fluid interaction. Another factor enhancing the solvent power is vapour pressure; the increase in a component vapour pressure, which increases with temperature, decreases solute-solute interaction.

The influence of temperature on the solubility varies with pressure; at high pressures, the solubility increases with temperature, at low pressures, a temperature increase causes a decrease of solubility. This behaviour comes about because at low pressures (near critical point), the decrease in density with increasing temperature is much more important than at high pressures (see Figure 1.3). Therefore, although the solvent power is enhanced by increased temperature, the effect on solubility is negative due to the decrease in density. The crossover pressure is a very important factor when a process involving solids must be optimized. [4], [2], [1]

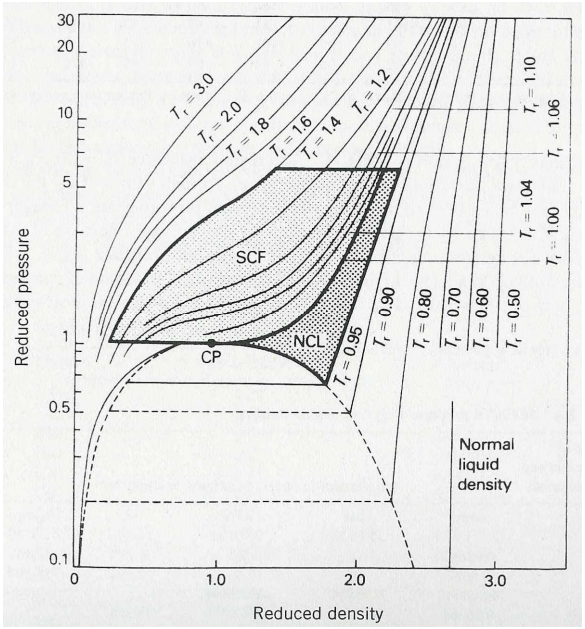

Figure 1.3. Reduced pressure (P_C) – reduced density (ρ_C) diagrams at various temperatures (T_R). SCF – supercritical fluid region, NCL – near critical region [1].

1.1.2 Transport properties

Usually, values of transport coefficients for a gas are extremely sensitive to pressure, and therefore prediction in high-pressure region is required. On the other hand, small changes in transport properties of liquids with pressure can be disregarded. The basic laws governing transport phenomena in laminar flow are Newton's law, Fick's law and Fourier's law. Proportionality constants of these equations, viscosity η, diffusion coefficient D and thermal conductivity λ, respectively, will be discussed in following paragraphs. A comparison of general values for gas, liquid and supercritical phase is given in Table 1.2.

Table 1.2. General range of values of density and transport properties for a gas, a liquid and a supercritical fluid

	Density (kg/m^3)	**Dynamic viscosity (10^{-3} N· s/m^2)**	**Diffusivity (mm^2/s)**
Gas	1	0.01	1-10
Supercritical fluid	100-1000	0.05-0.1	0.01-0.1
Liquid	1000	0.5-1.0	0.001

1.1.2.1 Viscosity

Most of pure liquids, simple mixtures and gases are Newtonian fluids, thus their dynamic viscosity is independent on shear stress and velocity gradient, and depends only on conditions of state.

For a gas, the effect of pressure on the viscosity depends on the region of P and T of interest relative to the critical point. Near the critical state, the change in viscosity with temperature at constant pressure can be very large. Two branches can be observed on a curve of viscosity as a function of temperature; one in which the viscosity rapidly decreases with increasing temperature (liquid-like behaviour) to a minimum near the critical point, and the other, where the viscosity increases with increasing temperature (gas-like behaviour). Critical values of several gases and liquids are available [5]. Besides, different correlations have been proposed for both pure compounds [6] and mixtures [7].

1.1.2.2 Thermal conductivity

Thermal conductivity of gases is connected with viscosity and heat capacity. Under ambient conditions, thermal conductivity of gases is in the range of 0.01 to 0.025 W/(K m); except of higher values for helium and hydrogen. For most organic liquids, the value is in the range of 0.1-0.2 W/(K m) at temperatures below the boiling point. (Water, ammonia and strongly polar liquids have higher values by a factor of 2 to 3; liquid metals and some silica compounds have very high thermal conductivities.) Under supercritical conditions, the conductivity decreases with increasing temperature, goes to a minimum and then increases with temperature. On the other hand, at constant temperature, it increases with pressure [2].

1.1.2.3 Diffusion coefficient

Diffusion coefficient (diffusivity) as defined by Fick's law is a molecular parameter and is usually reported as an infinite-dilution binary diffusion coefficient. As it can bee seen from Table 1.2, it is about one order of magnitude higher than for liquids and two orders of magnitude lower than for gases. Components of similar structure and molecular weight have also similar diffusion coefficients; the coefficient decreases with molecular weight. As it is known from correlations, the diffusion coefficient is inversely proportional to pressure at constant temperature. On the other hand, at constant pressure, the gas diffusivity increases with power 1.5 of the absolute temperature [2], [8].

1.2 Supercritical CO_2 extraction of natural matter

More than 130 years ago, Irish chemist Thomas Andrews gave a lecture to the Royal Society, reporting for the first time that supercritical fluids dissolve some non-volatile solvents. Andrews described the critical point as the end of the vapour pressure curve in a phase diagram. At temperatures and pressures above this point, many gases dissolve certain solids and liquids [9]. In 1879, Hannay and Hogarth had characterised the behaviour of supercritical fluids in more detail [10]. During a presentation to the Royal Society, they reported results from a series of experiments during which they dissolved solids with a melting point much above the liquid solvent's critical point. The solid remained diffused in the vapour even when they raised the temperature to 55°C above the critical point and considerably expanded the volume. Authors reported that "some solutions show curious reactions at the critical point". Ferric chloride, for example, precipitates from ether just below the critical point but it redissolves in the gas when heated by four or five degrees above the critical point. Sudden decrease in pressure precipitates the solute. They reported that the precipitate from supercritical fluids "is crystalline, and may be brought down as a "snow" in the gas, or on the glass as a "frost"". Increasing the pressure redissolved the crystals [11].

Chemists continued to experiment with supercritical fluids for almost a century, although they remained something of a curiosity for a long time. In the 1960's, a research oriented to separations with supercritical carbon dioxide (SCO_2) started, mainly in Germany [12]. Independently, Russian researchers studied extraction of plants with CO_2 near critical point [13]. Thus, advances in the solvent extraction of foods were made. For the first time, natural products such as coffee, tobacco, tea, cocoa, hops, spices and oil seeds could be extracted without the use of organic solvents [14].

Nowadays, various applications of supercritical fluids are studied, such as chemical reactions and synthesis under supercritical conditions, enzymatic reactions, preparation of nanoparticles, sterilization, drying; however, the extraction of compounds from natural sources remains the most widely studied application of supercritical fluids.

1.2.1 Supercritical extraction versus conventional techniques

There are two conventional techniques mostly used for separation of compounds from natural matrices: steam distillation and organic solvent extraction. The distillation is the most common process in essential oils production. Plant material is put into a still (distillation apparatus) over water; as the water is heated the steam passes through the plant material and vaporizes volatile compounds. The vapours flow through a cooler and condense back to liquid, which is then collected in the separator. The plant material can be also immersed directly in the boiling water (hydrodistillation). The main shortcoming of the distillation is high temperature that can cause a transformation of thermally sensible compounds into undesired products.

The use of organic solvents (the most common is hexane) permits to extract lipophilic compounds as well. However, their selectivity is low and thus, apart from the desired substances, non-volatile components of high molecular weight such as fatty oils, resins, waxes and colouring matters are co-extracted. Two other shortcomings are the solvent residues in the extract, with the subsequent toxicological risk, and the long extraction time required in most cases for achieving efficient extractions. In addition, operating temperatures (organic solvents' boiling points) can be harmful for thermally unstable compounds. Moreover, both solvent extraction and distillation are hardly feasible for automation [15]. Efficiency of these classical methods can be improved using microwaves or ultrasound assisted extraction. Further, the extraction process can be carried out under reduced pressure in order to lower the solvent boiling point.

Supercritical fluid extraction (SFE) provides several advantages over traditional extraction techniques. As the density and the solvent power of supercritical fluids are close to those of liquids and their transport properties are close to those of gases, they can penetrate into a porous solid material more effectively than liquid solvents. Moreover, after the extraction, the solute can be easily separated from the extract by decrease in pressure, in contrast to conventional extraction techniques using organic solvents which are difficult to remove completely from the extracts. The solvation power of supercritical fluid can be manipulated by changing pressure and temperature, which enables a selective extraction. The extraction is fast and feasible for automation; it can be extended by a direct coupling with chromatographic analysis.

Table 1.3. Critical point of some compounds tested as supercritical solvents [16]

Fluid	**Critical temperature (K)**	**Critical pressure (10^5 Pa)**
Carbon dioxide	304.25	73.8
Ethane	305.4	48.8
Ethylene	282.4	50.4
Propane	369.8	42.5
Propylene	364.9	46.0
Trifluoromethane (Fluoroform)	299.3	48.6
Chlorotrifluoromethane	302.0	38.7
Trichlorofluoromethane	471.2	44.1
Ammonia	405.5	113.5
Water	647.3	221.2
Cyclohexane	553.5	40.7
n-Pentane	469.7	33.7
Toluene	591.8	41.0

Different compounds have been examined as SFE solvents. For example, hydrocarbons such as pentane and butane, nitrous oxide, sulphur hexafluoride and fluorinated hydrocarbons [17], [18], [19]. Critical points of some of them are listed in Table 1.3. However, carbon dioxide (CO_2) is the most popular SFE solvent because it is safe, readily available and has a low cost. With critical point at 31.1°C and 7.38 MPa, it allows supercritical operations at relatively low pressures and at near-room temperatures, which preserves thermally unstable compounds [20].
In the text that follows, the term of supercritical extraction is to be understood as the extraction with supercritical CO_2.

1.2.2 Process description

A scheme of an extraction plant is shown in Figure 1.4. The liquid CO_2 from the storage (or bottle) is pressurized, heated and transferred to the extractor, where it gets loaded according to adjusted conditions (temperature and pressure). The starting material is put into a basket located inside the extractor that allows fast charge and discharge of the extraction vessel. The nature of the material and its pre-processing are parameters that can largely influence the separation performance and they will be discussed in detail later in this work. On a laboratory scale, the extractor is usually immersed in a water bath to maintain the extraction temperature constant; industrial plants use a heating agent in a double jacket extractor. The SCO_2 at the exit of the extractor flows through a depressurization valve to a separator in which, due to the lower pressure, the extracts are released from the gaseous medium and collected. In the case of a larger scale apparatus, the gaseous CO_2 can be condensed, intermediately stored and recycled.

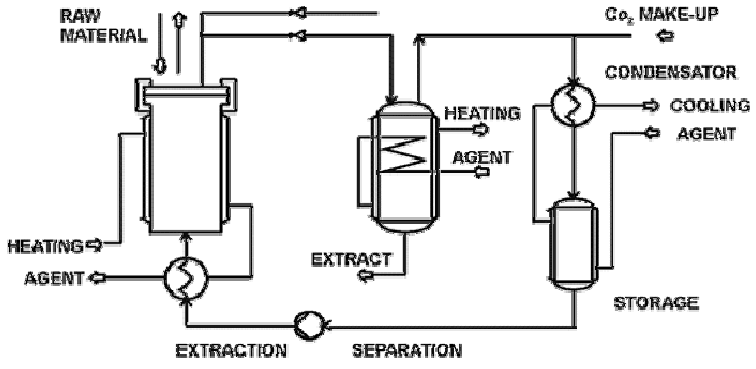

Figure 1.4. General flow diagram of the SF extraction process (NATex Prozesstechnologie web site).

Up to now, a continuous process providing continuous feeding and emptying of solid materials in the extractor under high pressure has not been sufficiently brought off. In different research studies, a screw press to pressurize and shift the material through a high pressure vessel was described but the technical realization for industrial plants is too difficult. Therefore, solid materials are extracted by cascade operation in two or more batch extractors combined in series (Figure 1.5a). The compressed gas passes the extractors in the sequence 1-2-3-4 until extraction in extractor 1 is finished. This

extractor is separated from the cycle, decompressed, emptied, refilled with the fresh material and added as last one to the sequence which is now 2-3-4-1. Due to this sequence high extraction yields are obtained because the pure solvent flow is contacted with pre-extracted material so that a concentration difference is present and on the other side, the pre-loaded solvent flow enters the extractor with fresh material so that the maximum of solvent capacity is used.

Although it is not possible to avoid the co-extraction of some compound families (with different solubility, but also with different mass transfer resistance in the raw matter), it is possible to carry out an extraction process in order to fractionate the extract (i.e. to allow selective precipitation of different compound families). This type of operation called fractional separation is based on changes in the solubility of compounds in the supercritical fluid in dependence on extraction conditions. There are two ways to obtain the fractionated extract: (a) the solubility of compounds can be progressively enhanced by increasing the pressure in the extractor and extract fractions are successively collected using just one separator; (b) faster way is to set directly the maximal solubility conditions in the extractor and to separate the extract in two or more separators in series operated at different pressures and temperatures (Figure 1.5.b) [21].

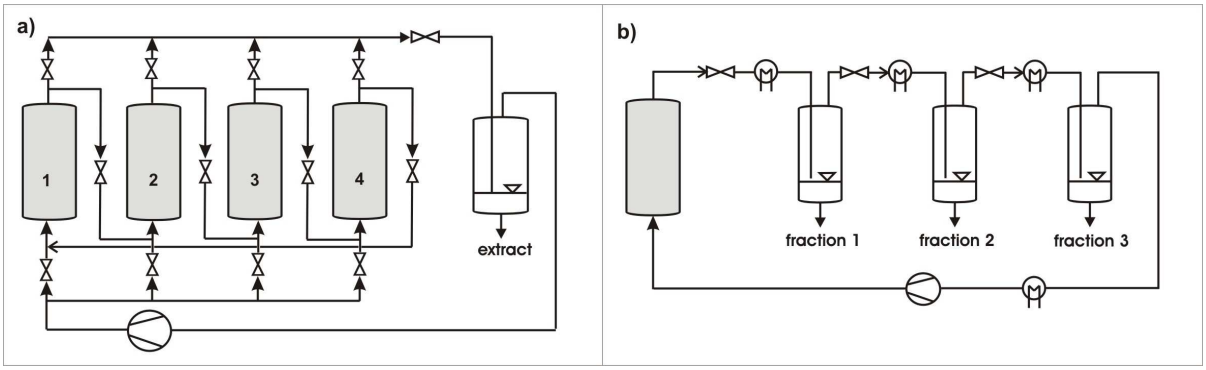

Figure 1.5. a) Cascade operation for extraction of solid materials; b) multi-step separation of extract.

1.2.3 Potential of SCO_2 to extract natural compounds

Knowledge of solubility of a solute in supercritical fluid is crucial. Molecules of CO_2 have no dipole moment and the fluid is usually regarded as non-polar, but it has also a little affinity for polar solutes, probably due to high quadrupole moment of molecules. Nevertheless, the presence of hydroxyl, amino, and nitro groups is known to diminish the solubility, especially if two or more of these groups are present in the solute molecule [1]. To increase the solvent power of SCO_2 towards polar molecules, a liquid co-solvent can be added. Small quantities of liquid solvents (e.g. ethyl alcohol) are readily solubilized by SCO_2. When in solution, they modify the solvent power of SCO_2 [22], [23]. This strategy has the drawback that a larger solvent power could also lower selectivity of the process; moreover, since the co-solvent is liquid at atmospheric pressure, it will be collected in the separator

together with extracted compounds. A subsequent processing is required to eliminate the solvent; therefore, one of the advantages of the SFE - solventless operation - is lost.

The solubility of solids and liquids in supercritical fluids has been measured extensively. The early studies provided by Francis [24] concern solubility of many classes of organic compounds such as aliphatics, aromatics, heterocyclics, and compounds with a large variety of functional groups in near-critical liquid CO_2. Later, Bartle [25] reviewed experimentally measured solubility of single compounds of low volatility in SCO_2, together with the temperature and pressure ranges of the experimental measurements and method employed to determine the solubility. Up to now, a wealth of information on the solubility of materials in supercritical CO_2 has been published in the literature and it forms an important part of establishing the technical and economic feasibility of any supercritical fluid extraction process. Most of the investigations on solubility have been concerned with binary systems consisting of a single solute in contact with a single supercritical fluid, solubility data derived from multicomponent systems have been reported less frequently [26].

As the extraction process has been studied on laboratory scale since many years, hundreds of publications have been published. Besides essential oils and vegetable oils, a large spectrum of compounds with nutritional and pharmaceutical properties has been isolated from various matters, such as tocopherols, carotenoids, alkaloids, unsaturated fatty acids. Detailed description is outside the scope of this work, it can be found in numerous published reviews [27], [19], [20], [21], [28]. Apart from natural products separation, the extraction process has been applied for example to neutralization and consequent impregnation of paper, the elimination of pollutants and pesticides from natural matter [29], the bone tissue treatment (a delipidation of bones decreases infection effects). The supercritical extraction has been also widely used in chemical analysis domain [30].

Besides the experimental work, the accent has been put on mathematical modelling of the extraction process so that the process could be scaled up. This topic is discussed closer in chapter 1.5.

1.2.4 Operating parameters

Selection and optimization of operating conditions plays a decisive role in extraction process industrialization. Although character of compounds to be extracted, their molecular weight, polarity and their localization in plant matrix must be considered for every particular case, some general remarks on the most important factors can be made here:

1.2.4.1 Temperature and pressure

As the critical temperature of CO_2 is 31.1°C, it is favourable to work in the range of 35-60°C to avoid degradation of thermally unstable compounds. An increase in temperature (at constant pressure) reduces the density of SCO_2, thus it reduces the solvent power of the supercritical solvent; but it increases the vapour pressure of compounds to be extracted.

However, the most relevant process parameter is the extraction pressure that can be used to tune the selectivity of the extraction. The general rule is: the higher the pressure, the larger the solvent power and the lower the extraction selectivity; however, it must be noted that the solvent power of the fluid is given by its density which is strongly non-linear function of both pressure and temperature (as discussed in chapter 1.1, see Figure 1.3). Hence, the proper selection requires the use of accurate tables of SCO_2 properties.

1.2.4.2 CO_2 flow rate

Solvent flow rate is a relevant parameter if the process is controlled by an external mass transfer resistance or by phase equilibrium; in this case, the amount of supercritical solvent feed to the extraction vessel determinates the extraction rate. The direction of the solvent flow (gravity-opposite or gravity-assisted flow) can play a decisive role if natural convection occurs in the extractor; this problem is discussed in chapter 1.4.

1.2.4.3 Material pretreatment

If the extraction process is controlled by internal mass transfer resistance, the material pretreatment is very important factor because it can change substantially the diffusion rate within the particles. Mechanical disintegration is mostly used as material pretreatment. For more details see chapter 1.3.

1.2.4.4 Extraction time

Process duration is interconnected with CO_2 flow rate and particle size and has to be properly selected to maximize the yield of the extraction process.

A study of Yin et al. [31] can be cited as an example of analysis of the operation parameters of seed oil supercritical extraction.

1.2.5 Industrial scale applications

Several applications have been fully developed and commercialized in the food and flavouring industry and in the pharmaceutical industry: environmentally friendly separation of volatile and lipid soluble compounds, extraction of high value oils, isolation of lipid soluble compounds, extraction of high grade natural aromas, purification of raw materials, extraction of hop resins, extraction of spices, reduction of nicotine in tobacco, coffee and tea decaffeination, recovery of aromas from fruits, meat, fish, etc. A terse review on SFE applications in food industry was published recently by Brunner [32].
A quite large number of industrials plants (around 100) of different sizes has been built during the last 20 years for the extraction of solid material with supercritical fluid in a batch mode. Since the early 1980's till 2005, a total number of about 100 vessels bigger than 100 litres in volume have been ordered for about 50 plants. They are mostly distributed in Europe, the USA, Japan, and in the South East Asian Countries [32].

The largest industrial application is the decaffeination of coffee beans and tea leaves [33]; this is valid for both investment costs and capacities of the plants. From the beginning of the seventies to the beginning of the nineties, nearly 50% of the whole production capacity for decaffeination of coffee and tea changed to the supercritical extraction process.

The second largest application is the extraction of bitter flavours from hops. In the last twenty years nearly all producers of hop extracts changed to the supercritical extraction process [34], [35].

Plants for extraction of spice oleoresins, medicinal herbs and high value fats and oils are much smaller compared to the decaffeination plants and hops extraction plants, and their introduction into the industry is slow.

Generally, industrial applications of SCO_2 extraction are limited by high investment costs compared to classical low pressure extraction techniques. On the other hand, operating costs for very large units are low (Figure 1.6). A continuous operation mode of extraction (continuous passage of the material through the extractor) could lower the operation costs [36]. Nevertheless, it is applicable only when extraction from liquids is carried out [37]; solid materials are extracted in batch mode due to the lack of satisfactory technologies of continuous feeding for high pressure equipments. Therefore, in the case of vegetable oils, although large quantities of raw materials are treated, the supercritical extraction remains more expensive than the traditional hexane extraction which can be carried out at continuous mode at atmospheric pressure.

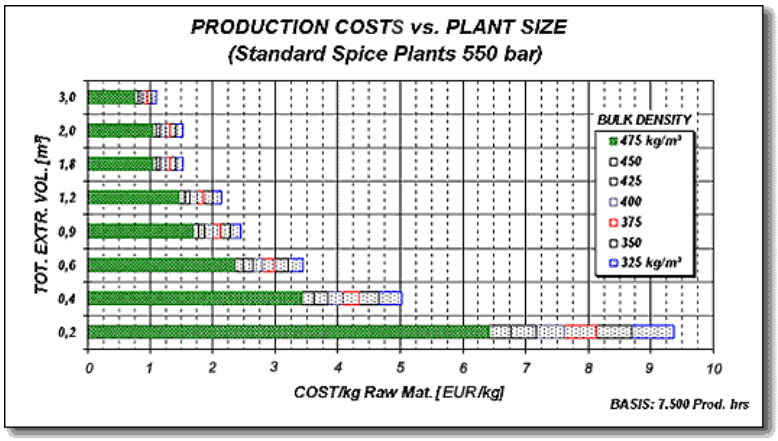

Figure 1.6. Production costs of a SFE plant versus the plant size (NATex Prozesstechnologie web site).

We can conclude, that the supercritical extraction can be competitive to the conventional techniques when large amounts of material are treated (as demonstrated by the examples of coffee, tea and hops plants) or when thermally sensible compounds of high nutritional value are extracted (e.g. vegetable oils with a high content of γ-linolenic acid). These high value products issued from a "green" treatment are competitive enough to their equivalents extracted with organic solvents, even when produced in small quantities.

1.3 Material pretreatment and internal mass transfer

Internal mass transfer is represented by diffusion inside extracted particles to their surface. The diffusion depends on the initial distribution of the substances to be extracted within the solid matrix and on the size of particles and type of pretreatment. To choose optimal method of pretreatment, first location of the substances must be evaluated; further, it is necessary to know whether the desired substance is bounded in any chemical reaction to the matrix or bounded to a complex. Generally, the distribution of solute depends on the type of solute and on biological aspects (e.g. waxes are deposited on the plant parts surface, vegetable oils are evenly distributed in seed endosperm, essential oils are located in well-defined plant secretory structures [38]).
In our experiments, we provided extraction from seeds (amaranth, soybeans, coffee beans), thus, next lines will concern mainly seeds; however, the techniques of pretreatment, generally, are applicable in a wide range of natural matrixes and they are applied in other extraction techniques as well.

1.3.1 Structure of seeds

A typical seed includes three basic parts: a seed coat (testa), an embryo and a supply of nutritients for the embryo; this supply can be represented by an endosperm (which is mostly the case of oil seeds) or a part of female gametophyte (conifers). Seeds store starch and triacylglycerols as food reserves for germination and postgerminative growth of the seedlings. The oil is evenly distributed in the seed endosperm in small, discrete intracellular organelles called oil bodies (Figure 1.7). Isolated oil bodies have a spherical shape and possess diameters ranging from about 0.5 to 2.0 μm. They contain mostly triacylglycerols and small amounts of phospholipids and oleosins [39]. Reverchon et al. [40] published micrographs from scanning electron microscopy (SEM) of grounded coriander and grape seeds (Figure 1.7d) and stated that the seed endosperm consists of oil-bearing cells “filled with oil” which should not be confused with biological cells that are much smaller. Shape and size of oil-bearing structures are characteristic for a given species of seeds. In another study, Reverchon et al. examined grounded rosehip seeds and they found there was no oil-bearing structure and the oil was located in long lignified channels [41]. (On the other hand, del Valle et al. [42] claimed that oil-bearing structures are present in rosehip seeds and they hypothesised that it might had been the lignified thick testa what Reverchon et al. observed.) To reduce the barrier represented by rigid inert structures, different techniques of material pretreatment are used.

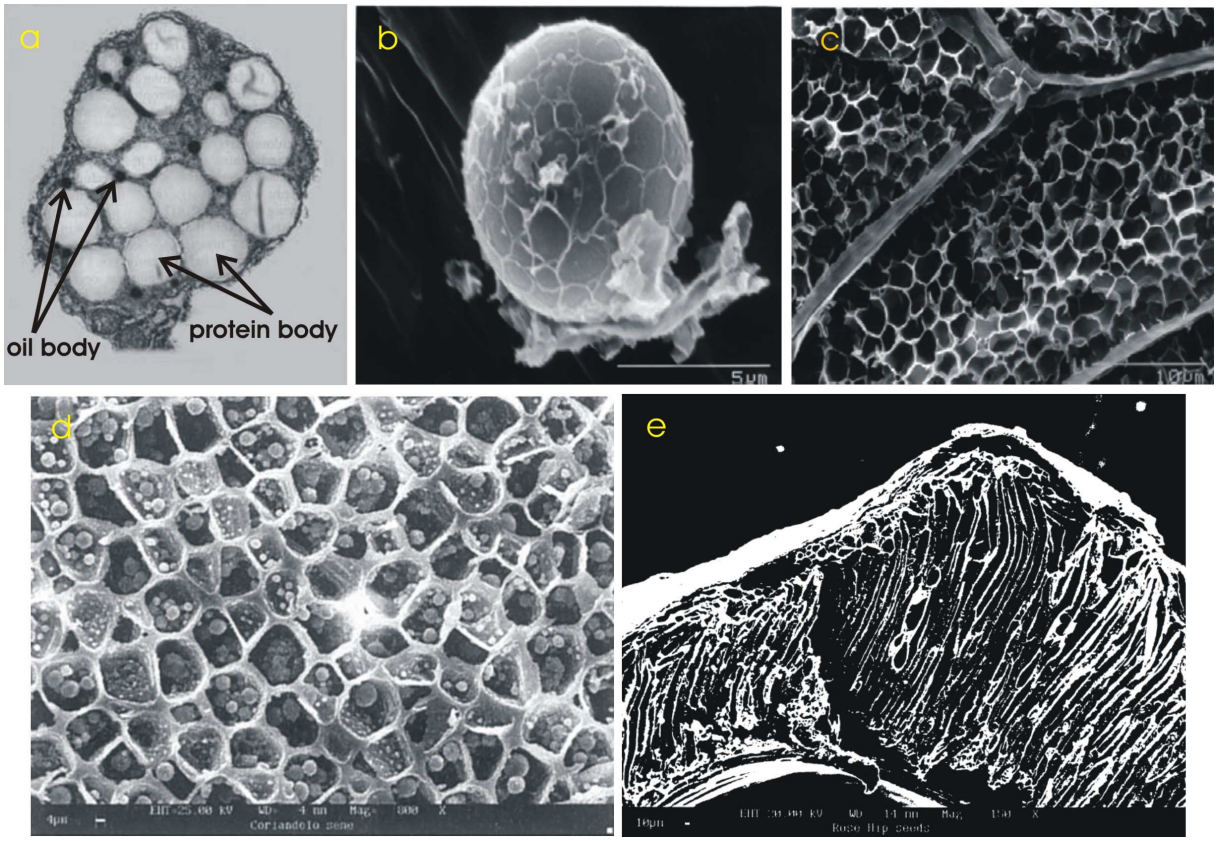

Figure 1.7. Examples of seed structure. Borage seed (transmission electronic microscopy): (a) gland cell as a whole, where protein and oil bodies within the cell, (b) gland cell before extraction, (c) gland cell after extraction [43]; (d) coriander seed (SEM): broken oil-bearing cells after extraction with non-extracted spherical starch bodies [40] ; (e) rosehip seed structure (SEM) after extraction [41].

1.3.2 Material pretreatment

Supposing that extracted compounds are not chemically bounded to the matrix, the diffusion can be influenced by following pretreatment processes:

1.3.2.1 Mechanical disintegration

The common experimental observation, which is not limited to just supercritical extraction, is that the extraction from whole uncracked seeds is nearly impossible and very low yields are obtained (virtually no oil is extracted from intact colza seeds, only 3% of oil is extracted from halved peanuts and only 1.3 g oil/kg is extracted from coriander seeds cracked in halves) [42].

Particle size depends both on the original shape and rheological properties of the material (leaves, needles, seeds) and on technique of disintegration. In the extraction process controlled by internal mass transfer resistance, particle size becomes a very important factor because a smaller mean particle size reduces the length of diffusion path of the solvent [21] and increases the interfacial area. Moreover, size-reduction techniques such as grinding, crushing and chopping do not only decrease the particle size, but also release oil from cells. They lead to a breakage of superficial cells, therefore,

the amount of released oil is inversely proportional to the final diameter of particles. In order to examine the effect of particle size on extraction yield, samples of defined particle size fraction are prepared by using a single size-reduction device whose working conditions can be set up to achieve different milling grades or by separating different size fractions from grounded mixture by sieving. However, del Valle et al. [42] pointed out that when the latter technique is applied, a segregation of seed parts with different oil contents may occur, especially when seeds with thick and/or hard testa and small germ are treated. Authors showed that rosehip seed fractions of large particles contained mainly testa fragments, whereas that of small particles contained mostly seed germ fragments.

Two possible drawbacks, however, may be associated with the decreasing particle size. The production of very small particles by grinding can produce the loss of volatile compounds; it limits the degree of material disintegration for essential oils extraction. A use of cool medium during the pretreatment stage can be used to prevent the loose [44]; a promising technique is to grind the matrix under cryogenic conditions, e.g. with liquid nitrogen. Moreover, if the particles are too small, channelling inside the extraction bed can occur. A part of solvent goes fast through the extraction bed without contacting the material which causes a loss of both efficiency and yield of the process. Therefore, mean particle diameter used for extractions ranges from 0.25 to 2.0 mm [21].

On the other hand, a reduction in particle size is not strictly required to release the oil from the cells in prepressed or flaked seeds, because the cell walls and other barriers to the mass transfer within the solid substrate are destroyed by high shear stresses during the pressing and flaking.

To describe internal mass transfer in a particle, generally, the particle is assumed to be a porous sphere and a differential equation for a solute diffusion based of Fick's law is used

$$\frac{\partial c}{\partial t} = D_i \left[\frac{1}{r^2} \frac{\partial}{\partial r} \left(r^2 \frac{\partial c}{\partial r} \right) \right] \tag{1.1}$$

where D_i represents intraparticle diffusion coefficient, it means an effective diffusivity of the solute in the porous vegetable matrix. (Effective diffusivity is also marked D_e in literature; the term "diffusion coefficient" applied in this work means exclusively "effective diffusion coefficient". Description of internal mass transfer makes a part of the extraction process modelling which is discussed in chapter 1.5.)

Migration rate of the solute is therefore related to the D_i value which can be estimated as a function of the binary diffusion coefficient (D_{12}) of the solute in the solvent, adjusted to quantify the effect of inner barriers in the substrate

$$D_i = D_{12} \frac{\varepsilon_p}{\tau} \tag{1.2}$$

where ε_p is the particle porosity and τ is the tortuosity of the interconnected pore network in the particle [45]. The value of binary coefficient can be estimated using for example the correlation of Catchpole and King [46] (D_i as a function of reduced temperature, reduced density, critical volume and molecular weight), particle porosity can be determined by Hg porosimetry. To estimate the tortuosity of prepressed oil seeds, Uquiche et al. [47] applied a fractal-texture analysis of binary light-microscopy images. The images are binarized and the values of fractal dimension and spectral dimension are evaluated; the tortuosity is calculated as a function of these two parameters.

Unlike the approach given above and assuming constant particle porosity and diffusion coefficient during the extraction process, Simeonov et al. [48] proposed a model where these parameters change with concentration; to describe such a system, authors applied a basic diffusion model wherein the simultaneous effect of concentration-dependent diffusivity and variable porosity was included.

1.3.2.2 Moisturizing

There is an enhancement of diffusion due to the swelling of cell walls by simple moisturizing the raw material. The transport of substances through biological cell walls can be described as the transport through various membrane systems. Elementary membranes - parts of these systems - consist of several layers, and lamellas are made of bimolecular lipid layer. These lipid pillars change with water content. If there is not enough water in the system, the pillars close the membrane, making it impermeable; if enough water is available, the membrane stretches and becomes permeable [2].

This step is particularly important in the case of SCO_2 extraction, because SCO_2 does not cause any swelling of the material contrary to the organic solvent extraction or a distillation where the cell walls are swelled directly by the solvent. Further, in the case of essential oils extraction from leaves and flowers, steam or boiling solvent cause a disruption of secretory structures containing oils, thus the mechanical disintegration is not so important.

An example of seed moisturizing is caffeine extraction from whole coffee beans that cannot be mechanically pretreated before the extraction (moreover, water has a kind of co-solvent role in this process) [49].

Further, some complex bonds retaining the solute in the matrix can be broken by the moisturizing (this might be done also by changing pH value).

1.3.2.3 High extraction pressure

The high extraction pressure itself was proved to help the breakage of the cell walls in the case of almond fruit [50]. High-pressure treatments do not cause the formation and destruction of covalent bonds but have effects on hydrogen, ionic, and hydrophobic bonds. Authors presented that the application of SCO_2 extraction modifies, initially, the cell wall matrix, in particular pectic polymers and hemicelluloses. At this initial phase of extraction, the breakage of ionic links within the pectin structure might increase the porosity of the wall, regulating the transfer of oil from the inner

cell. (Pectins are among the cell wall components with the ability to contain the turgor pressure of the cell.) The breakage of hydrogen bonds between hemicelluloses and cellulose might also contribute to increase the porosity of the wall.

1.3.2.4 Fast CO_2 pressure release

Apart from the constant high pressure imposed on a material, the sudden release of pressure (rapid evacuation of the CO_2 from the extractor) was proved to disrupt cell walls of some natural matter as well. After it had been successfully applied to disintegration of bacterial and yeast cells [51], [52], Gaspar et al. [53] examined an effect of the fast decompression treatment on subsequent dynamic SCO_2 extraction of essential oils from bracts of *Origanum virens* L., specifically the effect of pre-expansion and post-expansion pressures, the time of exposure to high pressure CO_2 and the decompression rate. They found as the most efficient a decompression from 7 MPa to atmospheric pressure, the extent of disruption of glands containing oil was strongly influenced by both exposure time and the rate of decompression. Further, they stated that the effect of the fast decompression pretreatment on the extractability of essential oil was greater than that obtained from ambient mechanical disintegration and similar to that obtained by cryogenic comminution.

1.3.2.5 Enzymatic hydrolysis

Enzymatic hydrolysis is a bioconversion process that offers an option for pre-conditioning of oilseeds prior-to conventional oil extraction processes. This pretreatment breaks the seed structure as it opens up the cell walls by converting the cellulose materials into glucose. It also converts the complex lipoprotein molecules into simple lipid and protein molecules. Therefore, this process helps in obtaining extra oil from various oilseeds (for example, soybean, sunflower, canola, rapeseed, mustard, sesame, peanut). Aqueous enzymatic extraction is another promising technique where a hydrothermal pretreatment is applied prior to oil extraction to inactivate the native enzymes present in the oilseeds and to loosen their structure, before the enzymatic treatment is applied [54]. Although a simple centrifugation is often used to separate the liberated oil, these methods can be coupled with classical extraction techniques [55].

1.4 Effects of natural convection in supercritical extractors

Previous chapter dealt with internal mass transfer during the extraction process, now we present the problem of natural convection in the extractor which concerns external mass transfer.

Natural convection is fluid motion as result of buoyancy forces induced by density gradient in a system. A ratio of buoyancy forces to viscous forces is presented by the Grashof number; it has a similar significance for natural convection as the Reynolds number has for forced convection (Table 1.4). The density differences are usually caused by temperature differences in the system; however, in the case of supercritical extraction from solid fixed bed, changes in density of the fluid phase (solvent + solute) can occur at constant temperature and invoke natural convection.

Researchers in supercritical fluid extraction generally coincide in concluding that depending on system conditions (pressure, temperature, flow rate), the prevailing mass-transport mechanism in supercritical fluids (SCF) extraction can be considerably affected by natural convection. It was early pointed out theoretically and proved experimentally by Debenedetti and Reid [56] that buoyancy effects (differences of density between the fluid at the interface and in the bulk) cannot be neglected when dealing with SCF. Near the critical point, properties of fluids change substantially and are very sensitive to changes in pressure and temperature. In supercritical region, density of supercritical fluids is high, close to liquids, and their dynamic viscosity, on the other hand, is small. Therefore their kinematic viscosity is extremely low, about 10^{-9} m^2/s, compared to both liquids (~10^{-7} m^2/s) and gases (~10^{-5} m^2/s), and the Grashof number (see Table 1.4) becomes important. Proneness to natural convection is even amplified by low flow velocities usually used for the extraction.

The phenomenon of natural convection was experimentally proved in numerous studies. Beutler et al. [57] found the rate of piperin extraction from black pepper to be accelerated by gravity-assisted solvent flow (downflow) when compared to gravity-opposed (upflow) solvent flow. They related the effect of flow direction to higher density of solute-laden SCO_2, compared to the density of pure solvent: the heavier solute-laden solvent is easier withdrawn from extractor bottom than from its top. The easier flow of solute to solvent outlet leads to higher concentration gradients along the extraction bed and thus to higher mass transfer driving force. A similar phenomenon was observed by Barton et al. [58] in a work concerning the extraction of peppermint oil. Sovová et al. [59], studying the SCO_2 extraction of grape oil from milled seeds, reported that the extraction in upflow mode was retarded due to free convection. Moreover, the extraction retardation increased with decreasing interstitial velocity of the solvent and height of extraction bed.

A strong effect was observed by Stüber [60] et al. who extracted 1,2-dichlorobenzene from the pores of an inert sintered metallic pellet. At conditions near the critical point, the extraction time for 50% recovery of solute under upflow mode almost tripled compared to the time for the same recovery with downflow of fluid.

The extraction retardation at low interstitial velocities in upflow mode is also evident from several published graphs of extraction yield plotted versus passed solvent [61], where the yields at lower solvent flow rates are lower than at higher flow rates, though the contact time is higher.
Description of natural convection effect on the extraction process provided by the literature is focused on two basic concepts relating the phenomenon (a) to changes in flow pattern described by axial dispersion and (b) to changes in mass transfer coefficient with a flow pattern a priori assumed.

Table 1.4. Definition of used dimensionless numbers: D - diffusion coefficient (m^2/s), D_a - dispersion coefficient (m^2/s) , g - gravity acceleration (m/s^2), k – mass transfer coefficient (m/s), l – characteristic length (m), u_0 – fluid superficial velocity (m/s), ρ – fluid density (kg/m^3), ν – kinematic viscosity (m^2/s)

Grashof	Gr	$\frac{l^3 g \Delta\rho / \rho}{\nu^2}$	buoyancy forces / viscous forces
Sherwood	Sh	$\frac{kl}{D}$	mass transfer velocity / diffusion velocity
Péclet (axial)	Pe	$\frac{lu_0}{D_a}$	flow velocity / diffusion velocity
Reynolds	Re	$\frac{u_0 l}{\nu}$	inertial forces / viscous forces
Schmidt	Sc	$\frac{\nu}{D}$	diffusivity of momentum / diffusivity of mass

1.4.1 Changes in external mass transfer coefficient

The external mass transfer coefficient characterizes dissolution of a free solute into the supercritical fluid during the fast regime of the extraction. To express the mass transfer in liquids or gases flowing in packed bed contactors at atmospheric pressures, Wakao and Kaguei correlated the Sherwood number with the Reynolds and Schmidt numbers (for *Re*=3-3000; *Sc*=0.5-10000) [62]

$$Sh = 2 + 1.1\,\mathrm{Re}^{0.6}\, Sc^{1/3} \tag{1.3}$$

However, deviations from the correlation occur at slow flow rates, when the conditions are propitious to natural convection [63], [64], [65].
In order to account for natural convection effects on the dissolution rate, several correlations including Grashof number have been published [66], [67], [68]. An overview of available correlations of mass transfer in fixed beds and packed columns was given by Puiggené [64]. The natural convection is considered to act on microscale, affecting external mass transfer coefficient, but not the flow pattern. Therefore, the flow pattern is assumed to be of plug flow or mixed-flow regime and mass transfer

coefficients are evaluated in dependence on the extraction conditions (pressure, temperature, flow direction).

The importance of natural convection can be assessed by the Grashof number as well as the ratio Gr/Re^2. This ratio represents the relative magnitude of buoyant to inertial forces; only when $Gr/Re^2 << 1$, natural convection can be disregarded, on the other hand, the influence of natural convection tends to vanish as the Reynolds number increases. Significant values of Gr (10^7-10^9) were found under supercritical conditions [56], [64].

The contributions of forced and natural convection on the mass transfer can be taken into account separately [60]. Based on a heat transfer expression in terms of Nusselt numbers proposed by Churchill [69] , an analogical equation, first applied by Knaff and Schlünder [70], can be used for the mass transfer

$$Sh_{Tot}{}^{n} = \left| Sh_{For}{}^{n} \pm Sh_{Nat}{}^{n} \right| \tag{1.4}$$

where the plus sign is for assisting (downward) flows and the minus sign is for opposing flows, Sh_{For} = f(Re, Sc) and Sh_{Nat} = f(Sc, Gr). Particular expressions of Sh_{For} and Sh_{Nat} for different conditions can be found in the literature [60].

Puiggené [64] measured extraction curves of 1,2-dichlorobenzene deposited on glass spheres under upflow mode. Two flow patterns were used for data modelling; model expecting the mixed flow gave better fit to the data that the one expecting the plug flow. Correlation of the experimental data based on eq.(1.4) examined the importance of free convection and showed a decrease of Sh_{Nat} with increasing Reynolds number.

Stüber [60] studied a system of toluene and 1,2-dichlorobenzene deposited on sintered porous pellets and focused on the impact of flow direction on mass transfer. The extraction was obviously enhanced under downflow mode, and extraction regime was concluded to be the one of mixed free and forced convection. A simple correlation of Sh = f(Re, Sc, Gr) was proposed to fit the experimental data.

Later, CFD simulations based on these experimental results were provided by Guardo et al. [65].

1.4.2 Changes in flow pattern

Another approach to describe the effect of natural convection is based on changes in flow pattern. Dams [71] examined the extraction of naphthalene from packed bed in both flow directions. For the upflow mode he observed deviations of the solid phase concentration profile from the profile calculated by a plug flow model, and explained them by flow irregularities induced by natural convection. He proposed to carry out extractions under downflow mode, because bypassing can occur when the upflow is realized at slow flow velocity. In accordance with this hypothesis, Sovová [59] proposed a model for SFE where the flow pattern in downflow mode was represented as plug flow and

the flow in upflow mode consisted of several parallel solvent flows of different velocities in different parts of extraction bed cross-section.

1.4.2.1 Measurement of axial dispersion

It must be pointed out that all presented conclusions on the flow pattern are based solely on extraction rate and concentration profiles. To study the phenomenon properly, a more direct observation of flow pattern simultaneously with the extraction is necessary.

Deviations from plug flow can be easily revealed and evaluated in terms of axial dispersion by the method of response to tracer injection. The axial dispersion is usually expressed with the axial Péclet number, which is less than 2.0 for liquids and greater than 2.0 for gases. The literature focusing on dispersion in packed beds under supercritical systems is sparse in comparison to that available for liquid and gaseous systems. All studies presented in next paragraphs deal with CO_2 as the solvent.

Tan and Liou [72] were the first to present extensive dispersion data under supercritical conditions. They measured dispersion coefficients for methane pulses in supercritical carbon dioxide passing through three sizes of glass beads (d_p=0.5, 1.0 and 2.0 mm). The supercritical fluid properties and flow rates were varied and resulted in values of the Reynolds number ranging from approximately 0.4 to 30. The corresponding Péclet numbers ranged from 0.6 to 2.7. Their results demonstrated a slight dependence of Péclet number on particle size, and, as expected, a strong correlation of the dispersion coefficient with interstitial velocity.

Catchpole et al. [73] performed the measurements of dispersion coefficients of squalene, benzoic acid and oleic acid at different conditions (313-333 K, 10-30 MPa, *Re* = 2-80) in columns packed with glass beads or ball bearings of variable diameter. The tracer was injected to the system by a six-port valve and detected by UV detector; the majority of the experimental apparatus was housed in a water bath in which the temperature was controlled. Results were expressed in the form of axial *Pe* = f (*Re*), column diameter, particles size and flow direction (horizontal and vertical position of the testing tube), and showed no significant influence of these parameters on the Péclet number. In the case of small particles, authors found the axial Péclet numbers lower than literature gas and liquid-phase data at ambient conditions. For the large particles, the values were in agreement with the literature data obtained under supercritical conditions.

Later, Ghoreishi and Akgerman [74] used a similar experimental arrangement to measure the axial dispersion coefficient of hexachlorobenzene (at conditions in the range of 298-323 K, 82.7-27.58 MPa, solvent flow rate 120-160 ml/h). Results showed that the axial dispersion coefficient increases with increasing temperature and flow rate and decreasing pressure. The values of the experimental Péclet number were found between those for liquid and gases. The dependence on the flow direction was not measured in the work.

In the study of Funazukuri et al. [75], the axial dispersion coefficients obtained at supercritical conditions under both upflow and downflow mode, with acetone as a tracer (313.2 K, 11-35 MPa)

were compared with the values obtained for different organic solvents at atmospheric pressure. No influence of the flow direction was found at supercritical conditions.

In all presented cases, the radial dispersion and the heat transfer resistances were neglected in the models due to geometry of used columns and constant density of the fluid. In most cases, the value of the Reynolds number is higher than 0.1, thus, mechanical dispersion can be assumed to dominate over molecular diffusion. On the contrary, for the lower flow rates (approximately $Re < 0.1$, $Pe < 2$), applied for example at some environmental processes such as soil treatment, diffusion dominance was observed [76].

The presented studies [71], [72], [73], [74], [75], [76] have in common that the measurements were carried out in a pure solvent of constant density, which was not affected by small amount of used tracers. Therefore, the natural convection could not develop and the flow direction does not seem to affect the flow pattern. However, no data are available to us on axial dispersion measured in the course of the supercritical extraction. Such measurements would show if a natural convection exists in extraction bed under upflow mode. They would also indicate flow irregularities caused e.g. by imperfect flow distribution at the entrance of extraction bed.

1.4.3 RTD – background information

Element of fluid: an amount of fluid small with respect to vessel size, but large with respect to molecular size, such that it can be characterized by values of (macroscopic) properties such as temperature, pressure, density and concentration.

Age (of an element of fluid): length of time, from entry, that an element of fluid has been in a vessel at a particular instant.

Residence time (of an element of fluid): length of time that an element of fluid spends in a vessel (i.e. from entry to exit); a residence time is an age, but the converse is not necessarily true.

Residence-time distribution (RTD or E(t)): relative times taken by different elements of fluid to flow through a vessel; a spread in residence times leads to a statistical treatment, in the form of a distribution; whether or not there is a spread in residence times has important implications for reactor (or contactor) performance.

To find the E(t) curve from the concentration curve is to change the concentration scale such that the area under the curve is unity

$$E_i = \frac{C_i}{M / v}; \int_0^\infty E(t)dt = 1 \tag{1.5}$$

where C_i is concentration of tracer at the exit of the vessel, M is amount of tracer injected to the vessel (kg or mol, depending on the concentration unit), v is volumetric flow rate of the fluid (m^3/s) [77].

Dispersion model

Dispersion (of longitudinal dispersion) can be described as a diffusion-like process superimposed on plug flow that causes that the pulse of tracer spreads as it passes through the vessel. It is represented by dispersion coefficient D_{ax} (m^2/s), the larger the coefficient is, the more the pulse is spread; D_{ax}=0 means plug flow. Dimensionless group D_{ax}/uL can be also used to characterize the dispersion in the vessel of length L, with superficial velocity of the fluid u.

Two moments are directly linked by theory to D_{ax} and D_{ax}/uL: the mean t_{mean} and the variance σ^2 defined as

$$t_{mean} = \frac{\int_0^\infty t\,C\,dt}{\int_0^\infty C\,dt} \cong \frac{\sum t_i C_i \Delta t_i}{\sum C_i \Delta t_i}; \qquad \sigma^2 = \frac{\int_0^\infty t^2\,C\,dt}{\int_0^\infty C\,dt} - t_{mean}{}^2 \cong \frac{\sum t_i{}^2 C_i \Delta t_i}{\sum C_i \Delta t_i} - t_{mean}{}^2 \tag{1.6}$$

In a closed vessel with a large deviation from plug flow, the dispersion coefficient can be evaluated using expression

$$\sigma_\Theta{}^2 = \frac{\sigma^2}{t_{mean}{}^2} = 2\left(\frac{D_{ax}}{uL}\right) - 2\left(\frac{D_{ax}}{uL}\right)^2\left[1 - e^{-uL/D_{ax}}\right] \tag{1.7}$$

where Θ signifies relation to dimensionless time

$$\Theta = \frac{t}{t_{mean}}. \tag{1.8}$$

E curve can be converted to

$$E_\Theta = t_{mean} \cdot E \tag{1.9}$$

The area under E_θ curve plotted versus t/t_{mean} is unity.

Response curves for close vessels with large deviation from plug flow (i.e. D/uL>0.01) can be found in Levenspiel [77].

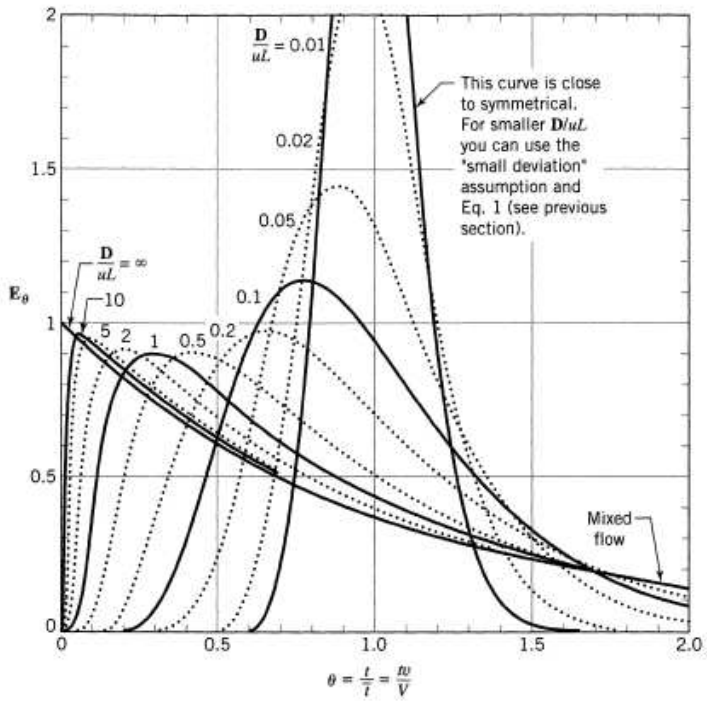

Figure 1.8. Tracer response curves for closed vessels and large deviation from plug flow [77].

1.5 Mathematical modelling of supercritical extraction from natural matter

Course of extraction is graphically expressed by so called extraction curve, which is usually dependence of mass of extract on time or on amount of solvent passed through the extractor. Shape of the extraction curve is generally very variable and depends on extraction conditions as well as plant character and sample pretreatment (some examples from literature are shown in Figure 1.9). Most of authors tend to describe mathematically their experimental data, therefore, numerous models have been proposed, both applicable just in some specialized cases and more universal ones.

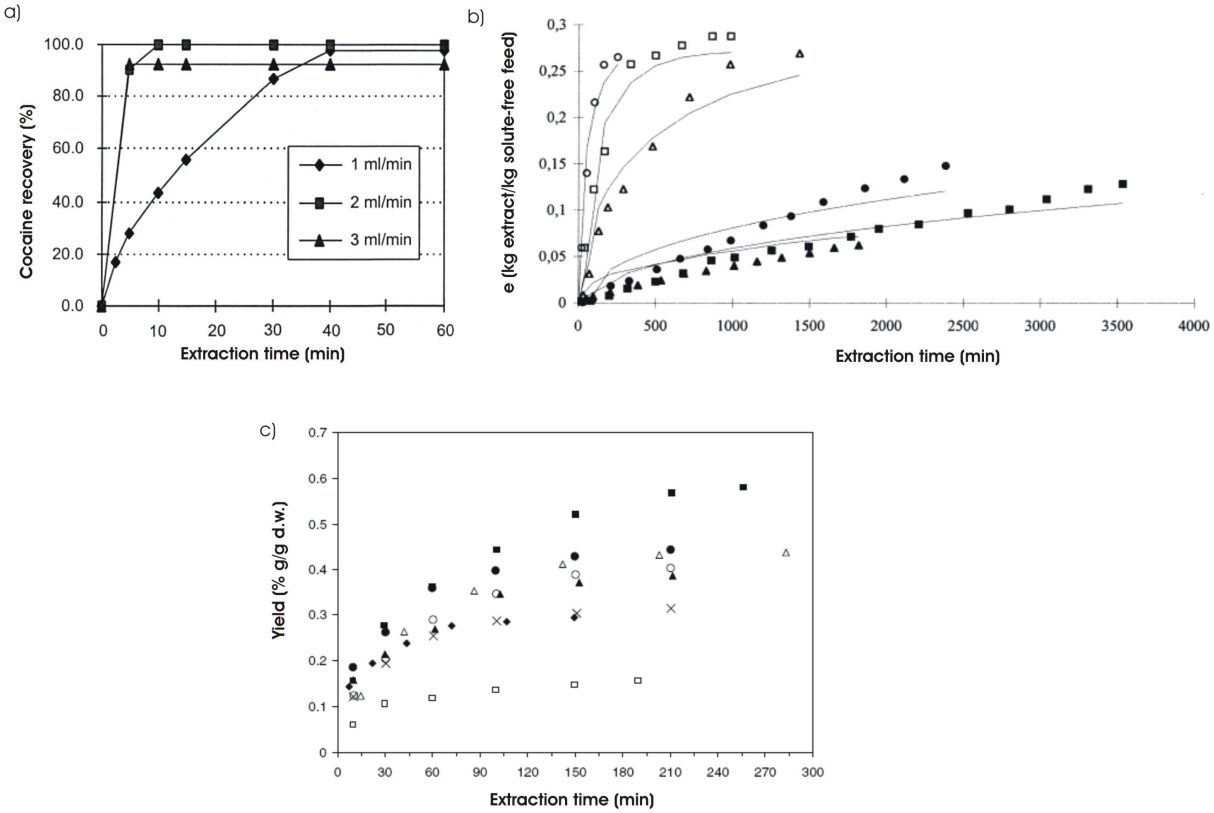

Figure 1.9. Examples of extraction curves. **a) cocaine from coca leaves** [78]: extraction at different flow rates for a particle size distribution between 150 and 170 μm; **b) oil from olive husk** [79]: T=313 K. U~6 ×10−4 m/s: Δ - P=12 MPa; □ - P=15 MPa; ○ - P=18 MPa. U~0.1×10−4 m/s :▲- P=12 MPa; ■ - P=15 MPa; ● - P=18 MPa; **c) volatile oil from coriander seeds** [80]: yields obtained for different SFE conditions: pressure and temperature (▲– 90 bar/40°C, □ – 90 bar/50 °C, ○ – 100 bar/40 °C and ■ – 150 bar/40 °C) for a mean particle size of 0.6 mm and a flow rate of 1.10 kg/h; mean particle size (● – 0.4 mm, ▲– 0.6 mm, × – 0.8 mm) using 90 bar, 40 °C and a flow rate of 1.10 kg/h; and flow rate (Δ – 0.79 kg/h,▲– 1.10 kg/h, ♦ – 1.56 kg/h) for 90 bar, 40°C and 0.6 mm of mean particle size.

Three different approaches that have been proposed for the mathematical modelling of SFE will be discussed:

– empirical

- based on heat and mass transfer analogy
- differential mass balances integration

The last approach is mostly applied, because it provides the most proper analysis. Comparison of the three approaches can be found in work of Esquivel et al. [79], who fitted the models to experimental data obtained for olive husk oil SCO_2 extraction.

1.5.1 Empirical approach

1.5.1.1 Adsorption analogy

Naik [81] showed that extraction by liquid CO_2 of several vegetable materials (clove, cardamom, ginger) conformed well to the Langmuir-like empirical equation:

$$Y = \frac{Y_\infty t}{B + t} \tag{1.10}$$

where Y is the extraction yield, t is the extraction time, B is an adjustable constant and Y_∞ is the asymptotic extraction yield.

1.5.1.2 Chemical reaction analogy

An assumption that the rate of extraction is proportional to the concentration of extracted solute left in the vegetable particle (x) was used by Nguyen et al. [82]. A kinetic constant k_c was used instead of the mass transfer and equilibrium relationship in the differential equation

$$\frac{dx}{dt} = -k_c x \tag{1.11}$$

Applying the initial condition $x(t=0)=x_0$, the equation was integrated, the kinetic constant was expressed as a function of the diffusion distance and the diffusion coefficient was evaluated from experimental data. Authors found a strong dependence of the extraction rate on the particle size which confirmed the controlling role of internal diffusion.

So and McDonald [83] extracted rapeseeds with hexane and presented a two stage washing/desorption model with kinetic constant for each stage; similar approach was used by Khandiah and Spiro [84] for supercritical extraction from ginger rhizomes.

Although the empirical approach can interpolate the experimental results, it does not take into account interactions between the solute and the solute matrix, equilibrium relationships in the system nor mass transfer mechanisms. Therefore, it cannot be used for a scale-up, nevertheless the estimation of the equation parameters may be useful for predicting extraction curves for the same solute-solvent system within the range of conditions used in their determination.

1.5.2 Approach based on heat and mass transfer analogy

SFE is considered analogical to heat transfer phenomenon where every single vegetable particle is described as a hot ball cooled in a uniform medium. The initial solute distribution within particles is assumed to be uniform, therefore the analogy of heat and mass transfer can be taken in account, applying Fick's second law of diffusion and the Fourier transforms. The mass balance across an internal surface of the particle is expressed as

$$\frac{\partial c}{\partial t} = D_i \left[\frac{1}{r^2} \frac{\partial}{\partial r} \left(r^2 \frac{\partial c}{\partial r} \right) \right] \tag{1.12}$$

where D_i is the diffusion coefficient of the solute in the sphere. The analytical solution of the equation (1.12) was published by Crank [85]. This so called hot ball model was applied to SFE by Bartle et al. [86]; it is explained in detail in chapter 3.3. The authors explained deviations from the model predictions qualitatively in terms of particle shape, solubility limitation and a non-homogeneous distribution of the solute within the material. The model was later modified with respect to the effect of solubility on the extraction [87].

Reverchon et al. [88] applied the hot ball model extended by including an external film resistance on the extraction of essential oil of various plants (marjoram, basil, rosemary). Intraparticle diffusion was found to be the controlling stage for all the analyzed matrices.

1.5.3 Approach using differential mass balance integration

Mass balance models have been widely used to describe the behaviour of fixed bed during solid-liquid operations like absorption/desorption, chemical reaction and extraction. To simplify the description, they usually assume constant solvent density and flow rate along the bed and neglect axial dispersion. The extract is mostly considered as a single compound.

A general model of extraction in packed bed can be found among others in Reverchon's review [27]. The model consists of mass balance equations completed with an equilibrium expression. For the extraction bed as schematized below, two independent mass balances can be written:

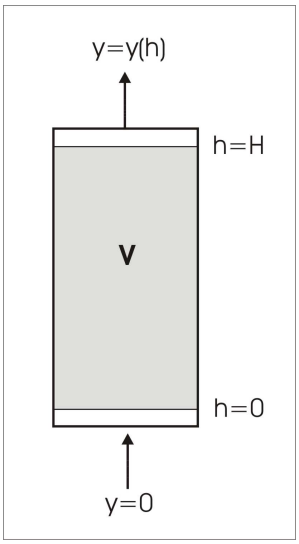

$$U\rho \frac{\partial y}{\partial h} + \varepsilon\rho \frac{\partial y}{\partial t} + (1-\varepsilon)\rho_S \frac{\partial x}{\partial t} = 0 \tag{1.13}$$

$$(1-\varepsilon)\rho_s \frac{\partial x}{\partial t} = -k_s a_0 \rho_s (x - x^*) \tag{1.14}$$

where

a_0	specific surface of particles (1/m)
h	axial coordinate along the bed (m)

k_s	internal (solid-phase) mass transfer coefficient (m/s)
t	extraction time (s)
U	superficial solvent velocity (m/s)
x	solute concentration in the solid phase (kg/kg of raw material)
x^*	concentration at the solid-fluid interface which is assumed to be in equilibrium with the fluid phase (kg/kg of raw material)
y	solute concentration in the fluid phase (kg/kg of solvent)
ε	void fraction of the extracted material (-)

System of equations (1.13) and (1.14) can be solved numerically with initial conditions t=0, y=0 and x=x_0 (where y_0 is the initial concentration of the solute in the solvent) and boundary condition h=0, $y(0,t)$=0. To define the solid-fluid phase equilibrium describing solid matrix interaction, a linear relationship is usually used in modelling

$$y^* = K\,x^* \tag{1.15}$$

where K is the mass partition coefficient of the extract between the solid phase and the fluid phase at equilibrium, it is supposed to be a function of pressure and temperature only. Mostly, the external mass transport resistance (solute – solvent) is negligible compared to the internal mass transfer resistance; therefore, it can be presumed that the concentration in the bulk of solvent is equal to the equilibrium concentration on particle surface, i.e. y=y^*.

When a system of porous particles with the solute trapped in pores is described, and if it can be assumed that the solid has no affinity for the liquid, the driving force for the extraction process will be represented by the equilibrium solubility of the solute in the fluid phase. Such a situation can be described by the shrinking core model [89]. The model might be applicable especially in extraction from seeds, as their oil content is usually high, so we can neglect the matrix-solute interactions, and the seed structure can be described by porous particles.

If the concentration profile along the extracted particle is required, equation (1.12) can be used as a solid phase mass balance for porous spherical particles, where D_i is the effective intraparticle diffusion coefficient. In the case of extraction from leaves, Goto et al. [90] used the mass balance for a single slab-like particle, including porosity of the leaf β

$$\beta\frac{\partial c_i}{\partial t} = D_i\frac{\partial^2 c_i}{\partial w^2} - (1-\beta)\frac{\partial c}{\partial t} \tag{1.16}$$

with w as the leaf coordinate and c_i as the concentration in the pores of the leaf.

In equation (1.14), the group $k_s a_0 /(1-\varepsilon)$ depends on the geometry of particles through $k_s a_0$. As this group is dimensionally equal to 1/s, it is possible to define the internal diffusion time t_i

$$t_i = \frac{(1-\varepsilon)}{k_s a_0} \tag{1.17}$$

It is so called characteristic time for the extraction process, i.e. the theoretical time necessary to extract all solute on condition that the extraction proceeds at initial velocity.
Therefore, equation (1.11) can be rewritten as

$$\frac{\partial x}{\partial t} = -\frac{1}{t_i}(x - x^*) \tag{1.18}$$

Further, assuming uniform rate of extraction along the extraction bed ($\partial y/\partial h$=const.), the time remains the only variable and a system of ordinary differential equations obtained this way can be solved numerically by the method of Runge-Kutta. Another simplification, neglecting of the accumulation of the extract in the fluid ($\partial y/\partial t$=0), allows a simple analytical solution of the problem.
To estimate internal diffusivity D_i, Reverchon [27] introduces the relation

$$t_i = \mu \frac{l^2}{D_i} \tag{1.19}$$

proposed by Villermaux [91] for dynamic modelling of linear chromatography for the case of simultaneous diffusion and adsorption in porous particles having a single porosity (see chapter 3.2.)
Lack [92] used an analogy with drying process to describe the supercritical extraction. The first part of the extraction was assumed to be analogical to the first drying stage of a wet material, where the humidity from the surface is being evaporated fast depending on the properties of the drying air. Consequently, the slow part of extraction is controlled by diffusion analogical to the diffusion of the humidity from inside of the wet material.
Inspired by this analogy, Sovova [93] proposed a model of broken and intact cells. The model assumes that a part of the solute, which is initially deposited in plant structures and protected by cell walls, is deliberated during a mechanical disintegration of the material. This solute situated in the area of broken cells close to the particle surface is therefore directly exposed to the solvent, whilst the core of the particle still contains intact cells with undamaged cell walls. The model results into three extraction periods – period of fast extraction of accessible oil, transient stage and slow period controlled by the diffusion. Detailed description of the model is given in chapter 3.1. The model was applied on the extraction of the grape oil [59] and caraway oil [44]. Experimental results were provided with different extraction conditions and effect of milling grade and flow direction was examined. The slow down of the extraction observed in the upflow operation was explained as a consequence of natural convection and channelling in the bed. Later, the author proposed a general model approach [94] applied to seed oil and essential oil extraction. The first extraction period is

described considering different types of phase equilibrium with and without solute interaction with matrix and different flow patterns, mainly with axial dispersion.

1.5.4 Material structure and solute location in the mathematical modelling

Optical or scanning electron microscope can be applied to visualize the structure and to adapt the used mathematical model to the given system. This approach was used for example by Reverchon and Marrone [40] in the extraction from seeds. SEM images of disintegrated particles were taken and the fraction of the free solute containing cells was determined graphically and used as one of model parameters.

Micro-scale model proposed by Zizovic et al. [95] incorporates closer botanical aspects of extracted material. Mass balance equations are extended by a so called Source and Transfer term (ST) which describes essential oil transfer from specific secretory structure to supercritical fluid phase.

This chapter gives just a brief review on mathematical modelling of SFE; for each individual case, the degree of simplification or extension of the model applied must be considered. A more detailed description exceeding the scope of this work can be found in the literature. [27], [40], [96].

1.6 DIC process – Instantaneous Controlled Pressure Drop

The DIC process was developed in the laboratory LMTAI (Laboratire maîtrise des technologies agro-industrielles, presently LEPTIAB) at the University of La Rochelle [97] and issued from the earlier theoretical study of Allaf concerning expansion by alveolation [98].

1.6.1 Principle of the process

The process is based on the thermomechanical processing induced by subjecting a substance partially humid to high pressure steam followed by a rapid expansion to vacuum (about 5 kPa, valve opening time of 0.2 s). Generally, the operating pressure is lower than 20 bar, hence the temperature in the autoclave is lower than 200°C, and the heating period ranges from seconds to minutes. The rapid pressure drop ($\Delta P/\Delta t > 2.5 \cdot 10^5$ Pa.s^{-1}) causes a bursting evaporation of a part of the moisture from the bulk of the material, which blows and breaks the walls of cavities. The degree of structural changes depends strongly on the nature of the treated material as well as on conditions of the treatment. The auto-vaporization as an adiabatic transformation induces also instantaneous cooling of the material in the autoclave.

Temperature and pressure histories of one DIC cycle are shown in Figure 1.10. Successive steps of the process are the following:

a) at the beginning, the material is placed in an autoclave (see DIC set up schema in chapter 2) that is at the atmospheric pressure;
b) an initial vacuum is installed in the autoclave in order to improve the penetration of the heating fluid through the material and thus, to enhance heat transfer;
c) saturated steam is injected to the autoclave;
d) fixed pressure is maintained in the autoclave for a fixed period of time;
e) steam feed is cut off and the valve connecting the autoclave to a vacuum tank is opened rapidly which results in an abrupt pressure drop in the autoclave
f) and (g) the valve is closed and the atmospheric pressure is installed

A similar process, steam explosion, has been used for pretreatment of biomass containing lignocellulosic structures [99]. It results in a hydrolysis of glycosidic bonds in the hemicelluloses and, to a lesser extent, in the cellulose. It also leads to a cleavage of hemicellulose–lignin bonds. Unlike the steam explosion the DIC process does not use the release to atmospheric pressure but the pressure drops to vacuum. Therefore, to reach the same degree of destruction, temperature applied on the material may be lower in the DIC process.

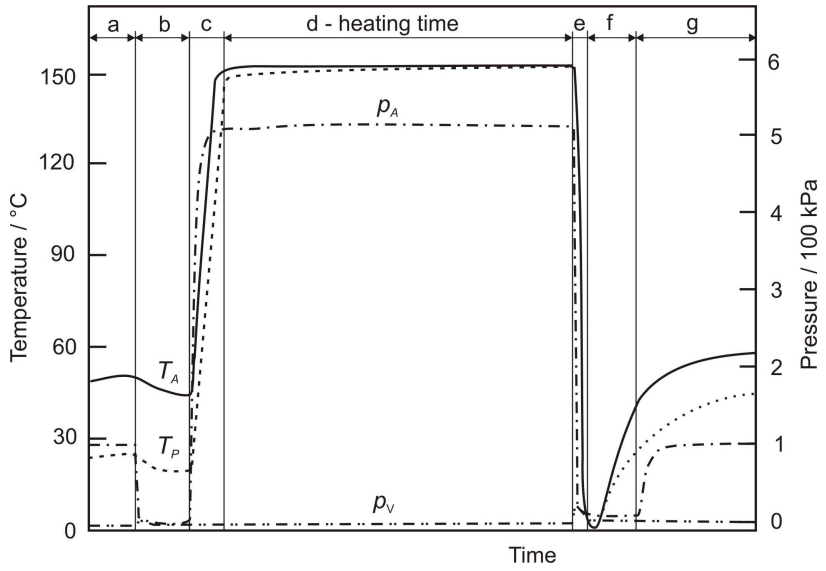

Figure 1.10. Temperature and pressure history of a DIC processing cycle. p_A pressure in autoclave, p_V pressure in vacuum tank, T_A temperature in autoclave, T_P temperature of product.

1.6.2 Theoretical background

Although many applications of the DIC process have been tested and experimental studies have been performed since last 20 years, the theoretical bases of the process have been proposed quite recently. As no classic thermodynamic theory was found appropriate to describe the phenomena observed, Allaf proposed a specific theory of instantaneity [100], which was recently extended by Allaf and Al Haddad [101].

Further, the problem of pressure-drop rate was closely examined [102]. If we neglect pressure losses in the valve and connecting pipe, the connection between the autoclave and vacuum tank can be simulated by an orifice. The flow through an orifice is sonic if the ratio of the pressures after and before the orifice, β, is equal or lower than the value β_c:

$$\beta_c = \left(\frac{2}{\gamma+1}\right)^{\gamma/(\gamma-1)} \tag{1.20}$$

Due to very low pressure in the vacuum tank, this condition is fulfilled for a great deal of the expansion. For this period, the discharge of the autoclave happens at the sonic velocity in the pipe exit. Approximating the autoclave discharged by an orifice towards the constant pressure p_V, neglecting friction loses in the pipe and assuming that the temperature T_A in the autoclave is constant during the pressure-drop, the pressure in the autoclave can be expressed in a form of exponential function of time:

$$p_A = p_I \exp\left(\frac{-t}{k_{theor}}\right); \quad k_{theor} = \frac{V}{a}\sqrt{\left(\frac{\gamma+1}{2}\right)^{\gamma+1/\gamma-1}\left(\frac{M_W}{\gamma R T_A}\right)} \tag{1.21}$$

where

a	orifice area
k_{theor}	characteristic time (s)
M_W	molar mass of gas
p_I	initial pressure in the autoclave
R	gas constant
V	volume of the autoclave
γ	ratio of the specific heat at constant pressure and constant volume, $\gamma=C_p/C_v$

The theoretical pressure drop-rate at the beginning of the expansion is equal to

$$\left.\frac{dp_A}{dt}\right|_{t=0} = \frac{-p_I}{k_{theor}} \tag{1.22}$$

Theoretical and experimental pressure histories are plotted in Figure 1.11. The rate of valve opening manifest itself at the beginning of the expansion The evaporation of the water condensed in the autoclave, starting at the pressure of about 300 kPa, increases considerably the amount of the discharged fluid and hence the deviation of the exponential function. In the case of air, there is no evaporation, thus the curve shape is close to the exponential one except of the very beginning which is influenced by the final rate of valve opening.

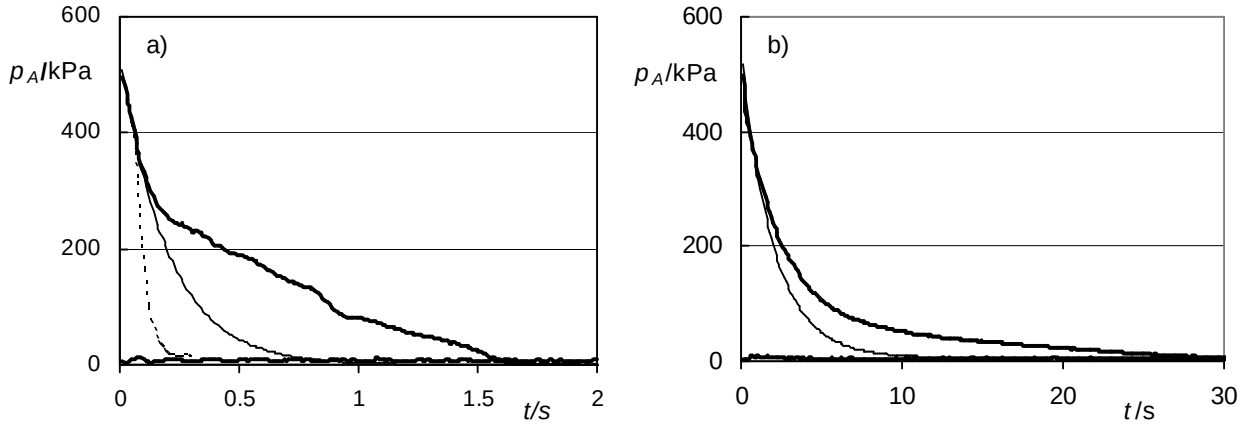

Figure 1.11. Pressure-drop history in autoclave (upper thick line) and vacuum tank (lower thick line) connected with different openings: (a) 80 mm, (b) 6mm. The solid thin line stands for exponential curves that best fit the beginning of the expansion. The dashed thin line in (a) stands for pressure drop of compressed air. [102]

1.6.3 Applications

The DIC process has been already applied for drying of vegetable materials [103], fish [104] and pharmaceutical products,[105], drying/texturation [106], treatment of archaeological waterlogged wood [107], rice expansion, inactivation of microorganisms, DIC treatment by microwaves [108] and

also extraction of volatile compounds like essential oils [109], [110]. Numerous patents have been applied [97], [111].

2. EXPERIMENTAL

2.1 Impact of structure modification on SCO_2 extraction

2.1.1 Material

- commercial amaranth seeds
- soybeans, type Sapporo, provided by INRA Surgères, France
- green coffee beans, type Arabica, Ethiopian origin, purchased from local markets

Plants containing volatile compounds (such as odorous plants with essential oils) had to be avoided, because these compounds would be partially lost in the DIC process. Therefore, we focused on seeds, containing mostly vegetable oils. **Soybeans** were chosen as model material because they contain relatively high amount of oil (~20%). Amaranth seeds and coffee beans were chosen from the practical point of view. **Amaranth seed** is perspective for its high nutrition value and the presence of squalene [112]. Decaffeination of **coffee beans** is one of the most important industrial applications of the supercritical extraction [49]. Extraction from whole beans is selective for caffeine, but the process is slow. The aim of this work was to enhance the extraction by structure modification of beans.

2.1.2 Experimental procedure

One part of seeds was treated by DIC process (see chapter 2.1.4), the other part was used as a reference sample. From each part, samples of whole seeds and milled seeds were prepared and extracted (2.1.3). To complete the material characteristics, in the case of soybeans and coffee beans, textural properties were analyzed (2.1.5) and grain size analysis of milled samples was carried out (2.1.6). Total content of extractable solute was determined by solvent extraction (Randall extraction, see chapter 2.17). Extracts from coffee beans were analysed by high pressure liquid chromatography to determine caffeine content (2.18).

2.1.3 SCO_2 extraction

2.1.3.1 Experimental apparatus

The SFE experiments were carried out in the ICPF AS CR laboratory.

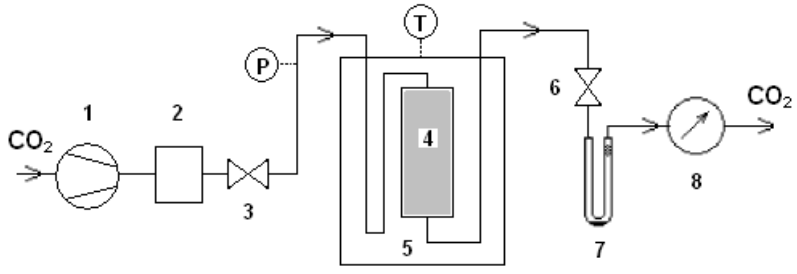

Figure 2.1. Schematic diagram of the extraction apparatus.

The material was placed in a cylindrical extractor between layers of glass beads to improve the solvent flow distribution. Carbon dioxide was pumped by compressor (1) from pressure bottle into a surge tank (2) where it was maintained at a set pressure, then introduced through a shut-off valve (3) to a capillary immersed together with the extractor (4) in a water bath (5), preheated this way and supplied to the extractor. The solute-laden CO_2 flowing out of the extractor was expanded to atmospheric pressure in a heated micrometer (6) valve. The oil was collected in a U-tube (7). During the extraction, the U-tube was replaced and weighed at regular intervals to determine the evolution of the extract amount. Constant solvent flow rate was manually maintained by setting of micrometer valve and controlled by gas meter (8).

2.1.3.2 Extraction conditions

The extraction pressure and the temperature of the water bath were maintained at 28 MPa and 40°C in all runs with soybeans and amaranth seeds, and 24 MPa and 50°C in all runs with coffee beans. The constant solvent flow of 0.5 L/min (expanded CO_2) was adjusted by the metering valve and measured using a gas meter at the outlet of the U-tube. These conditions are in the range of extraction conditions used in the literature to extract vegetable oils [41] and caffeine from coffee [113]. The pressure of 28 MPa is the limit pressure that can be achieved by used apparatus.

The milled beans and all amaranth samples (4.0-4.7 g) were extracted in a 12-ml extractor with an inner diameter of 8 mm and the whole beans (15.7 - 25 g) in a 150-ml extractor of 33 mm inner diameter.

2.1.4 DIC treatment

2.1.4.1 Experimental apparatus

DIC experiments were carried out at the LMTAI laboratory.

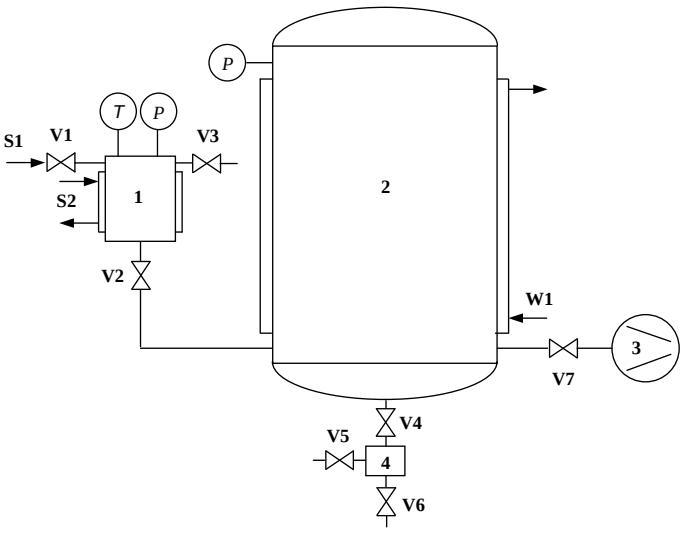

Figure 2.2. DIC set-up.

The DIC set-up is shown in Figure 1. It consists of an autoclave (1), a reservoir under a vacuum (2), a water ring vacuum pump (3) and a trap (4). The 18 L autoclave is separated from the 1600 L reservoir by a butterfly valve with a diameter of 200 mm and opening time of 200 ms. Saturated vapour (S1) is supplied through the valve (V1). The pressure in the autoclave is controlled manually by this valve. Saturated vapour (S2) heats the autoclave by means of a double jacket. The atmospheric pressure is adjusted after a DIC cycle through a vent (V3). The vacuum pump installs a vacuum of about 5 kPa in the reservoir. The reservoir is cooled by tap water (W1) circulating in a double jacket. Condensate can be removed through the trap (4) equipped with a system of valves. The autoclave and reservoir are equipped with manometers and pressure transducers. Several thermocouples are mounted in the autoclave for temperature measurements of material and steam. The treated material is enclosed in a perforated steal container with a diameter of 175 mm.

2.1.4.2 Conditions of the treatment

a) Amaranthus seed

Before the DIC treatment itself, a part of amaranthus seeds was soaked in water at room temperature for 1 hour, then softly dried in an oven at 45°C for 1 hour and stored in a refrigerator at 4°C for 24 hours, the other part was treated dry. The treatment of samples was carried out at 0.6 MPa for 1 minute. After the expansion the samples were dried at 45°C and stored in a refrigerator in plastic bags.

b) Soybeans

Before the DIC treatment, decorticated soybeans were soaked with water at 70°C for 15 minutes, then dried softly in an oven at 45°C for 1 hour and stored in a refrigerator at 4°C for 24 hours. Homogenous moisture distribution within the material, necessary for the subsequent DIC treatment, was obtained in this way. The treatment of samples consisted of one-minute treatment at 0.3 MPa followed by 2 minutes at 0.7 MPa. After the expansion the samples were dried at 45°C and stored in a refrigerator in plastic bags.

c) Coffee beans

Beans were moisturized to a water content of 27.5 % (dry basis), then stored in a refrigerator at 4°C for 24 hours. The DIC treatment of samples was carried out at 0.5 MPa for 45 seconds. After the expansion the samples were dried at 45°C and stored in a refrigerator in plastic bag.

d) Study of DIC conditions effect on soybeans

A set of DIC treatments of soybeans at different pressures (0.117-0.68 MPa) and times of treatment (0.6-3 min) was carried out to investigate the influence of DIC conditions on the extraction rate. The conditions of the treatment were selected using two-factor experimental design (see later).

The beans were not moisturized in these runs; the samples were dried at 45°C after the DIC treatment and stored in a refrigerator in plastic bags.

2.1.4.3 Experimental design

Experimental design is an efficient way how to optimize a process with a reduced number of experimental runs.

COST method (Changing One Separate Factor at a Time), consisting of fixation of all factors except one to find an influence of this factor on the process response, request a lot of experimental runs, thus it is expensive, and does not provide information about optimum conditions if there are interactions between parameters. On the other hand, experimental design idea proposes reduced number of experiments with systematic variation of all factors. Statistic analysis of results obtained with these runs permits to determine optimal conditions of the process, as well as particular effect of all parameters on the response (e.g. extraction yield) and their interactions.

Central composite experimental design was applied in this work to determine DIC effect (time of treatment, pressure) of experimental runs to find the influence of DIC on the mass transfer in soybeans during supercritical extraction. This design uses response surface method and mathematical modeling is based on second-order polynomial functions. Hence, the response is a function of two factors in our case

$$\eta = f(X_1, X_2) \tag{2.1}$$

and it is expressed as

$$\eta = \beta_0 + \sum_{i=1}^{n} \beta_i X_i + \sum_{i=1}^{n} \beta_{ii} X^2{}_i + \sum_{i=1}^{n-1} \sum_{\substack{j=2 \\ j>i}}^{n} \beta_{ij} X_i X_j + \varepsilon \tag{2.2}$$

where β_i , β_{ii} et β_{ij} are regression coefficients and X_i are the factors, n is number of factors and ε is random error. The experimental points correspond thus to

1. complete factorial experimental design with points at corners of the square (the square represents the studied region of conditions),
2. central points are used to estimate the variance (reproducibility) of experiments,
3. axial points, marked $-\alpha$ and $+\alpha$, complete the points of factorial experimental design and allow evaluation of quadratic effects of factors. Value of α depends on number of factors n and it is calculated as

   $$\alpha = \sqrt[4]{2^n} \tag{2.3}$$

   with value of α = 1.41 corresponding to two factors.

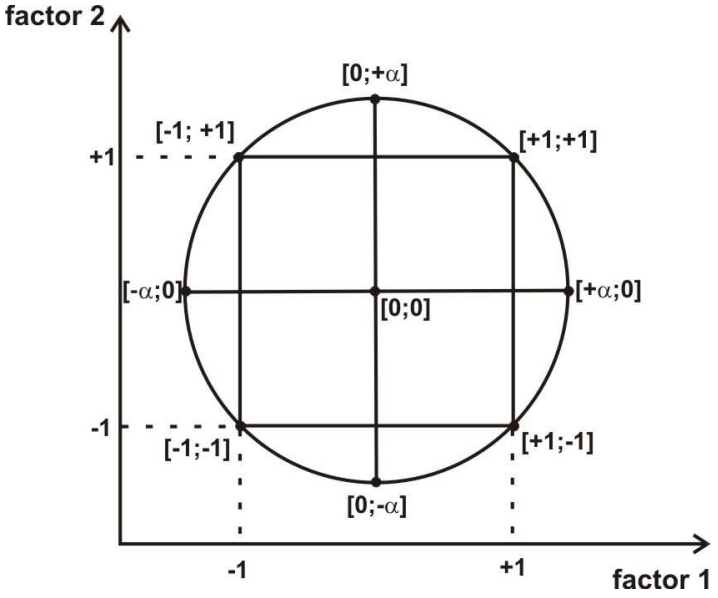

Therefore, the number of experimental runs corresponding to two factors (parameters) can be determined as $2^n + 2n + n_0 = 12$ (Table 2.1) (number of central points n_0=4 was applied in this work).

Table 2.1. Experimental conditions of DIC applied on soybeans

exp. run	t (min)	pressure ($\cdot 10^5$ Pa)
1	0,59	4
2	1	2
3	2	4
4	3	2
5	1	6
6	2	1.17
7	3.41	4
8	3	6
9	2	4
10	2	6.83
11	2	4
12	2	4

2.1.5 Textural properties analysis

Textural properties of the extracted materials were determined by mercury porosimetry in the range 0.1-400 MPa (AccuPyc 1330, Micrometrics, USA) and helium pycnometry (AutoPore 9600, Micrometrics, USA). Measurements of all tested samples were tripled to confirm reproducibility of the results, and pore-size distribution curves were plotted. Bulk and skeletal density determined by the porosimetry and helium pycnometry, respectively, were used to calculate the porosity

of the materials. Measurements were kindly performed by Dr. O. Šolcová and Mrs. H. Šnajdaufová from ICPF AS CR.

Scanning electron microscopy type JEOL 5410LV (CCA – Centre commun d'analyse of University in La Rochelle) was employed to examine the internal structure of soybeans. Samples were put on a stand and covered by adhesive carbon under vacuum. Potential difference of electron acceleration of 20 kV was applied.

2.1.6 Disintegration characteristics

Disintegration was carried out using a coffee grinder adjusted to constant degree of milling. Grain size analysis of milled material was made using a set of standardized sieves of mesh diameter 1, 0.63, 0.5, 0.315 and 0.2 mm. Mass of sieved samples varied between 4 and 10 g. The sieved fractions were weighed and average values of limiting mesh diameters were used as fraction particle diameters. For the largest fraction, particle diameter of 1.25 cm was used with respect to real size of particles.

Void fraction of packed bed of solid particles in the two used extractors was determined by means of graduated cylinders of approximately the same diameter as the extractors and of volume of 5 and 40 ml. Void fraction was calculated as

$$\varepsilon = \frac{V_{void}}{V_{total}} = 1 - \frac{m/\rho_s}{V_{total}} \tag{2.4}$$

where m is mass of material in the cylinder, ρ_s is bulk density of beans determined by mercury porosimetry, and V_{total} corresponds to volume of the graduated cylinders of 5 and 40 ml.

2.1.7 Randall extraction

This method was used to determine the total content of solute (oil) in the material.

2.1.7.1 Experimental apparatus

The Randall modification of the standard Soxhlet extraction (also called the Soxtec method or the submersion method) submerges the sample in boiling solvent, reducing the time needed for extraction. It is a 2-step process: in the first step, a thimble containing the test portion is immersed into the boiling solvent. The intermixing of matrix with hot solvent ensures rapid solubilization of extractables. The thimble is then raised above the solvent and the test portion is further extracted by a continuous flow of condensed solvent to remove the rest of extract.

Extraction was realised on device VELP Scientifica SER 148.

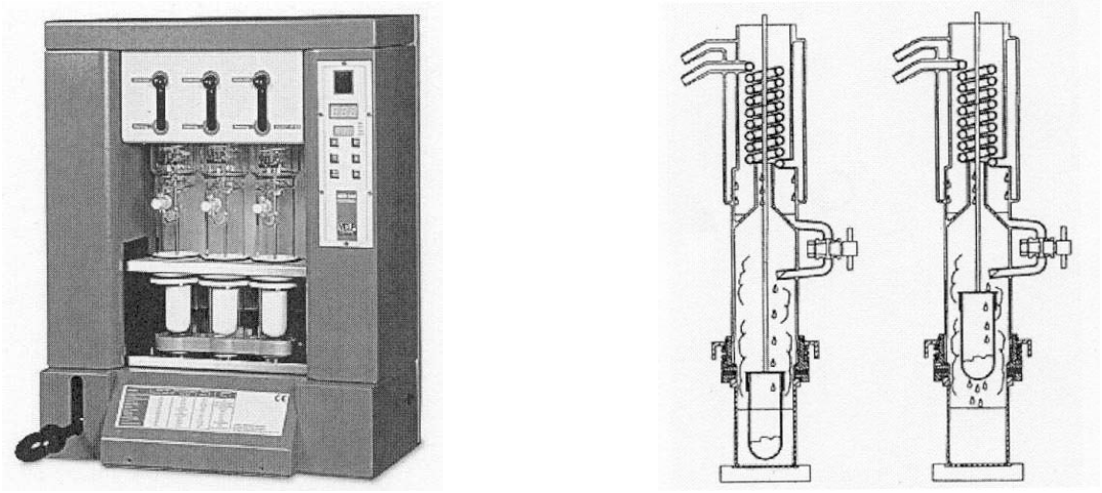

Figure 2.3. Randall extraction apparatus (left); schema of the two extraction steps - immersion and washing (right).

2.1.7.2 Extraction conditions

Samples of milled soybeans with a mass of 7-10 g were placed in paper thimbles and extracted for 5 hours in 80 ml of boiling hexane (69°C), then rinsed with condensed solvent for 15 minutes. Whole coffee beans were soaked in water up to water content of 40 wt.% and samples of 15.7-19.2 g were extracted for 5 hours in 80 ml of boiling chloroform (61°C), then rinsed for 15 minutes.

Samples of milled coffee beans of 3-4 g of weight were extracted for 3 hours in 80 ml of hexane, then they were rinsed for 30 minutes.

Low pressure evaporation, provided by Buchi Rotavapor R-114 and ILMVAC vacuum pump, was applied to remove the solvent at pressure of 200 mbar and temperature of water bath of 40°C. The extract was weighted regularly until constant weight; it was kept in an exsiccator to cool down to room temperature before each weighing.

2.1.8 HPLC Analysis

Analysis was performed on a HPLC device (Watrex Praha) with a reversed phase column Nucleosil C18 (250×8mm, 5 µm, Watrex Praha). The mobile phase consisted of mixtures of acetonitrile: water (25:75, v/v), the flow rate was 1 ml/min, analysis was carried out at room temperature. Retention time of caffeine was found 12.6 min. DAD-UV detection at 272 nm was applied. External standard method was used for identification and quantification of caffeine; pure caffeine (anhydrous, ≥ 99% (HPLC); Fluka) was used as standard. The injection volume was 10 µl.

2.2 Impact of natural convection in solvent on SCO_2 extraction

2.2.1 Experimental procedure

Experimental apparatus described in chapter 2.2.2 was used to measure residence time distribution (RTD) under subcritical and supercritical conditions (2.2.3). A thermoregulatory box was constructed to maintain constant temperature of test section; its characteristics can be found in chapter 2.2.4. Benzoic acid was chosen as tracer in all experiments (2.2.5). To study RTD during extraction, experiments were carried out with both natural vegetable material containing solute, and with a solute deposited on inner glass beads. Milled soybeans were used as natural material. Two different solutes were deposited on glass beads (2.2.6).

2.2.2 Installation

Experimental apparatus is shown schematically in Figure 2.4.

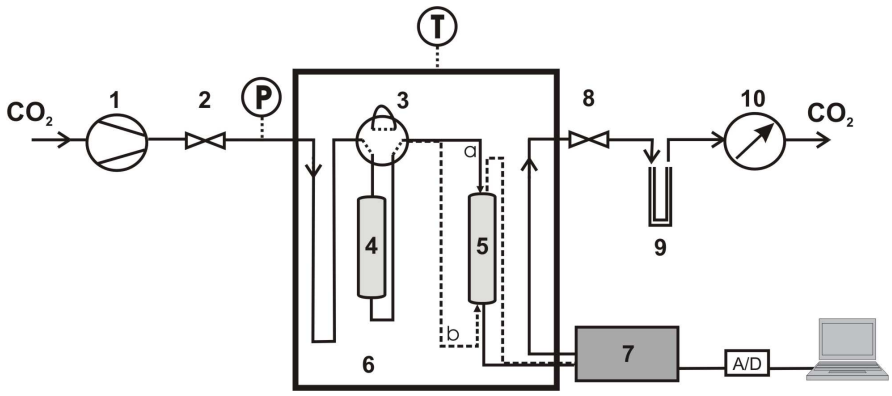

Figure 2.4. Experimental set-up for RTD measurement.

Carbon dioxide was supplied from a pressure bottle and compressed to the required pressure by a syringe pump (1) (model 260D, Teledyne ISCO, USA). It was introduced through a micrometer valve (2) to the experimental section consisting of six-port valve (3), saturator (4) and extractor (5). The experimental section was placed in a thermoregulatory box (6) and maintained at constant temperature by hot air. Benzoic acid (BA) was used as a tracer and placed in the saturator. The closed loop of the saturator was kept pressurized with CO_2 to obtain saturated solution of BA in SCO_2 at given conditions. A solution of BA in SCO_2 was injected to the extractor from the sample loop by switching the six-port valve. Extractor was filled with either glass beads or milled vegetable material placed between two layers of glass beads. Inlet and outlet capillary of the extractor were long enough so that the flow direction could be switched from downflow to upflow easily without dismantling the installation.

The fluid stream flowing out of the extractor was analyzed at λ=230 nm by a UV/VIS detector (7) equipped with a high pressure resistant microcell of 0.5 μm in volume (pressure limit of 20 MPa). The fluid phase leaving the detector was expanded to ambient pressure in a heated micrometer valve (8) and the extract was collected in a U-tube (9). Constant pressure of 12 MPa was maintained by the pump and solvent flow (0.5±0.1ml/min and 1.0±0.1 ml/min) was adjusted with the micrometer valve at the outlet, the flow rate was verified by a gas meter (10) (taking into account actual temperature and pressure). The response of the detector was transformed to a digital output and analysed by chromatography software ECOMAC (v. 0.103, ECOM Ltd, s.r.o.).

2.2.3 Extraction conditions

Experimental runs with subcritical CO_2 were carried out at room temperature and pressure of 12 MPa; extractor of 4 ml in volume (80 mm in height and 8 mm in diameter) was used, tracer was placed in a column of 7.5 ml in volume (150 mm in height and 8 mm in diameter). Total length of capillaries connecting the extractor to the six-port valve and the detector was 130 cm, their diameter was 1 mm.
Experimental runs at supercritical CO_2 were carried out at 40°C and pressure of 12 MPa; this time, the larger column of 7.5 ml in volume was used as extractor and the tracer was placed in the 4 ml column. Total length of capillaries connecting the extractor to the six-port valve and the detector was 130 cm, their diameter was 1mm. To examine the flow pattern without extraction, glass beads of 2 mm in diameter were filled into the extractor. To study the flow pattern during the extraction process, either milled soybeans containing vegetable oil or glass beads coated by a thin layer of a solute were used. As all solutes used in this work, except hexadecane, are waxy solids, the coating was made in a water bath by immerging glass beads to melted solutes. Hexadecane ($C_{16}H_{34}$) in mixture with dotriacontane ($C_{32}H_{66}$) was treated this way as well; pure hexadecane (liquid) was deposited on small pieces of glass wool and evenly distributed in the extractor filled with glass beads.
Note: As noticed in later experiments with trilaurin, the even deposition of waxy solids on glass beads could be reached as well if small amounts of the solid are just put regularly between layers of glass beads along the extractor. As the solute melts under applied pressure and partially dissolves in the SCO_2, after depressurization we could observe that the beads were evenly coated with the solid.

2.2.4 Thermoregulatory box

Dimensions of the box are 60 x 70 x 80 cm. It is made from particleboard (8mm of thickness) with two walls made from plexiglass (6 mm of thickness). The thermoregulation is assured by a hot air ventilator (AEG VH 227, Stiebel Eltron) connected to a control circuit using one thermocouple. Time dependent evolution of temperature at four places in the box, measured under simultaneous fluid phase flow of 1 ml/min at pressure of 12 MPa) is shown in Table 2.2. The temperature at the detector can be assumed to be the same as at the outlet of the box, because the detector was placed in the immediate vicinity of the box and connecting capillaries were enwrapped with foam plastic.

Table 2.2. Temperature profile in the thermoregulatory box: T1 – extractor (control circuit thermocouple), T2 - tracer column (saturator), T3 – entrance/exit of fluid phase to the box, T4 – entrance/exit of the fluid to the detector

t (min)	T1 (°C)	T2 (°C)	T3 (°C)	T4 (°C)
2	39	32	32	40
5	40	36	37	42
10	40	37.5	37	41
25	40	38.5	37	40
40	40	39	37	40
60	40	39	37	40

2.2.5 Tracer characteristics

Solubility of benzoic acid in supercritical CO_2 can be found in the literature [114], [115]. Rough estimation of solubility at 40°C (temperature used in this work), can be made based on the data for 45°C. Published data show that there is the retrograde solubility (crossover pressure) at approximately 17 MPa (Figure 2.5). Therefore, at the extraction pressure of 12 MPa, an eventual temperature drop in capillaries at the exit of the thermoregulatory box would not cause any clogging by precipitated benzoic acid, because its solubility increases with decreasing temperature. This is important from the experimental point of view.

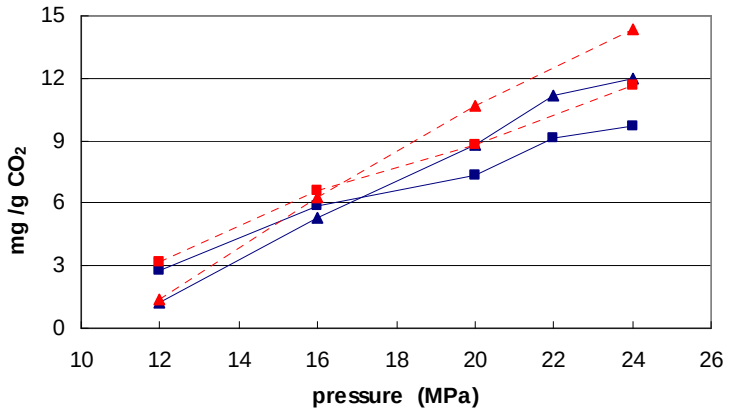

Figure 2.5. Solubility of benzoic acid in SCO_2 at 45°C (■) and 55°C (▲): blue points - [115], red points – [114].

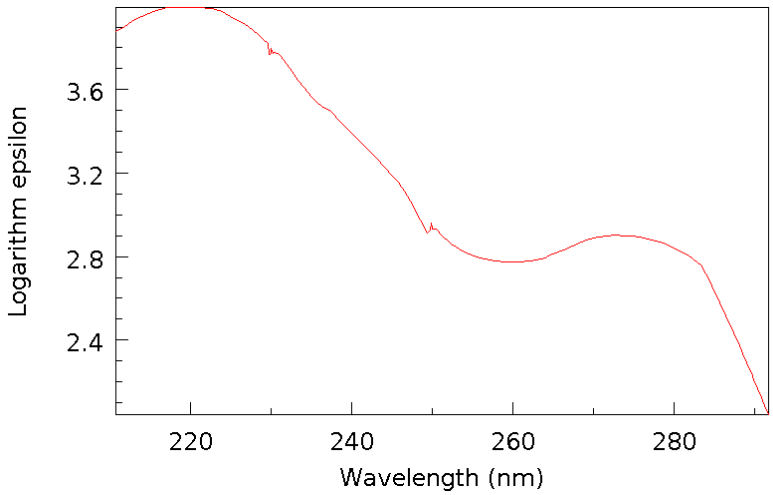

Figure 2.6. Benzoic acid UV/VIS spectrum in 100% sulphuric acid. ε - molar absorptivity coefficient (1/mol.cm) [116].

2.2.6 Solutes characteristics

Tetracosane ($C_{24}H_{50}$)

Solubility data at 37°C are available in [117].

Trilaurin ($C_{39}H_{74}O_6$)

Solubility data for 40°C can be found in [118]; a correlation based on Chrastil's equation is available in [119].

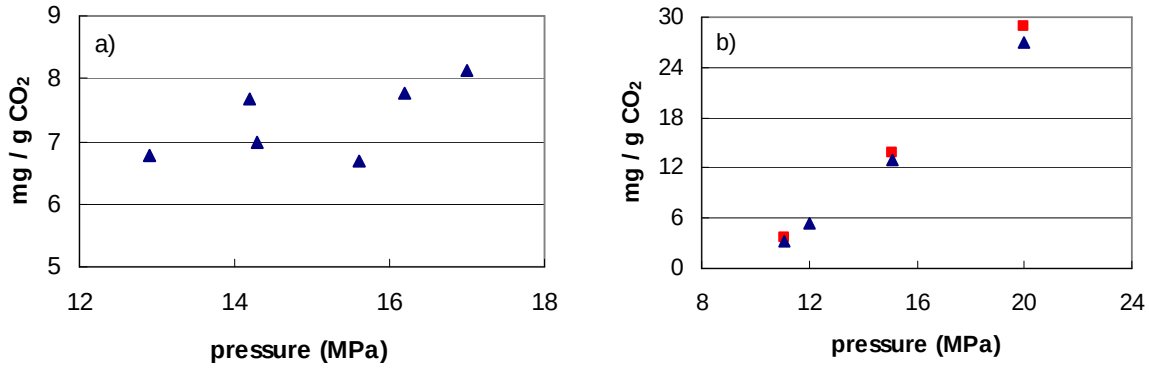

Figure 2.7. a) solubility of tetracosane in SCO_2 at 37°C [117], b) solubility of trilaurin in SCO_2 at 40°C: ■ - [118], ▲ - [119].

Tables of solubility data can be found in Annexe 2 (enclosed on the CD support).

3. MATHEMATICAL MODELS

3.1 Model of broken and intact cells (BIC)

This model [93] assumes that close to the surface there is a region of broken cells whose walls were damaged by mechanical pretreatment. Extraction of easily accessible oil from this region is fast and depends in particular on the oil solubility in the supercritical fluid. On the other hand, the particle core contains intact cells whose mass transfer resistance is high. Therefore, the extraction from intact cells is much slower.

The model solves the mass balance in the packed bed reactor; the system of equations is similar to equations (1.7) and (1.8)

$$-\rho_s(1-\varepsilon)\frac{\partial x}{\partial t} = J(x,y) \tag{3.1}$$

$$\rho\varepsilon\frac{\partial y}{\partial t} + \rho U\frac{\partial y}{\partial h} = J(x,y) \tag{3.2}$$

where x is the solute concentration in the solid phase (kg/kg raw material), y is the solute concentration in the solvent phase (kg/kg solvent), ρ_s is the density of the solid phase (kg/m^3) and ρ is the density of the solvent (kg/m^3). J is the mass transfer rate (kg/m^{3}s) during the extraction defined as

$$J(x > x_k, y) = k_f a_0 \rho(y_r - y)$$

$$J(x \le x_k, y) = k_s a_0 \rho_s x \tag{3.3}$$

Assuming that the solubility of the solute in SCO_2 is low, we can consider the amount of solute in the solvent in the extractor to be negligible in comparison with the amount of solute present in the material; therefore, the first term in eq. (3.2) can be neglected. (We can do this simplification in the case of vegetable oils, however, the first term should be taken into account when highly soluble solutes, such as some essential oils, are concerned.) Then, initial and boundary conditions are determined: $x(h, t=0) = x_0$; $y(h = 0, t) = 0$.

Analytical solution of the model was found introducing dimensionless variables

$$r = \frac{x}{x_k}; \quad Y = 1 - \frac{y}{y_r}; \quad z = \frac{k_f a_0}{U} h \tag{3.4}$$

where x_k is the initial content of solute in intact cells (kg/kg raw material), y_r the solubility of the solute in the supercritical fluid (kg/kg CO_2), k_f the external mass transfer coefficient (m/s), a_0 the specific surface (1/m).

The dimensionless mass transfer rate defined as

$$J^*(r,Y) = \frac{J(x,y)}{k_f a_0 \rho y_r} \tag{3.5}$$

is then assumed to be a product of Y and a function $f(r)$ varying for the fast and slow period of extraction:

$$J^*(r,Y) = f(r)Y; \quad f(r>1) = 1; \quad f(r \le 1) = \frac{k_s \rho_s x_k}{k_f \rho y_r} r \tag{3.6}$$

Model leads to three extraction periods. In the initial fast period the rate of extraction is constant and determined by the solubility and solvent film resistance. As the particles at the reactor inlet loose all the accessible solute, the transition period starts, reflecting the exhaustion advancing through the extraction bed. At the end of this period, all accessible solute has been removed from the bed. Then, only the solute captured in closed cells is extracted during the third period controlled by slow diffusion to particle surface through intact tissue inside the particles.

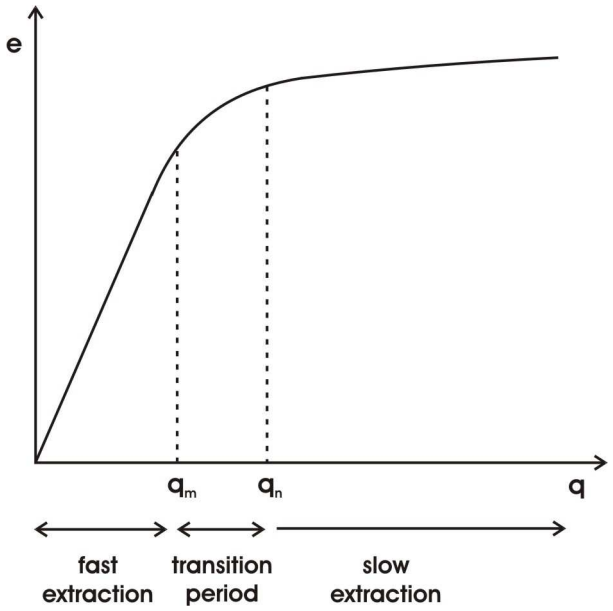

Figure 3.1. Three periods of an extraction curve. Dimensionless amount of extract *e* plotted versus dimensionless amount of solvent *q*.

The process is represented by extraction curve where the extraction yield is plotted versus the extraction time or the mass of solvent passed through the extractor per unit mass of extracted material (Figure 3.1). The amount of extract *e* corresponding to each extraction period is expressed by eq. (3.7), derivation of the solution in detail can be found in [93]

$$\begin{aligned} e &= q y_r \left[1-\exp(-Z)\right] && q < q_m \\ e &= y_r \left[q - q_m \exp(z_W - Z)\right] && q_m \le q < q_n \\ e &= x_0 - \frac{y_r}{W} \ln\{1 + \left[\exp(W x_0 / y_r) - 1\right] \cdot \exp[W(q_m - q)] \frac{x_k}{x_0}\} && q \ge q_n \end{aligned} \tag{3.7}$$

where q_m and q_n representing the amount of solvent at the beginning and at the end of the transition period respectively are expressed as

$$q_m = \frac{x_0 - x_k}{y_r Z} \tag{3.8}$$

$$q_n = q_m + \frac{1}{W} \ln \frac{x_k + (x_0 - x_k)\exp(W x_0 / y_r)}{x_0} \tag{3.9}$$

$$\frac{z_W}{Z} = \frac{y_r}{W x_0} \ln \frac{x_0 \exp[W(q - q_m)] - x_k}{x_0 - x_k} \tag{3.10}$$

Z and W are parameters related to the mass transfer in solvent and solid phase, respectively. Dimensionless axial coordinate z_w/Z indicates the position of the boundary between fast and slow extraction in the extraction bed and varies in the range of 0-1.

$$Z = \frac{k_f a_0 \rho}{q'(1-\varepsilon)\rho_S} \tag{3.11}$$

$$W = \frac{k_s a_0}{q'(1-\varepsilon)} \tag{3.12}$$

Mass transfer parameters for the fast and the slow extraction period can be evaluated by fitting the model to experimental data. The flux from broken cells to bulk solvent is described by volumetric external mass transfer coefficient $k_f a_0$ where a_0 is the specific surface (particle surface area per unit volume of extraction bed). Similarly, the flux from intact cells is characterised by volumetric internal mass transfer coefficient $k_s a_0$. The third evaluated parameter is the volumetric fraction of broken cells in the particles $r_b = 1 - x_k / x_0$, depending generally on the grade of disintegration.

3.2 Approximation of effective diffusion coefficient

The third part of the extraction curve corresponding to the slow extraction can be approximated by exponential dependence

$$\frac{e}{x_0} \approx 1 - C \exp\left(\frac{k_s a_0 t}{1-\varepsilon}\right) = 1 - C \exp\left(-\frac{t}{t_i}\right) \tag{3.13}$$

where t_i is the characteristic time of extraction which can be expressed also as

$$t_i = \mu \frac{l^2}{D_i} \tag{1.19}$$

l is the volume-to-surface ratio for the particles (the characteristic particle dimension). The parameter μ depends on the shape of extracted particles (1/3 for slabs, 1/2 for long cylinders and 3/5 for spheres). These values were suggested by Villermaux [91] for dynamic modelling of linear chromatography under assumption of simultaneous transient diffusion and instantaneous adsorption in porous particles having single porosity. The approximation was applied in supercritical extraction by Reverchon [61]. Approximate relationship between the internal diffusivity and effective mass transfer coefficient results from eqs. (3.13) and (1.19)

$$D_i = \frac{k_s a_0}{1-\varepsilon} \mu l^2 \tag{3.14}$$

3.3 Hot ball model

Hot ball model proposed by Bartle et al. [86] is based on the diffusion in a sphere. Therefore, the extracted particles are assumed to be spherical with initially uniformly distributed solute diffusing through the matrix analogously to the heat diffusion and the solute concentration in the solvent is assumed to be close to zero. Unlike the BIC model which is well applicable in the situations where some of the solute is readily accessible to the solvent on particle surface, the hot ball model is suggested for a matrix which contains small quantities of extractable solute. In such a case, due to the small quantity of solute with respect to the large amount of solvent, the solute solubility does not limit the mass transfer in the fluid phase. The time dependence of extraction yield is described by equation

$$\left(\frac{e}{x_0}\right)_{HB} = 1 - \frac{6}{\pi^2} \sum_{n=1}^{\infty} \frac{1}{n^2} \exp\left(\frac{-D_i n^2 \pi^2 t}{r^2}\right) \tag{3.15}$$

where e is the dimensionless extraction yield, t is the extraction time, r is the radius of the sphere and x_0 is the initial solute content in the plant (i.e. the extraction yield at infinite time).

However, as the extraction proceeds in the packed bed reactor, the solvent saturates progressively with the solute and the concentration of solute in the bulk cannot be considered to be zero. Moreover, if the surface of particles is covered by an amount of accessible solute, this solute dissolves preferentially and its solubility in the solvent limits the extraction. Thus, the model was later modified with respect to the effect of solubility on the extraction [87]. The concentration of the solute in the fluid is not anymore assumed to be zero, but is finite and determined by the rate of loss of solute out of the matrix. It is considered to be proportional to the concentration in the matrix at the surface and the partition

coefficient is assumed to be proportional to the solubility of the solute in the fluid. Equation (3.15) is therefore modified

$$\left(\frac{e}{x_0}\right)_{HB} = 6\sum_{n-1}^{\infty}\frac{\left(\frac{hr}{a_n}\right)^2}{hr(hr-1)+a_n{}^2}\exp\left(\frac{-a_n{}^2 D t}{r^2}\right) \tag{3.16}$$

where *hr* is the parameter depending on the flow rate, particular matrix and solute, its solubility in the fluid and the temperature and a_n are roots of the equation

$$a\cot(a) = 1 - hr \tag{3.17}$$

For high values of *hr* the model converges to the simple hot ball model (eq. (3.15)) and the lower the value of *hr* is, the larger solubility limitation occurs during the extraction process (Figure 3.2).

3.4 Comparison of hot ball model and Villermaux approximation

Comparison of hot ball model, Villermaux approximation and modified hot ball model is given in Figure 3.2. Curves are calculated for a random model system: diffusivity D_i = 5.10^{-14} m^2/s, particle diameter r = 0.5 mm. Number of terms n used for sum calculation in hot ball models affects the curve shape at the very start; in the case of simple hot ball model, the higher value of n, the closer the extraction yield is to zero at t = 0. In all calculations in this work, the value of n = 1000 was employed.

Unlike the approximation of Villermaux, the curve predicted by the simple hot ball model is steep at the beginning; this predicted initial velocity is progressively slowed down when modified hot ball model with decreasing *hr* is applied. Therefore, the value of D_i evaluated from the beginning of the experimental curve by the approach of Villermaux will be always much higher that the one issued from the simple hot ball model fit for the same experimental data; the extraction curve should be treated as complete as possible.

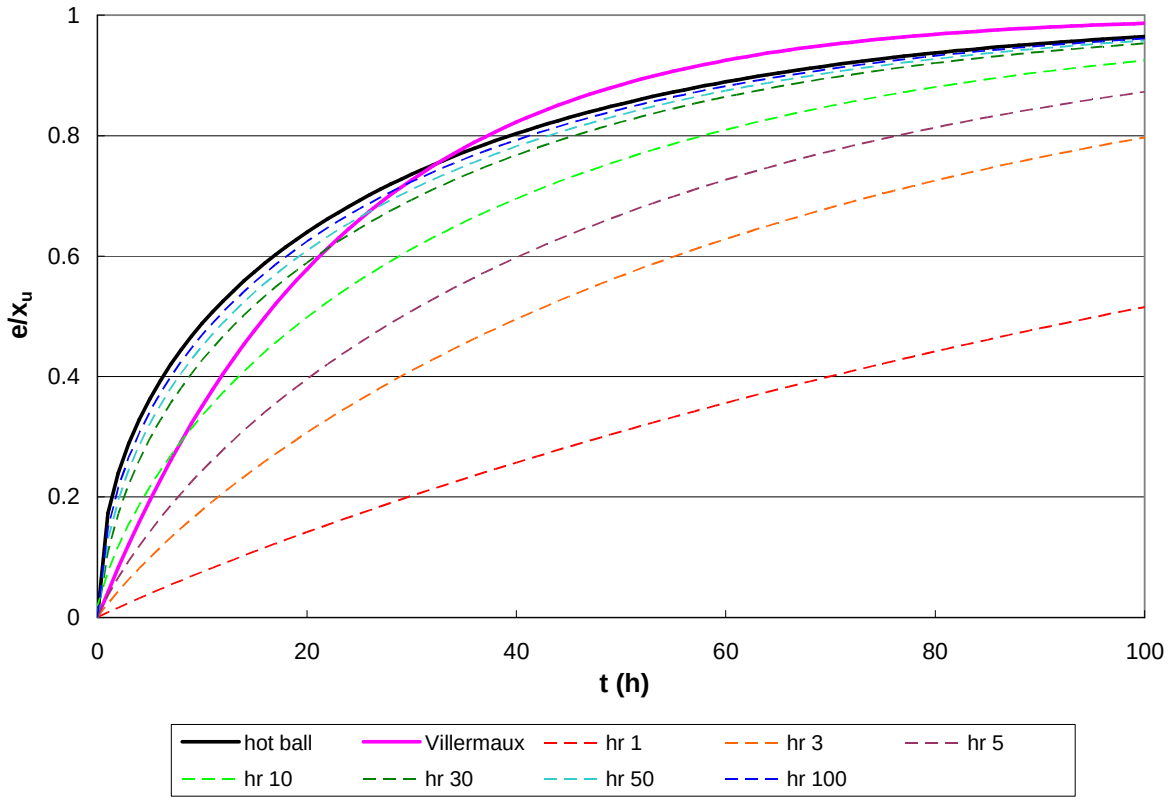

Figure 3.2. Comparison of models applied for extraction of whole beans. (Data calculated with Matlab using eqs. 3.13 – 3.17)

4. RESULTS AND DISCUSSION

4.1 Impact of seed structure modification on SCO_2 extraction

Three types of seeds were tested in this work: amaranth seeds, soybeans and green coffee beans. Experimental data can be found in Annexe 1 (enclosed on the CD support).

4.1.1 Amaranth seeds

Amaranth seeds are small and protected by a rigid hull which is difficult to remove. When treating whole seeds by DIC process the hull stayed compact (whether the seeds were moistened before the treatment or not), and negligible yield of subsequent extraction was observed. To obtain the amaranth oil, hard seeds have to be disintegrated; as the seeds resisted to a coffee grinder, we used a poppy seed mill and obtained a very fine powder where majority of the oil was deliberated and then extracted in the fast linear period. Therefore, in such case, mechanical destruction of seeds seems to be the most efficient pretreatment technique, and no further enhancement of extraction rate can be brought by the DIC pretreatment.

4.1.2 Soybeans

Note: Samples of non-treated beans and DIC-treated beans were prepared as described in chapter 2. In section 4.1.2, if not stated otherwise, the term “DIC treatment” means the treatment for 1 minute at 0.3 MPa followed by 2 minutes at 0.7 MPa.

4.1.2.1 Porosity and pore-size distribution

Scanning electron microscope (SEM) was employed to examine the internal structure of soybeans (Figure 4.1). In comparison to non-treated material which is rather compact and homogeneous, the internal structure of the DIC-treated material is substantially destroyed by the bursting moisture evaporation during the DIC treatment (see micrographs *a* and *c*). The largest pores of order of magnitude from 1 mm to 0.01 mm represent about 19 % of the seed cross-section area (estimated graphically from the micrograph *c* using a grid).

Non-homogeneities in structure destruction can occur as seen on micrograph *d*, which represents a dry soybean treated by DIC at 0.2 MPa for 4 minutes. This can be caused by position of beans in the reactor bed or by varying permeability of bean surface to the vapour. When a bean is soaked with water before the DIC treatment and hence the moisture is homogenously distributed in the bean, occurrence of these irregularities is reduced. On the other hand, the soaking of beans does not visually change the inner structure, as seen when comparing micrographs *a* and *b*, and has no influence on the final extraction yield, as will be shown further.

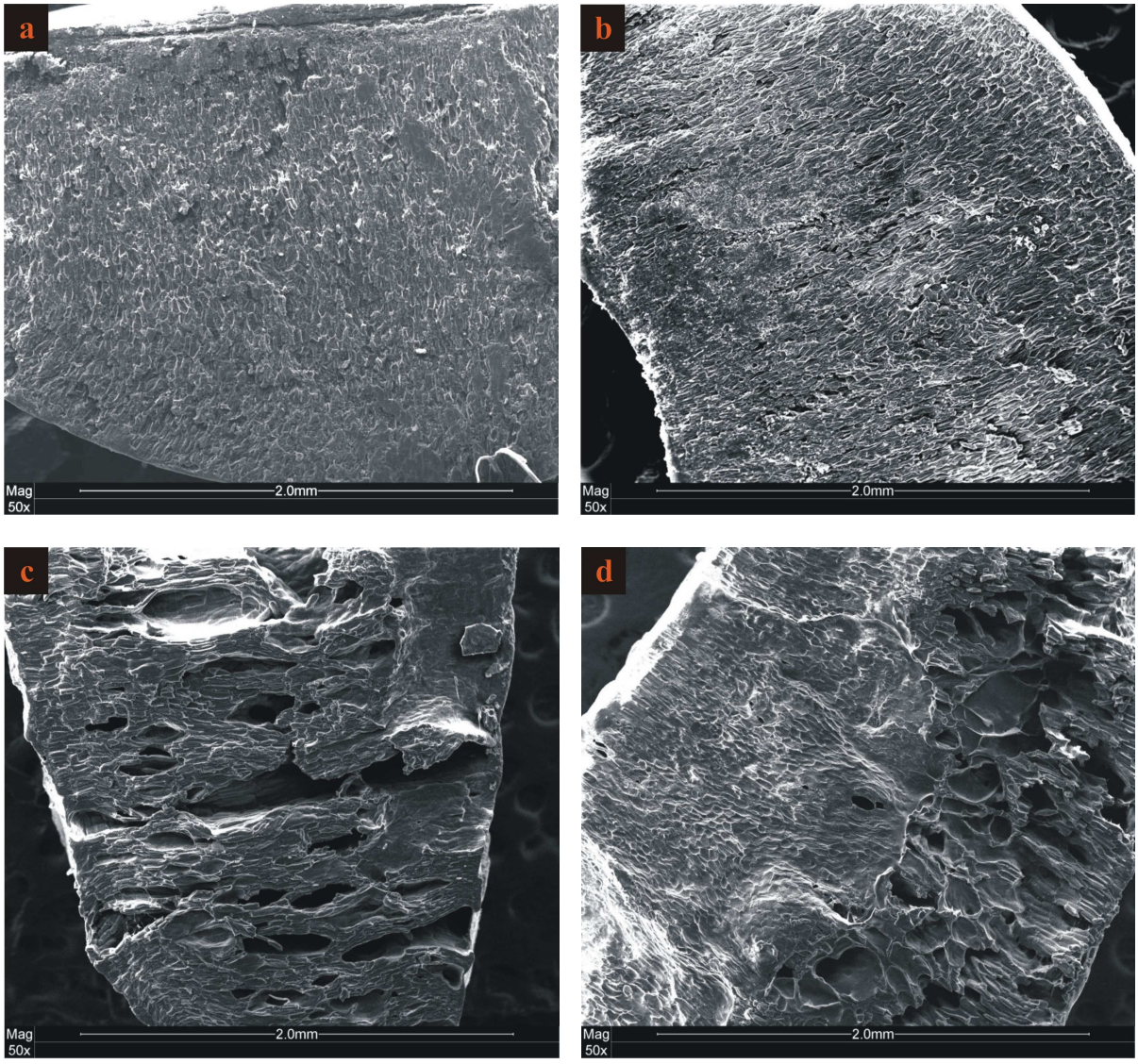

Figure 4.1. SEM micrographs (50x). (a) non-treated soybean, (b) non-treated soaked soybean, (c) soybean treated by DIC at conditions stated in 2.2.3, (d) soybean treated by DIC at 0.2 MPa/4 min.

The mercury porosimetry and helium pycnometry were used consequently to evaluate pore size distribution of smaller pores (less than 50 μm) and material density (Table 4.1).

Table 4.1. Density and porosity of raw soybeans and soybeans treated by DIC (1 minute of treatment at 0.3 MPa followed by 2 minutes at 0.7 MPa)

	bulk density ρ_s (g/cm^3)	**skeletal density ρ_{sk} (g/cm^3)**	**percentage of small pores ($1 - \rho_s / \rho_{sk}$) (%)**
non-treated beans	1.218	1.243	2.1
DIC-treated beans	0.903	1.124	19.6

Good reproducibility of the pore-size distribution curves for both cases of treated and non-treated material is evident from Figure 4.2. Both distribution curves are bidispersive, i.e. there are two

predominating sizes of pores: the smaller ones of the radius about 100 nm and the larger ones of 5-50 μm. The smallest pores of radius less than 10 nm were not influenced by DIC treatment but the number of larger pores grew considerably. The increase was about tenfold for 100 nm pores and even thirtyfold in the case of pore radius about 10 μm.

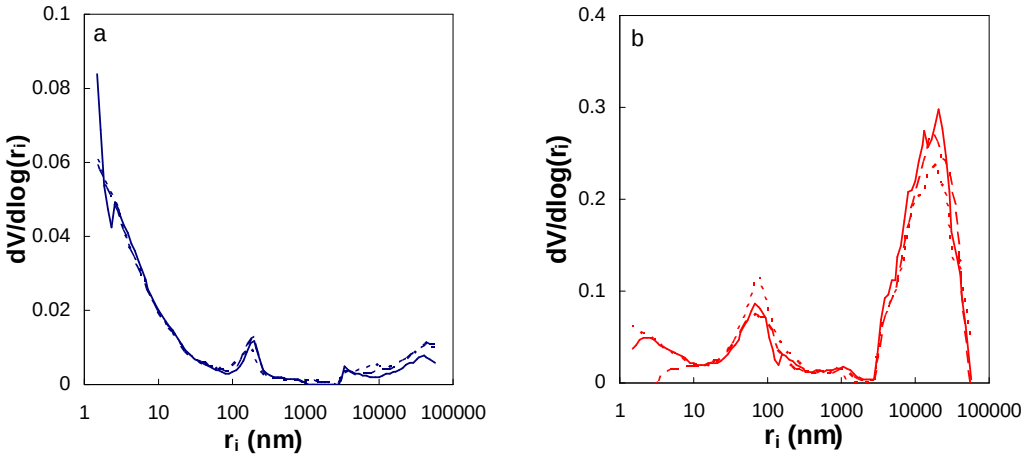

Figure 4.2. Pore-size distribution curves (r_i: pore radius). (a) non-treated soybeans; (b) DIC-treated soybeans.

This trend however cannot be generalized because the DIC treatment results in different structure modification depending on material internal structure and conditions of the treatment.

The structural changes of beans caused by DIC treatment manifest themselves by particle size distribution obtained by sieve analysis. In Figure 4.3a, particular distributions of several samples or sample mixtures are presented. Reproducibility of the grain size analysis was tested on a DIC treated sample (Figure 4.3b); the average deviation from the mean value was found 7.8 %. Although all samples were milled using the same conditions of milling, the DIC-treated milled material consists of smaller particles than the non-treated material. Especially the particles larger than 1 mm are practically missing in the DIC-treated material whilst in the non-treated material they represent more than 10 wt.%. Changes in rheological properties of the material make soybeans treated by DIC more porous and brittle in comparison with tough and more compact raw material. Therefore, they can be milled more efficiently.

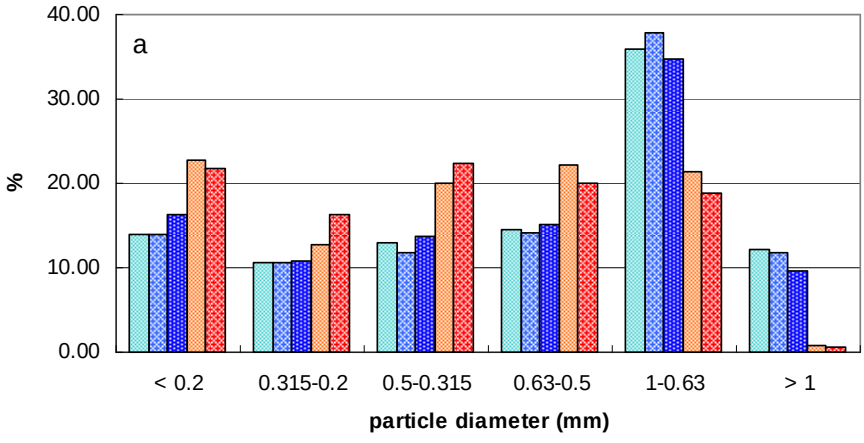

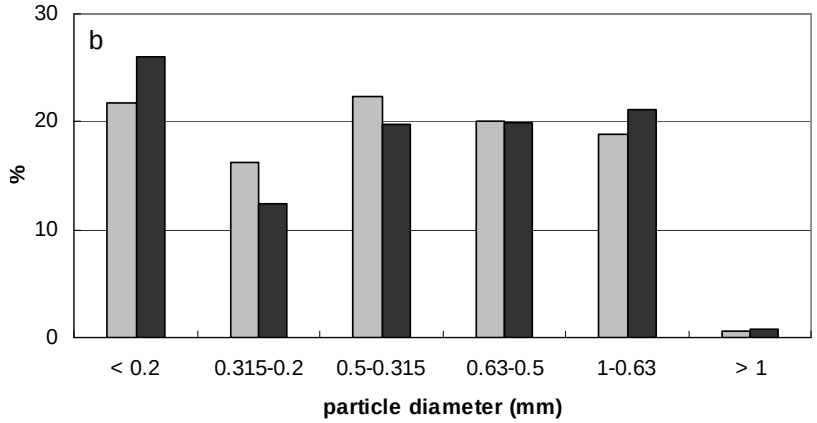

Figure 4.3. Particle size distribution. (a) comparison of non-treated beans (blue columns) and DIC-treated beans (red columns); (b) reproducibility of grain size analysis.

4.1.2.2 Extraction yield and kinetics

Solvent extraction

Total extraction yield was determined by Randall extraction with hexane. Experiments were tripled, average value was found 0.193 kg/kg raw beans for non-treated samples and 0.222 kg/kg raw beans for DIC-treated samples; therefore, there is an increase in extraction yield caused by the DIC process. This increase is related to the internal structure modification; it can be observed in the case of SCO_2 extraction as well, as shown further.

Supercritical extraction

Extraction data were obtained as a set of experimental points (Q, E), where E is the mass of extract obtained with the mass of solvent Q. To compare experiments with different solid feed N, dimensionless extraction yield e was plotted (Figure 4.4) against the dimensionless amount of solvent q.

$$q = \frac{Q}{N}; \qquad e = \frac{E}{N} \tag{4.1}$$

Figure 4.4 shows extraction data for milled (a) and whole (b) soybeans. Although the measurements were being performed within time space of 10 months, oil content in beans was not affected by the storage as proved by several repeated extraction runs.

Good reproducibility was reached in the case of milled beans. In the case of whole beans, differences in curve shape are more obvious and even emphasized due to the picture scale. Experimental error is caused partly by the extraction apparatus; there is a small irregular hold-up of oil in the micrometer valve, which affects the weighed amount of oil collected in the U-tube. Unlike milled beans, from which large amounts of extract are obtained and the hold-up is negligible, the small yields from

the whole beans are more burdened with this error. Moreover, biological tissue is not a homogeneous material, and particular solute content and distribution through a plant part may vary.

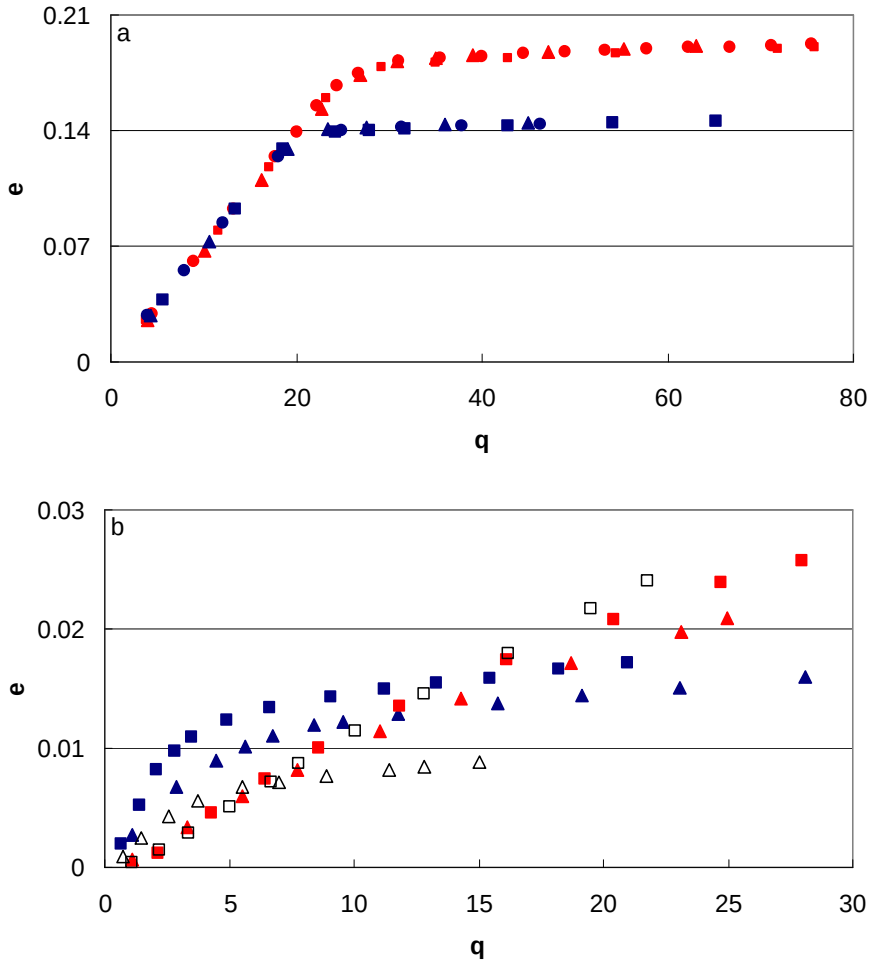

Figure 4.4. SCO_2 extraction of milled (a) and whole (b) soybeans. Blue points - non-treated beans; red points - DIC-treated beans; open points - impact of soaking.

Extraction data of milled material (Figure 4.4a) has a standard shape, which distinguishes fast and slow extraction period. Whole DIC-treated beans curves (Figure 4.4b) describe only the slow extraction period, as expected, because the beans were not disintegrated thus no accessible oil was supposed to be on their surface. On the other hand, non-treated beans curves consist of the two periods. The initial fast extraction is probably due to a small amount of easily accessible oil on the surface of decorticated beans. The oil would be surely wiped off during DIC treatment and therefore the extraction data of DIC-treated material correspond only to the slow extraction period.

As already reported, soybeans were soaked in water before the DIC treatment to obtain a homogenously moisturized sample and hence to improve the effect of the instantaneous pressure drop. As reported by open points in Figure 4.4b, the swelling has no significant impact on the extraction rate, which corresponds with negligible structure change (Figure 4.1 a, b). The curve of non-treated beans shows lower content of easily accessible oil on the surface; a part of oil was

probably washed out by water during the soaking. No acceleration of extraction rate is observed on the slow part of the curve, in contrast to DIC-treated beans (the slight variance between the two set of points corresponding to DIC-treated beans is within the limits of experimental error). Although there is no obvious improvement of extraction by swelling, it has an indirect positive effect, because the added moisture improves the homogeneity of the effect of the DIC treatment.

Model with broken and intact cells

Determination of model constants:

When applying the BIC model, particles are assumed to consist of a compact core covered with a layer of oil. Their internal porosity is not taken into account; therefore, to characterize the core, bulk density value from Hg porosimetry was used instead of skeletal density.

Similarly, void fraction is based only on the position of particles in the extraction bed, not accounting for the pores opened to the surface, for simplification. Void fraction was calculated as described in chapter 2; measurements were tripled, the average values are listed in Table 4.2.

To express mean particle size of a sample, Sauter mean diameter (i.e. the diameter of ideal sphere with the volume/surface ratio equal to the one of the particles) is calculated as

$$d_{32} = \frac{1}{\sum_{i=1}^{n} \frac{f_i}{d_i}} = 6\frac{V}{A} \tag{4.2}$$

where n is the number of fractions f_i of particles with diameter d_i , V and A correspond to particles volume and surface, respectively.

In the case of milled samples, d_{32} was calculated from their particle size distributions. To calculate the mean diameter of whole beans, we assumed that the surface and the volume of a halved soybean correspond to hemi-ellipsoid

$$V = \frac{4}{6}\pi a^2 c$$
$$A = \pi a^2 + \frac{\pi a c}{e}\sin^{-1} e + \pi a c \quad ; \quad e = \sqrt{1 - \frac{a^2}{c^2}} \tag{4.3}$$

A set of 20 beans was used to gain average values of dimensions a and c, for both non-treated and DIC-treated beans. Samples were considered to consist purely of halved beans; presence of fragments and whole beans was neglected.

A value of oil content in beans (x_0) was fixed the same in all calculations; however, generally, the choice of total amount of extract is debatable. The value depends strongly on technique of extraction, solvent used for the extraction and the pretreatment of material. This shows up also from comparison of hexane extraction yields for raw beans and DIC-treated beans (see above, solvent

extraction). Assuming that in both cases, the extraction was efficient enough to extract the most of soluble compounds, we see that "total" oil content corresponding to DIC-treated beans exceeds the "total" value for raw beans. As the supercritical extraction data tend to lower yields than those obtained by Randall extraction, we preferred to use in our models asymptotic values of exponential curves fitted on the slow period of extraction data. The average asymptotic values for non-treated and DIC-treated samples were found 0.145 and 0.205 kg oil /kg of raw beans respectively. The value corresponding to DIC-treated beans was used in our calculations and it was assumed that all extractions would gradually reach this "maximal" oil content. However, it must be pointed out, that this value results from particular DIC conditions used in this work and should not be generally considered as absolute oil content.

The oil solubility 0.007 g/g CO_2 was used in all calculations, it was obtained from correlation of del Valle and Aguilera [120]

$$y = [\exp(40.361 - 18\,708/T + 2\,186\,840/T^2)(0.001\rho)^{10.724} \pm 2.7]/\rho \qquad (4.4)$$

Carbon dioxide density ρ = 899.3 kg/m^3 was calculated using Altunin and Gadetski equation of states [121] for extraction pressure 28 MPa and temperature 313.15 K.

Table 4.2. Constants of soybeans applied for modelling

		ρ_s (g/cm^3)	ε (-)	x_0 (kg/kg beans)	y_r (kg/kg CO_2)	d_{32} (mm)
milled beans	**non-treated**	1.218	0.57	0.205	0.007	0.34
	DIC-treated	0.903	0.45			0.26
whole beans	**non-treated**	1.218	0.42			2.88
	DIC-treated	0.903	0.47			3.67

Data evaluation

Slopes of linear part of extraction curves were evaluated and compared with the solubility value. In the case of milled beans, the slopes of the linear part of extraction curves were close to 0.006 g/g of CO_2, which is within the interval given by eq.(4.4); hence the solution in the extractor was almost saturated due to relatively large residence times (at the flow rate of expanded CO_2 of 0.5 l/min, superficial velocity at given SCO_2 density in the small extraction column is about 2.2 cm/min). In the case of non-treated whole beans, the average slope of the linear part of extraction curves was only 0.0034 g/g CO_2; this can be explained by a substantially decreased contact surface of whole beans in comparison with milled beans. Mass transfer parameters are given in Table 4.3.

Table 4.3. BIC model coefficients for extraction of soybeans

		$k_f a_0$ (1/s)	r_b (-)	$k_s a_0$ (1/s)	k_s (m/s)	^aD_i (m^2/s)
milled beans	**non-treated**	$1.7.\ 10^{-2}$	0.67	$4.3.\ 10^{-6}$	$5.6.\ 10^{-10}$	$1.9\ .\ 10^{-14}$
	DIC-treated	$2.8{\cdot}10^{-2}$	0.85	$2.6.\ 10^{-5}$	$2.1.\ 10^{-9}$	$5.3\ .\ 10^{-14}$
whole beans	**non-treated**	$3{\cdot}10^{-4}$	0.058	$5.8.\ 10^{-7}$	$4.9.\ 10^{-10}$	$1.4\ .\ 10^{-13}$
	DIC-treated	-	0	$3.4.\ 10^{-6}$	$4.0.\ 10^{-9}$	$1.5\ .\ 10^{-12}$

a – D_i calculated using eq.(3.14)

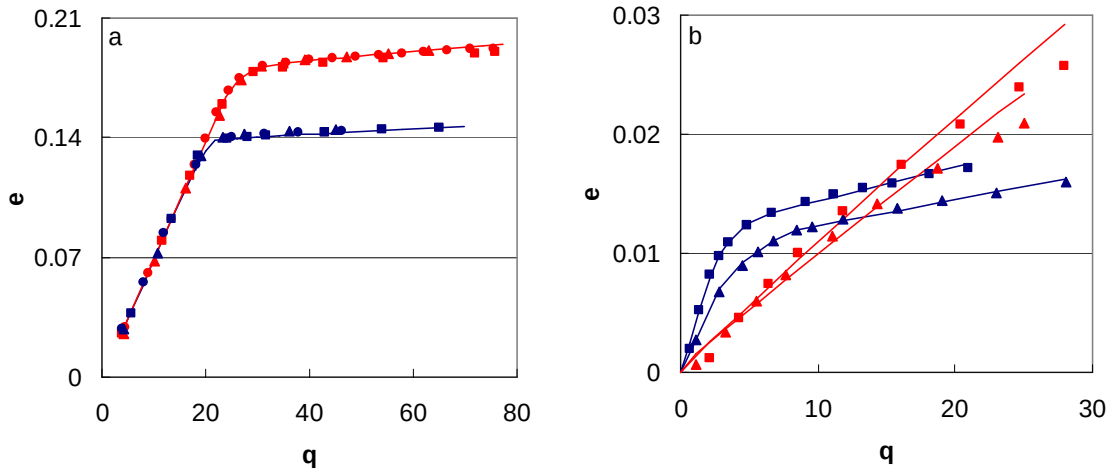

Figure 4.5. Extraction curves of non-treated (blue points) and DIC-treated soybeans (red points) fitted by BIC model: (a) milled beans, (b) whole beans.

The volumetric external mass transfer coefficient $k_f a_0$, describing the mass transfer from the layer of extracted oil on the surface of particles during the fast extraction period, does not change substantially by DIC treatment. The slight increase is probably related to the increase in the surface of the particles in the case of DIC-treated material (see below). The value of $k_f a_0$ is irrelevant in the case of whole DIC-treated beans because only the slow extraction period occurs.

Concerning the second extraction period, a large difference can be seen between the non-treated and DIC-treated material. The volumetric internal mass transfer coefficient $k_s a_0$ is substantially increased by the DIC treatment. This parameter however depends on particle size. The specific surface area is expressed as

$$a_0 = \frac{1-\varepsilon}{l} \tag{4.5}$$

and characteristic particle dimension l is for a spherical particle of diameter d equal to $d/6$. The Sauter mean diameter was used and the internal mass transfer coefficient k_s was calculated from the volumetric coefficient according to

$$k_s = k_s a_0 \frac{d_{32}}{6(1-\varepsilon)} \tag{4.6}$$

The k_s values in Table 4.3 show acceptable agreement between milled and whole beans, both for non-treated and DIC-treated material. The mass transfer is about six times faster than in the case of non-treated material. This improvement of extraction kinetics by DIC treatment is in agreement with the increased porosity of the material as discussed above, because the penetration of the solvent into the material as well as the extraction of solute out of the material is easier. The importance of the largest pores for extraction kinetics decreases with increasing degree of disintegration of the vegetable material as the large pores are destroyed by milling. The size of particles is mostly smaller than 1 mm after milling (Figure 4.3a). As the extent of the improvement is similar for milled and whole beans, we can conclude that micropores are much more important for the extraction kinetics improvement than large pores.

The increase in the volumetric fraction of broken cells r_b corresponds to the results on particle size analysis showed above, because the volumetric fraction of broken cells and the amount of easily accessible oil in milled material increases with decreasing particle size. Evidently, the value of parameter r_b is strongly influenced by the grinding whose reproducibility must be guaranteed in order to provide reproducible extraction results. Individual size fractions obtained by sieve analysis could serve for the extraction as material of defined and reproducible particle size. However, in thecase of material rich in oil, as soybean is, there is a risk that a part of easily accessible oil on particle surface will stick to the sieves. To avoid a decrease in extraction yield reproducibility, we chose not to sieve the material before the extraction.

In the case of whole beans, each experimental run was fitted by the BIC model separately (Figure 4.5b) because of slight differences between extraction data. Despite the differences, trend of both curves is obvious. Whilst the curves corresponding to DIC-treated samples are rather linear, curves corresponding to non-treated material show similar shape as for the milled material. Average values of mass transfer parameters are listed in Table 4.3. Better agreement of the BIC model with experimental data was reached in the case of non-treated material than for the DIC-treated one.

Using the approximation given by eq. (3.14) and supposing that the extracted particles are spherical, the internal diffusivity was calculated from the mass transfer coefficients evaluated for the slow part of the extraction curve (Table 4.3, Villermaux). The difference of approximately one order of magnitude can be seen between the D_i values for milled and whole beans. The mass transfer coefficient k_s which varies only slightly for milled and whole beans Thus, the mass transfer coefficient is a better characteristic of the mass transfer from beans than the diffusivity. With respect to the fact that the value of diffusivity for a rigid cellular tissue is reported to be in the range of orders of magnitude from 10^{-14} to 10^{-13} m^2/s it is obvious that the values calculated for DIC-treated whole beans are too high. This difference in D_i is probably caused by inaccurate description of the initial part

of extraction curve, simulated in the case of whole beans, by the simplified relationship derived by Villermaux. [122]. Besides, the whole beans are not ideal spheres as assumed. The surface of beans after the DIC-treatment is not smooth and their efficient interfacial area is therefore larger than would correspond to measured value of d_{32}.

Hot ball model

To fit better the extraction data of whole beans, where the extraction is controlled predominantly by internal diffusion, we applied the hot ball model, based on diffusion in a spherical particle.

DIC-treated beans

Extraction data of whole beans treated by DIC were fitted by both simple and modified hot ball models using equations (3.15) and (3.16) and diffusion coefficients were found by the least square method. When modified hot ball model is applied, the coefficient *hr*, representing the solubility restriction to the extraction from the particle, is to be found so that the model curve shape is close to the shape of plotted extraction points. Applying the value of *hr* in the range from 1 to 60, a set of diffusion coefficients was evaluated for a fixed value of *hr* by fitting the data with the modified hot ball model. The best fit was achieved with the value of *hr* = 25 for both curves, average value of corresponding D_i is presented in Table 4.4. and Figure 4.6.

In view of results, the simple hot ball model (eq.(3.15)) is discarded for further use, because it does not provide a satisfactory fit. It is probably due to the fact that the model simplifies the system when assuming the concentration at the bulk to be zero. Hence it predicts the curve shape corresponding to a fast extraction at the beginning (which is not slowed down by any solubility limitation), followed by a decelaration. Our data, however, do not demonstrate any fast extraction at the very start.

Concerning the difference between values evaluated by hot ball models and value issued from the approximation of Villermaux, we can refer to the comparison of models in Figure 3.2.

Table 4.4. Coefficients evaluated for whole soybeans with hot ball model

	$^{a}D_i$ (m^2/s)	$^{b}D_i$ (m^2/s)	m (kg/s. kg CO_2)	r_b (-)
non-treated beans	---	$2.2 \cdot 10^{-14}$	0.00067	0.048
DIC-treated beans	$1.1 \cdot 10^{-13}$	$3.9 \cdot 10^{-13}$	---	---

a – D_i calculated from simple hot ball model, eq.(3.15)

b – D_i calculated from modified hot ball model, eq.(3.16)

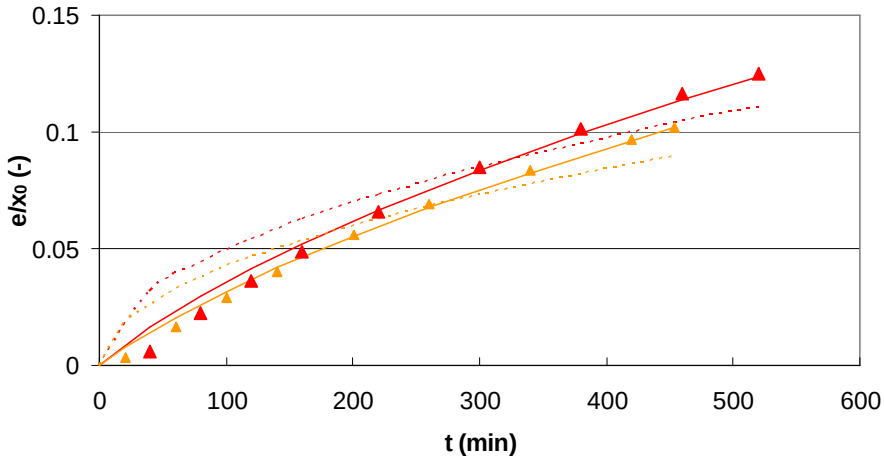

Figure 4.6. Extraction yield of DIC-treated samples (▲) fitted by simple hot ball model (--) and modified hot ball model (–).

Non-treated beans

The initial shape of extraction curves for non-treated beans indicates a fast extraction of a small amount of oil present probably on particle surface. We assumed that its extraction occurs simultaneously with the slow diffusion from the particle described by eq. (4.7), until it is depleted. Thus, the initial part of extraction curve as function of time is assumed to be a straight line with the slope m equal to the product of equilibrium concentration of the solute in the solvent y^* and the specific flow rate q'. The two parts of the curve were described as

$$\begin{aligned} \frac{e}{x_0} &= y^* q' t = m\, t \qquad && for \quad m \cdot t \le r_b \\ \frac{e}{x_0} &= \left(\frac{e}{x_0}\right)_{HB,m} + r_b \qquad && for \quad m \cdot t > r_b \end{aligned} \tag{4.7}$$

Optimal value of hr = 64 was found for both curves and diffusion coefficient D_i (Table 4, hot ball) was evaluated together with m and r_b by fitting the calculated curve to the experimental data.

To conclude, the values of diffusion coefficients evaluated by the modified hot ball model correspond better to D_i determined for the milled beans than those given by the approximation of Villermaux. The diffusivities for non-treated beans are very similar, the diffusivity for the whole DIC-treated beans is too large but after compensation for rough bean surface it would decrease. To describe the extraction from non-disintegrated beans, the modified hot ball model is more appropriate than the BIC model.

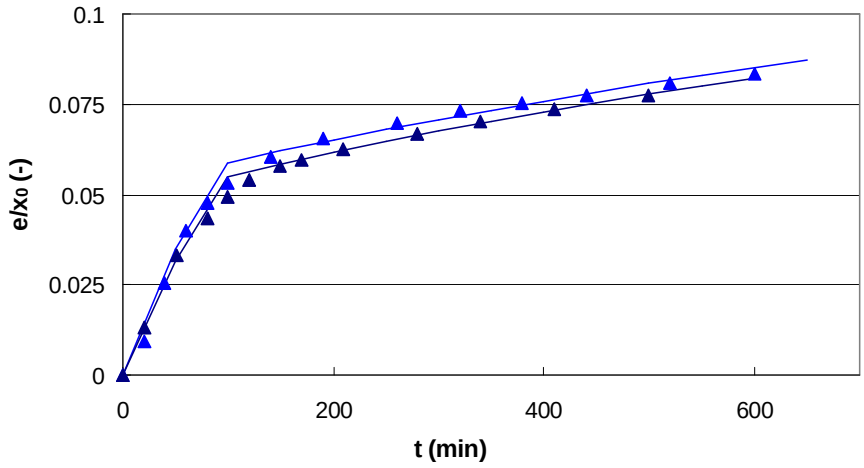

Figure 4.7. Extraction yield of non-treated samples (▲) fitted by the modified hot ball model (–).

4.1.2.3 Impact of DIC conditions on the extraction rate

The impact of DIC conditions on the extraction rate was tested on a set of 8 experiments. Samples were treated at conditions stated in the picture in Fig 4.8, initial humidity of samples were kept the one of the raw material. As a different batch of soybeans was treated here, extraction yields are slightly higher than those found in previous experiments. (Experimental points are interlined here just to better distinguish curves shapes to guide the eye, no model was applied.)

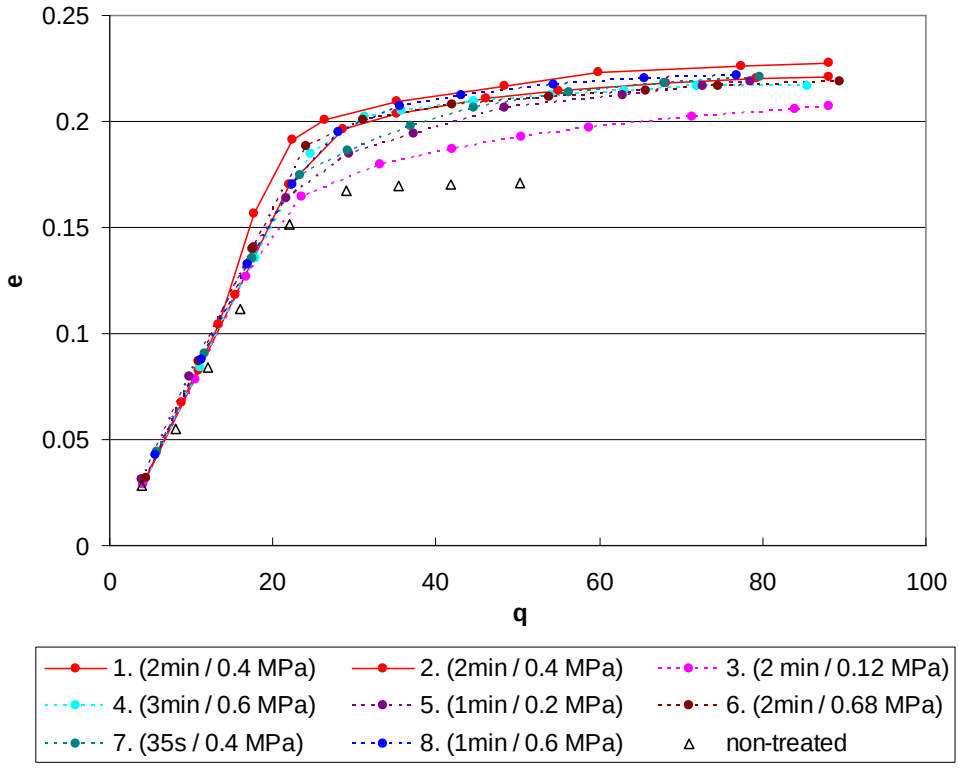

Figure 4.8. Impact of DIC conditions on the extraction rate.

Although the effect of changes in conditions of the DIC process on the extraction yield has been reported previously [123], our results could not confirm or disprove this fact. In comparison with non-treated beans, we can see the same enhancement in extraction rate as reported above for milled beans. However, if we estimate the experimental error from a comparison of two red curves corresponding to samples treated at same conditions, differences between two random curves are mostly not significant enough. Moreover, comparing sample 4 and 7 which can be considered to be treated at limiting conditions within the set of experimental runs, we can see practically no difference in the slope of the slow extraction period; it is improbable.

Thus, there is probably a coupling of experimental errors of the two used installations that made impossible the deeper study of this part of work. Nevertheless, we can state that

- for all applied conditions of DIC process, the extraction was enhanced in comparison with the raw material;
- although an effect of pressure on the extraction yield was not proved, there is an obvious increase in extraction yield in the pressure range from 0.2 to 0.68 MPa.

4.1.3 Green coffee beans

4.1.3.1 Moisturizing of coffee beans

In order to extract caffeine from coffee beans, the beans are moisturized before the extraction, because there are several limitations to the use of pure carbon dioxide for this purpose. As the pure supercritical CO_2 is not able to extract polar compounds, a polar modifier must be used to do that. Caffeine is a polar compound and it has been proved that the presence of water in the system coffee beans-SCO_2 increases the extraction yield. Moreover, it is well known that when extractions are carried out with organic liquid solvents, the material is soaked and moistened by the solvent which enables better diffusion of extracted compounds through cell walls; but on the other hand, any similar effect does not occur when the supercritical CO_2 is used as a solvent. Mass transfer through the cell walls in this case is substantially slowed down. The permeability of cell walls increases when water is added to the system SCO_2-coffee; diffusivity values in such a system differ from those of caffeine in pure water barely of about one order of magnitude [124]. Caffeine diffusion coefficient in SCO_2 has been studied by several authors, it varies around 10^{-10} m^2/s for moistened whole beans. However, polarity and bad permeability are not the only obstacles to caffeine extraction from coffee beans; even more polar methylenchloride, used as a solvent, is not able to extract the caffeine from dry whole beans, the extraction is feasible only from moistened beans. McHugh and Krukonis claimed that water added to a coffee bean disrupts chemical bonds bounding caffeine in a chlorogenic acid structure present in the bean [49]. To prove that these bonds decrease activity of caffeine, authors compared a theoretical amount of solvent necessary to extract all the caffeine from beans (knowing the solubility of caffeine at given conditions) with a real value issued from experiments; the real amount was higher

than the theoretical one, which proved that the caffeine bounded in beans does not dissolve as much as the free caffeine in water.

In practice, the green coffee beans are soaked in water before extraction, the water content varies from 40-50 wt.%. Peker et al. [124] reported that the water content in beans increases with time of soaking until it reaches a value of around 40 wt.% (corresponding to about 12 hours of soaking), further soaking does not change the water content substantially. To prevent a depletion of water when long extractions are carried out, the supercritical CO_2 entering to the extractor can be moistened as well. In our experiments, both whole and milled beans were moistened before the extraction so that the water content reaches 20 wt.% (value based on raw beans; recalculated to dry matter, the humidity is about 27%, as initial humidity in raw beans was found 9.7% (drying kiln at 105°C, 24 h)). Water coming out from the extractor does not cumulate in the extract, but it is leaving with the gaseous CO_2. The water solubility in SCO_2 at given conditions (24MPa, 50°C) is 2.9 mg/g CO_2, but as stated by Reverchon et al. [125], the real amount of water leaving the extractor is smaller than it theoretically should be. The authors found that the water content in the extract of sage was independent on the size of extracted particles and its extraction curve as function of specific solvent flow rate is linear (unlike the curve corresponding to oil extraction and depending on the extraction rate), thus, some kind of bonding between water and the matrix influences probably the final equilibrium concentration of caffeine in SCO_2. If we take into account this conclusion, we can state that the water content of 20% as used in this work was sufficient regarding to the amount of solvent consumed for both whole and milled beans. All experimental data in this work (i.e. extraction yields) were related to mass of raw (non-soaked) beans and used for the modelling under this form as well.

4.1.3.2 Porosity and pore-size distribution

Coffee bean is not as compact as soybean; the tissue is somehow rolled inside the bean, creating cavities within the bean. When contacted with moisture, the bean tissue swells up and fills these cavities. However, unlike soaked soybeans, there is no increase in particle size, as can be seen when comparing Sauter mean diameters of raw (non-soaked) beans and DIC-treated (soaked) beans (see Table 4.6, the value of d_{32} for DIC-treated beans was found even slightly lower than for raw beans, but this difference is just an experimental error due to the choice of the representative sample; in fact, the bean does not “shrink” when it is soaked). Roethe et al. [126] carried out an analysis of raw and soaked beans by scanning electronic microscope, and they concluded that the transport of caffeine dissolved in the water inside the coffee beans is realised predominantly through cell walls and only about 3% of the mass transfer take place in pores.

As issued from porosimetry results (Figure 4.9), the porosity increased remarkably on the level of very small pores, however, these pores are not significant for the extraction rate increase. On the other hand, the number of large pores (5-50 µm) did not increase by the DIC process. It should be emphasized that in accord with Hg porosimetry rules, the beans were dried before the porosity

measurement; therefore, regarding to conclusions about soaking stated above, however important the increase in porosity after the DIC process is (especially when very small pores are concerned), it probably looses its importance at the moment when the beans are soaked in water.

Table 4.5. Density and porosity of extracted coffee beans

	bulk density ρ_s (g/cm^3)	**skeletal density ρ_{sk} (g/cm^3)**	**percentage of small pores ($1 - \rho_s / \rho_{sk}$) (%)**
non-treated material	1.246	1.337	0.68
DIC-treated material	1.117	1.099	~ 0

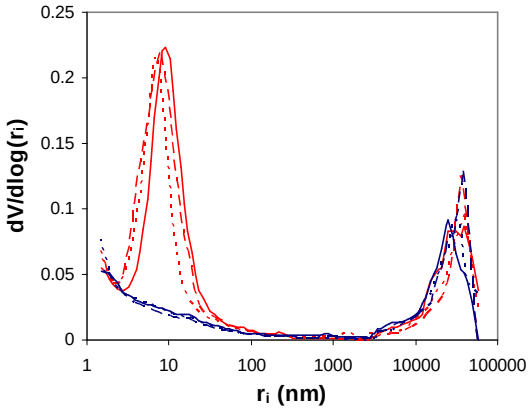

Figure 4.9. Green coffee beans non-treated (---) and treated by DIC at 0.5 MPa/45 s (---).

Unlike the soybeans, milled coffee beans samples were prepared by sieving the milled material in order to obtain well defined particle size distribution in all samples. The ratio was settled as follows: 10% fraction of particles >0.63mm, 40% fraction of 0.63-0.5mm, 30% fraction of 0.5-0.315mm a 20% fraction of 0.315-0.2mm in diameter.

4.1.3.3 Extraction rate and caffeine analysis

Unlike the soybean extracts, consisting of vegetable oil in the case of both milled and whole beans (the composition was not analysed in detail, but visually, there was no difference between extracts), coffee beans do not give the same result. Although the extract from milled beans was oily, similar to the soybean oil with addition of green pigments, in the case of whole beans, a white powder was obtained. In view of the fact that supercritical extraction of whole green coffee beans had been described in the literature as highly selective for caffeine (and the green coffee beans treatment is the most important industrial application of SCO_2 extraction), an HPLC analysis of caffeine content in our extracts from milled and whole beans was carried out as well, beside the total extraction yield observation.

Milled beans

Extraction curves of milled beans (Figure 4.10) have a characteristic shape corresponding to fast and slow extraction period; the BIC model was applied to describe the extraction rate. The same methods were used to evaluate material constants as for soybeans. Solubility of the extract in SCO_2 at given conditions (24MPa, 50°C) is in the range of 0.002 – 0.008 kg/kg CO_2 (calculated with the correlation proposed by del Valle, eq. 4.4), average value of 0.005 kg/kg CO_2 was chosen for the modelling; this value corresponds to average slope of linear extraction period of our extraction curves as well.

Table 4.6. Constants of coffee beans applied for modelling.

		ρ_s (g/cm3)	ε (-)	x_0 (kg/kg beans)	y_r (kg/kg CO_2)	d_{32} (mm)
milled beans	**non-treated**	1.246	0.66	0.102	0.005	0.48
	DIC-treated	1.117				

To give a better idea about how the extraction develops in real time, in the case of milled beans, the value of q=100 corresponds approximately to the extraction time of 300 min (this is a rough value, exaction time corresponding to a q value varies slightly as the feed of material in the extractor N is not constant for all runs (2.5-3.8 g) and $q=Q/N$). Parameters used for the BIC model are stated in Table 4.7.

Table 4.7. Model coefficients for milled coffee beans

		$k_f a_0$ (1/s)	r_b (-)	$k_s a_0$ (1/s)	k_s (m/s)	^aD_i (m^2/s)
milled beans (BIC model)	**non-treated**	$1.67.\ 10^{-2}$	0.7	$2.33.\ 10^{-5}$	$5.49.\ 10^{-9}$	$2.64.10^{-13}$
	DIC-treated	$1.67.\ 10^{-2}$	0.74	$2.67.\ 10^{-5}$	$6.27.\ 10^{-9}$	$3.01.\ 10^{-13}$

a – D_i calculated using eq.(3.14)

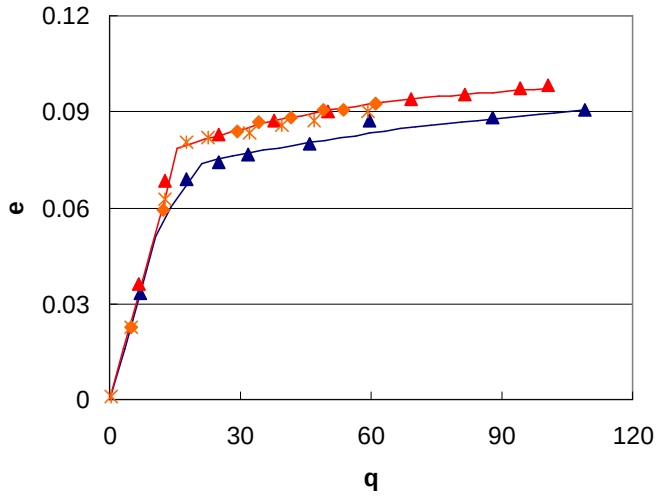

Figure 4.10. Extraction curves of non-treated (blue points) and DIC-treated (red points) milled beans, (–) BIC model.

Three extraction runs corresponding to extraction from milled beans treated by DIC are plotted in order to show a good reproducibility of extraction data. Similarly to soybeans, there is no change in coefficient $k_f a_0$, because this coefficient depends on the solubility of the free solute in the SCO_2. Neither the parameter r change significantly, as the particle size distribution was constant in all extraction runs with milled beans, anyway, it can be seen that the free solute fraction increased slightly with the DIC treatment. Next columns of the table prove the conclusion already made from porosimetry analysis results: the DIC process does not influence significantly the mass transfer in the material during the extraction.

Results of HPLC analysis shows that the final concentration of caffeine in the extract from milled beans is about 8%. Due to very small increase in extract weight between two successive points of extraction curve, we could not analyze the extract for each experimental point separately; hence, concentrations were evaluated generally for an ensemble of several successive samplings. Identically for non-treated and DIC-treated material, the first sample analysed by HPLC (i.e. corresponding to the beginning of extraction curve) is characterized by a low concentration of caffeine (order of magnitude of 10 mg/g of extract), but with the transition to the slow extraction period the concentration increases of about one order of magnitude. Obviously, the total extraction rate decreases, but the extraction of caffeine itself continues at the same velocity (see later).

Whole beans

The yields of total extract from whole beans are shown in Figure 4.11. As a larger-capacity extractor and larger feeds were applied for whole beans extraction (23.8-25.2 g), corresponding dimensionless amounts of solvent q are lower than those at milled beans extraction runs. It means that at the flow rate of CO_2 of 0.5 l/min, the value of q=10 corresponds to approximately 4.6 h of extraction.

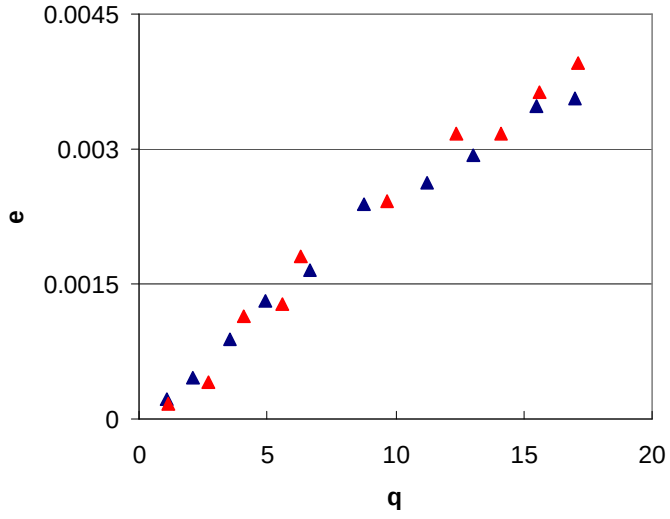

Figure 4.11. Extraction curves of non-treated (blue points) and DIC-treated (red points) whole beans.

HPLC analysis results confirmed that the caffeine represents the majority in the extract from whole beans. Unlike the milled beans the concentration of caffeine in the extract from whole beans stayed constant (order of magnitude of 10^2 mg/g of extract). Average value was found 700 ± 183 mg/g of extract, thus the result is burdened with an important experimental error caused by very small extraction yields (total amount of extract per run was about 0.9 g, extract increase between two successive experimental points was in the range of 0.002-0.02 g). There is a difference between total content of caffeine in the extract from non-treated and DIC-treated beans (61.4% and 72.6% respectively), but we consider this difference to be comparable to the experimental error explained above.

If we compare caffeine contents in extracts from milled and whole beans, we can deduce some conclusions about water influence in the extraction process. Extraction of oil from broken cells is not limited in any way by the presence of water and it proceeds in the same time as the extraction of caffeine. On the other hand, as soon as the extraction process reaches intact cells diffusion of oil through cell walls soaked with water becomes difficult and subsequently, concentration of caffeine as the main polar compound becomes more important in the total extract.

Figure 4.12 shows extraction yield of caffeine exclusively, for both milled and whole beans as a function mass of solvent (values related to raw beans feed).

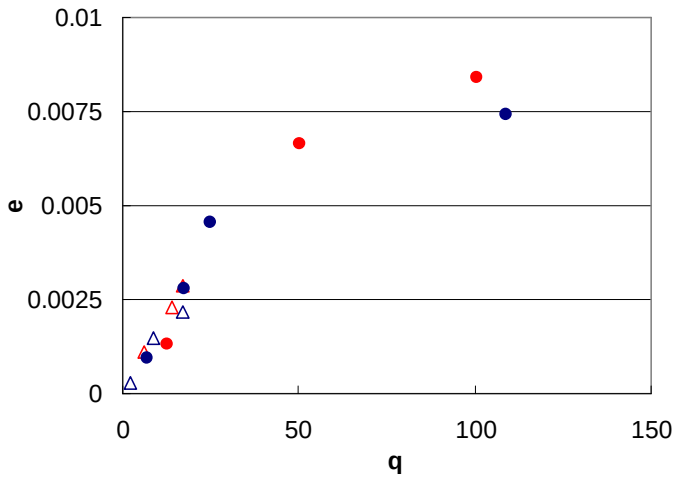

Figure 4.12. Extraction curves caffeine in non-treated (blue points) and DIC-treated (red points) beans. (●) milled beans, (Δ) whole beans.

The data for milled and whole beans samples agree very well no matter if the DIC pretreatment took place or not. There is visible decrease of extraction rate at the end of milled beans curves. This can be caused partially by the diffusion control already occurring at the end of extraction, as it is usually observed when oil is extracted from beans, but there is also the fact that the water content in beans decreases slowly during the extraction which causes the decrease in amount of caffeine extracted from beans. (Let's admit for a while, in contrast with the conclusions stated at the beginning of the chapter,

that the water is extracted from beans at the constant rate corresponding to its solubility in SCO_2; in this case, the depletion of water would correspond right to these last points of curves. Anyway, accepting the conclusions that there is an interaction of water with the matrix towards the end of the process decreasing the equilibrium concentration of water in the SCO_2, we can suppose that the material still contains some water till the end of extraction allowing the caffeine extraction, although the rate of extraction might be slowed down).

All points in Figure 4.12 follow the same trend at the beginning; this fact shows that in our case, the extraction rate of caffeine was not limited by diffusion but the process was controlled by the low solubility of caffeine in the solvent. Extraction would be controlled by diffusion if we could increase the solvent flow rate in the extractor; unfortunately, the installation we used for this work cannot assure higher flow rates.

For this reason, evaluation of diffusion coefficients was not possible, but we were able at least to estimate a partition coefficient (partition of the caffeine between the CO_2 and the water in a bean) characterising the phase equilibrium between the extracted particle and the solvent and to compare it with literature values.

The slope of the linear part of extraction curves plotted in Figure 4.12 varies in the range of $(1.4\text{-}2.0).10^{-4}$ g/g CO_2. And yet, solubility of free caffeine in SCO_2 at the same extraction conditions is of about one order of magnitude higher that this [113], therefore we can see the impact of the caffeine interaction with matrix. Peker et al. [124] described the extraction from whole beans by means of a model with only one parameter – equilibrium partition coefficient *m* defined as

$$m = \frac{caffeine\ concentration\ in\ SCO_2}{caffeine\ concentration\ in\ water\ in\ \ a\ bean} \tag{4.8}$$

This coefficient can be roughly estimated for our data as well, considering that the concentration of caffeine in SCO_2 is given by the slope of linear part of extraction curves, the concentration of caffeine in beans is about 1 wt.% and the water content is 20 wt.%.

$$m = \frac{1.6 \cdot 10^{-4}}{1/20} = 0.0032 \tag{4.9}$$

Peker et al. found values of *m* at temperature of 50°C as follows: 0.0054 for 16.5 MPa and 0.0215 for 19.3 MPa.

Another possibility to compare our data is given by the work of Roethe et al. [126] – concentration of caffeine in SCO_2 evaluated from their extraction data (extraction carried out at 20MPa and 60°C) is rather in agreement with our results, but in view of fact that they used higher water content in beans (50 wt.%) the value of partition coefficient would be about 0.01. We can conclude from these two comparisons that our results are roughly of the same magnitude as the values reported in the literature.

Solvent extraction

In view of the fact that extracts from whole and milled beans are of different character, different organic solvents were used for Randall extraction. Milled beans were extracted by hexane (which is mostly used for evaluation of oil content in seeds), whole beans were soaked with water and extracted with more polar chloroform to obtain the caffeine. Only raw beans non-treated by DIC were extracted, extraction yields for milled and whole beans was found 16.2 wt.% a 2.02 wt.% respectively (related to mass of raw beans). Asymptotic value determined from extraction curves of milled beans (10.2%) differs from the yield obtained by Randall extraction more than in the case of soybeans; it might be that a part of oil stayed stuck of sieves during the milled sample preparation. Different selectivity of SCO_2 and chloroform caused probably the yield difference in the case of whole beans.

4.1.3.4 Conclusions

Finally, we can sum up the conclusions about the DIC pretreatment and the extraction of coffee beans as found in this work. Number of pores large enough to have an influence on the extraction rate in beans does not change by the DIC treatment, moreover, as we know from the literature, mass transfer in beans takes place mostly through cell walls. Therefore, due to the soaking of beans in water applied generally before the extraction, cell walls become more permeable and the extraction is subsequently enhanced just by the soaking, without regard to the DIC pretreatment of beans.

Extract from milled beans consists of vegetable oil and coefficients of mass transfer are equal for non-treated and DIC treated beans. When whole beans are extracted, the extraction of oil becomes impossible due to the presence of water in beans tissue and the caffeine is extracted preferentially; unfortunately, we could not compare mass transfer coefficients for caffeine in whole and milled beans, because the extraction of caffeine in our experiments was limited by low solubility of caffeine in SCO_2. So even if there were any changes in the internal structure of beans, their influence could not appear in this case.

4.2 Impact of natural convection in solvent on SCO_2 extraction

The aim of this work was to introduce the method of measurement of RTD characteristic into the laboratory to be able to follow the effect of flow direction on axial dispersion in a supercritical extractor. First results and conclusions are stated in this chapter; they are not final, but will serve to development of the method and further studies of natural convection at supercritical conditions. Experimental data can be found in Annexe 2 (enclosed on the CD support).

4.2.1 Choice of the method

Benzoic acid (BA) was chosen as a tracer; fluid phase saturated with BA was injected to the extractor. BA is slightly soluble in liquid and supercritical CO_2. Thus, an input of low tracer concentration in the fluid phase gives a reasonable response of the detector, and we do not take the risk that the narrow microcuvette in the detector will be blocked by tracer precipitation if its solubility changes due to potential pressure and temperature instability. Benzoic acid had been already applied as a tracer in supercritical experiments [73].

We tested both pulse and step input. Step experiment was found to be inconvenient, because it results in higher concentrations of benzoic acid passing through the microcuvette of the detector, which we want to protect from any potential blockage. Pulse input was chosen, though it must be noted that we have not reached yet satisfactory reproducibility in concentration of pulses. The injection of the tracer is manual, by switching the dosing valve, therefore the effect of opening/closing the valve is more important shorter the injection is. Two-second injection applied in experiments at subcritical conditions was replaced by ten-second injection in supercritical experimental runs in order to eliminate the influence of the valve switching, but the reproducibility stayed low.

4.2.2 Sequence of procedures

While the thermoregulation of the test section was being constructed to allow the work at supercritical conditions, preliminary experiments at room temperature, i. e. in liquid phase (12 MPa, temperature in the range of 23 to 27°C) were carried out.

Firstly, the detector and the injection system were tested, then the flow pattern in the extractor filled with inert glass beads was observed. Two flow rates were compared and flow rate of 1 ml/min was chosen for further experiments. Results are discussed in section 4.2.4.

As the main idea for which these preparative steps have been realized is to discover the effect of natural convection in real extracted systems, the next step was to test the method on a vegetable material. We avoided plant parts containing essential oils that could absorb the UV rays, and the choice was limited to seeds, because vegetable oils consist of esters of fatty acids absorbing light of shorter wave lengths than the tracer. Hence, soybeans were milled, loaded to the extractor between two layers of glass beads and extracted. A series of tracer injections in the range from 2 to 30 s was

applied in both flow directions, but the response was not detected. The tracer was completely adsorbed on the vegetable matrix; the limit of saturation was not reached even after a series of long injections. Thus, the use of real extractable material was discarded and the idea of a solute deposited on an inert support was adopted.

The choice of the model solute should conform following conditions:

- to be "invisible" in UV radiation
- to be soluble in CO_2, but not too much, so that the feed placed in the extractor would be sufficient to assure constant extraction rate during all the course of peak elution.
- to enable even distribution along the extractor (e.g. deposition on inert glass beads)

Aliphatic hydrocarbons do not absorb UV rays and their solubility in the CO_2 as well as their physical properties depends on the length of the chain. Four long-chain hydrocarbons were extracted at subcritical conditions: $C_{16}H_{34}$, $C_{18}H_{38}$, $C_{20}H_{42}$ and $C_{24}H_{50}$. The first one is liquid at normal conditions, the others are waxy solids that can be easily melted and deposited on glass beads filled into the extractor.

In order to examine a possible decrease in extraction rate due to mixing with an almost insoluble wax, the hydrocarbons were melted together with $C_{32}H_{66}$ (at ratio 1:1). The liquid hexadecane was either melted with the wax or deposited on small pieces of glass wool and evenly distributed in the extractor filled with glass beads. However, as we can see at Figure 4.13 in the case of hexadecane, the mixing with wax had almost no influence on the extraction rate; similar result was obtained with $C_{24}H_{50}$. Curves are expressed in terms of volume of liquid solvent supplied by the pump; therefore, at flow rate of 1 ml/min, the axis corresponds to the time of extraction as well. Although the space time is relatively short, about one hour should be reserved for each experimental run, because of long tails of peaks and time necessary for manipulation.

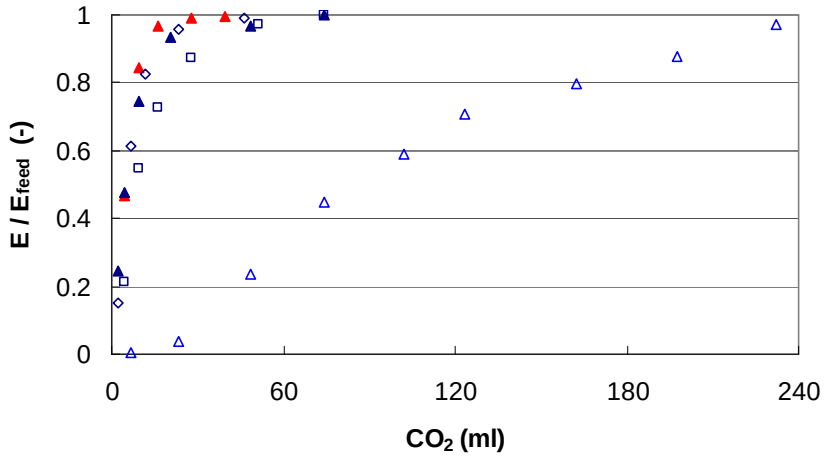

Figure 4.13. Extraction of aliphatic hydrocarbons by subcritical CO_2 (12 MPa, room temperature ~ 25°C).
▲ - C_{16}; ▲ - C_{16} / C_{32}; ◊ - C_{18} / C_{32} ; □ - C_{20} / C_{32}; Δ - C_{24} / C_{32}.

We can see that only tetracosane ($C_{24}H_{50}$) fulfils the condition of suitable extraction rate; it was chosen for further experiments. Thus, the residence time distribution with simultaneous extraction in liquid phase was measured using pure tetracosane as a solute deposited on glass beads by coating. See results in section 4.2.4.

(Note: Solubility of tetracosane of 0.9 mg/g of CO_2 was evaluated from the extraction curve (see Figure 4.14). Compared to the solubility corresponding to the nearest conditions to those used in this work that can be found in the literature, our value is much lower. (Furuya [117] reported the solubility of 6.76 mg/g of CO_2 at 37°C and 12.9 MPa; see Annexe 2.) This might be caused partially by lower temperature and pressure applied in this work, partially by accumulation of the solute near expansion valve. Although the valve is heated, the temperature in the capillary near the valve might have been influenced by the adiabatic cooling of the stream causing deposition of a thin layer of precipitated waxy solid on walls of capillary. It must be noted, that the feed of solute into the extractor was only about 0.2 g and the solubility is low, hence even a slight deposition would change substantially the extraction yield.)

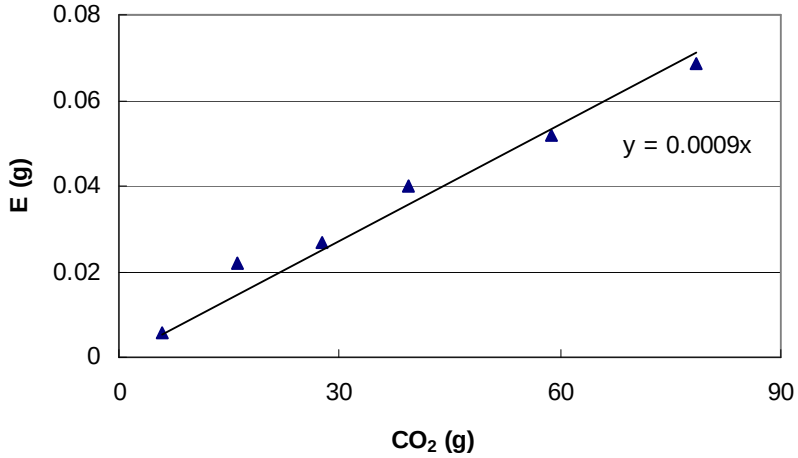

Figure 4.14. Linear part of the extraction curve of $C_{24}H_{50}$ extracted at 12 MPa / 25°C.

When the thermoregulatory box was finished, we started the measurements under supercritical conditions (12 MPa, 40°C).

The difficulties with deposition of $C_{24}H_{50}$ in capillaries and the microcuvette of the detector remained at supercritical conditions as well; therefore, we were searching for another possible solute whose melting point would be lower and then it would not block the capillaries if sudden pressure and temperature drops occurred. Trilaurin (lauric acid triglyceride) was chosen; generally, vegetable oils consist of esters of triglyceride of fatty acids, trilaurin makes a part of them. Its behaviour at supercritical conditions was observed in a high pressure cell with sapphire windows. Temperature was set at 40°C, pressure was gradually increased up to 14 MPa as the cell was filled with CO_2 supplied by the pump. Initially waxy solid started to melt at 7 MPa, at 12 MPa all feed was completely melted.

After slow decompression, trilaurin stayed liquid, and it solidified slowly while the cell was being cooled. Therefore, no precipitation of solid should occur when dealing with the compound at conditions used in this work – 12 MPa and 40°C. On the other hand, due to the liquid character of trilaurin at supercritical conditions, it can flow down slowly through the vertically placed extractor which could block the exit capillary, especially when the extractor is operated under downflow mode. Hence, RTD measurements were carried out firstly for upflow mode when a part of solute was extracted, then the extractor was switched to downflow mode. See results in 4.2.5.

4.2.3 Data treatment

In this first approach, conclusions are based on comparison of experimental data by means of moments and E-curves. Following simplification is assumed: flow pattern in all parts of the test section except the extractor (i.e. six-port valve and capillaries of 1 mm in diameter) is supposed to be the plug flow. Hence, the resulting flow pattern corresponds to the flow pattern in the extractor. This assumption is evidently disputable. However, it is acceptable for the purpose of this work, where only a simple comparison is made of RTD characteristics measured under upflow and downflow mode is made.

The raw data supplied by the detector were treated in several steps (see Annexe 2):

- baseline of the peak was reduced to zero
- as the plug flow is considered in capillaries, the time passed from the tracer injection to the start of the peak was reduced by the period corresponding to the passage through capillaries at the inlet and outlet of the extractor
- concentration of the tracer was evaluated using Lambert-Beer's rule. Molar absorptivity of benzoic acid at atmospheric pressure was applied for the estimation.
- moments t_{mean}, σ^2, $(\sigma_\Theta)^2$ were evaluated from the data using eq. (1.6) and (1.7)
- residence time distribution (or E curve) was calculated (eq.(1.5)) and plotted against time

4.2.4 Experiments at subcritical conditions

4.2.4.1 Flow pattern in the extractor without extraction

Extractor of 4 ml in volume (diameter 8 mm, length 8 cm) filled with glass beads of 2 mm in diameter was used in all runs. Experiments were carried out at two flow rates – 0.5 ml/min and 1 ml/min.
Void fraction ε in the extractor is 0.42 (determined by weighing the beads, glass density of 2600 kg/m^3 was used). Therefore, the space time τ is 4.64 min and 2.32 min at flow rate of 0.5 and 1 ml/min, respectively. Superficial velocity of the fluid phase is

$$v = \frac{V'}{\frac{\pi d^2}{4}} = \frac{1}{\frac{\pi \cdot 0.8^2}{4}} = 2 \text{ cm/min for volumetric flow rate 1ml/min}$$

and Reynolds numbers is

$$\mathrm{Re} = \frac{vd\rho}{\eta} = \frac{\frac{2}{6 \cdot 10^3} \cdot 0.008 \cdot 845.96}{7.91 \cdot 10^{-5}} = 28.5$$

Where d is extractor diameter, and density ρ and viscosity η correspond to 12 MPa and 25°C (ρ=845.96 kg/m^3, calculated from the Altunin and Gadetskii equation of state, and η=7.91.10^{-5} Pa.s,). In the case of 0.5 ml/min, v=cm/min and Re=14.2. Thus, laminar flow occurs in both cases. Two-second injection of tracer was applied.

Curves in Figure 4.15 correspond to measurement in upflow and downflow mode at two different flow rates; average values of moments are listed in table 4.8. Unfortunately, values of moments are strongly burdened with peak tailing, which is probably caused by mixing of the fluid at both ends of the extractor top and bottom where the flow diameter changes sharply from 1 mm in capillary to 8 mm in the extractor. Hence, the calculated values of t_{mean} are much longer than extractor space time; on the other hand, peak maximums are rather close to the space time value. The differences in peak height are related to bad reproducibility of concentration of tracer in injected amount. It is a common feature of all these preliminary experimental runs, and the problem should be solved in future work.

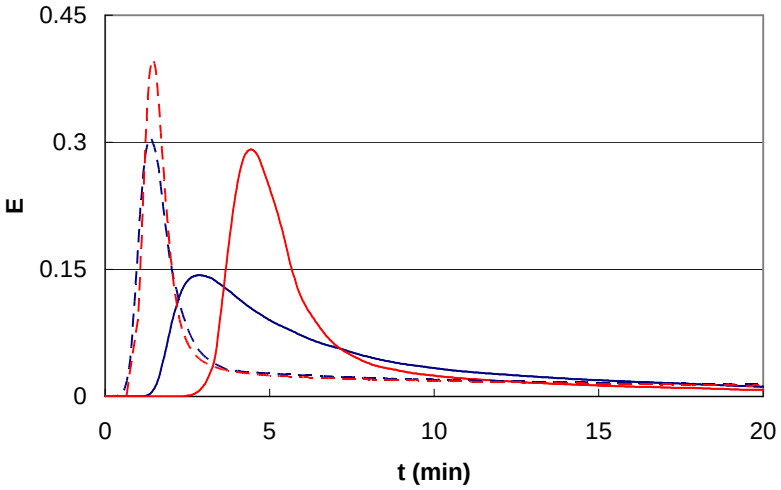

Figure 4.15. RTD data obtained with pure CO_2 at flow rate 0.5 ml/min (---) and 1 ml/min (—) under downflow (blue) and upflow (red) mode. Extractor of 8 mm in diameter and 8 cm in length, filled with glass beads.

Anyway, several conclusions can be made. The picture shows that there is no significant difference between upflow and downflow mode when the flow rate of 1 ml/min is set. On the other hand, at the flow rate of 0.5 ml/min, the mean t_{mean} is shorter for downflow mode. As there is only the pure

CO_2 and the tracer present in the extractor, we can imagine that the changes in flow pattern in the extractor are caused by changes in density when the solvent is laden with the tracer. The flow is faster at the downflow mode, on the contrary, when the fluid flows upwards, a mixing probably occurs. This situation could be in the future modelled rather by a compartment model with two ideally mixed vessels. Although the tracer is not ideal (it tends to change flow pattern itself), its use is acceptable when higher flow rate is applied. Therefore, the flow rate of 1 ml/min was chosen for further experiments in this work.

Table 4.8. Moments evaluated for subcritical conditions (12 MPa, 25°C). Extractor of 8 mm in diameter and 8 cm in length, filled with glass beads

	mode	**t_{mean} (min)**	**σ^2 (min^2)**	**σ_Θ^2 (-)**
pure CO_2 / 0.5 ml/min	downflow	8.73	55.92	0.67
	upflow	9.43	66.10	0.74
pure CO_2 / 1 ml/min	downflow	14.04	222.38	1.13
	upflow	14.48	235.44	1.12
extraction of $C_{24}H_{50}$ / 1 ml/min	downflow	12.82	181.24	1.10
	upflow	23.51	509.08	0.92

4.2.4.2 Flow pattern in the extractor with simultaneous extraction

The residence time distribution with simultaneous extraction in liquid phase was measured using pure tetracosane as a solute deposited on glass beads. The extraction was carried out under both upflow and downflow mode in the 4 ml extractor, with the flow rate of fluid phase of 1 ml/min and two-second injection. In Figure 4.16, the curves are plotted together with the ones corresponding to experimental runs without extraction; moments calculated from the data have been already listed in the Table 4.8. Again, peaks are burdened with long tails, differences in height and elution time of peak are related to experimental error, so we should not rely much on calculated moments. Visually, there are no significant differences neither between experiments carried out without extraction not those obtained with simultaneous extraction.

It must be taken into account that the kinematic viscosity of supercritical fluids is lower than the value for liquids. Therefore, the effect of natural convection reported for supercritical CO_2 might not occur at such extent when subcritical CO_2 (even near its critical temperature) is used.

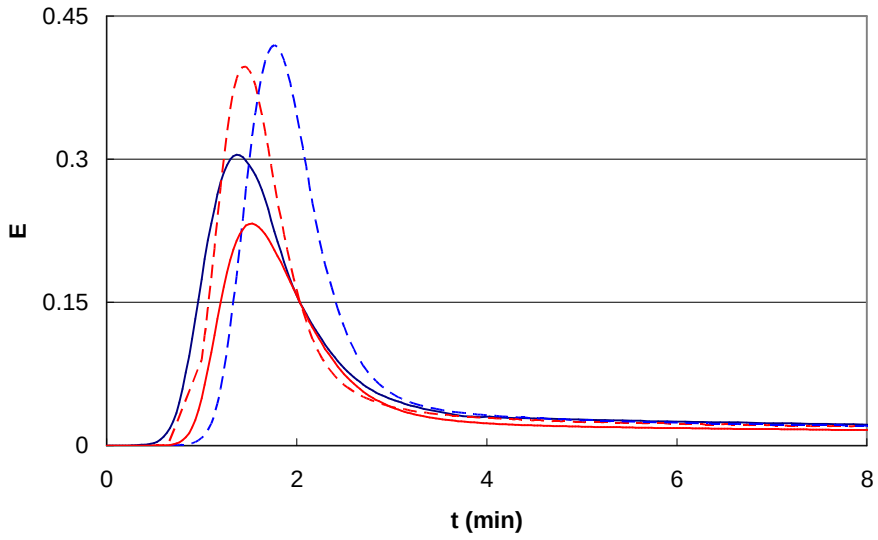

Figure 4.16. RTD data obtained during the extraction of $C_{24}H_{50}$ with subcritical (liquid) CO_2, 1 ml/min (—) compared with the data without extraction at flow rate 1 ml/min (---) under downflow (blue) and upflow (red) mode. Extractor of 8 mm in diameter and 8 cm in length filled with glass beads.

4.2.5 Experiments at supercritical conditions

Trilaurin is more soluble in SCO_2 than tetracosane, therefore, a larger extractor of 7.5 ml in volume (diameter 8 mm, length 15 cm) was used to allow higher feed of solute. Feed of solute varied around 1 g; thus, at the flow rate of 1 ml/min and the solubility of about 5.38 mg/g CO_2 (see Annexe 2), i.e. 3.86 mg/ml SCO_2, the extractor can be operated for more than 4 hours per charge. Preliminary experiments showed that the laborious deposition of the solute on glass beads was not necessary. When a reasonable amount of solute (~1g) is evenly distributed between glass beads, and then it melts under applied pressure and partially dissolves in the SCO_2, after depressurization we observe that the beads were evenly coated by the solid.

Experiments were carried out at 12 MPa, 40°C and flow rate of 1 ml/min. The test section was placed in hot air heated thermoregulatory box. The extractor was filled with glass beads of 2 mm in diameter. The space time τ is 4.35 min, superficial velocity of the fluid phase is 2 cm/min and Re=30.4, with ρ=718.9 kg/m^3 and η=5.73.10^{-5} Pa.s. Ten-second injection was applied.

The data are presented in Figure 4.17. The average values of calculated moments are listed in Table 4.9. It should be stressed again that in this first approach we rely rather on visual comparison of curves, in order to determine whether there are any differences in flow pattern when the solvent flow direction is switched from down to up. Moments are calculated to give us a rough tool to compare the data, but they are very sensible to long tails of peaks. Therefore, here again the values of t_{mean} are much higher than space time. A more appropriate method of data evaluation has to be found.

When comparing RTD for upflow and downflow without extraction, we can see that there is a long tail of peak in upflow mode. The explanation could be the same as proposed for runs liquid CO_2 at slower flow rate - that the tracer is not ideal but affects itself the flow pattern in the vessel; the natural convection occurs in the vessel under upflow mode due to changes in density. Further, as shown in detailed picture, the beginning of peak elution is not constant, significant retardation is obvious especially under downflow mode. Moreover, peak maximums correspond to times higher than space time, in contrary to experiments without extraction. Explanation of this behaviour during extraction could be a kind of temporary interaction of the benzoic acid with the melted trilaurin in the column. We did not observe the same effect in the case of tetracosane under subcritical conditions, but it might stay solid under lower temperate. This is just a hypothesis to verify, because we have not examined yet the behaviour of tetracosane under high pressure.

Anyway, Figure 4.17 shows an obvious increase in the mean and dispersion of peaks measured with simultaneous extraction, both under downflow and upflow mode. The higher degree of dispersion of peaks under upflow mode is obvious. (This is in contrast with the table, where dimensionless variance was calculated to be the same for both upflow and downflow mode.)

Table 4.9. Moments evaluated for supercritical conditions (12 MPa, 40°C) at flow rate 1 ml/min. Extractor of 8 mm in diameter and 15 cm in length, filled with glass beads

	mode	**t_{mean} (min)**	**σ^2 (min^2)**	**σ_Θ^2 (-)**
pure CO_2	downflow	6.30	4.01	0.10
	upflow	10.23	56.64	0.53
extraction of trilaurin	downflow	14.83	42.77	0.20
	upflow	26.33	152.13	0.20

Nevertheless, beside the natural convection related to changes in density due to the dissolution of the solute, three other phenomena occur probably in this case : a) the presence of the tracer itself may cause differences in density and subsequently changes in flow pattern; b) there might be an interaction of the tracer with the solute resulting in retardation of peak elution, c) it has to be kept in mind, that trilaurin used as solute melts under high pressure and it probably partially dribbles from through the layer of glass beads in the direction of gravity. It can have positive influence on downflow extractions and negative influence, on the other hand, on upflow extractions. This fact would surely affect the RTD data.

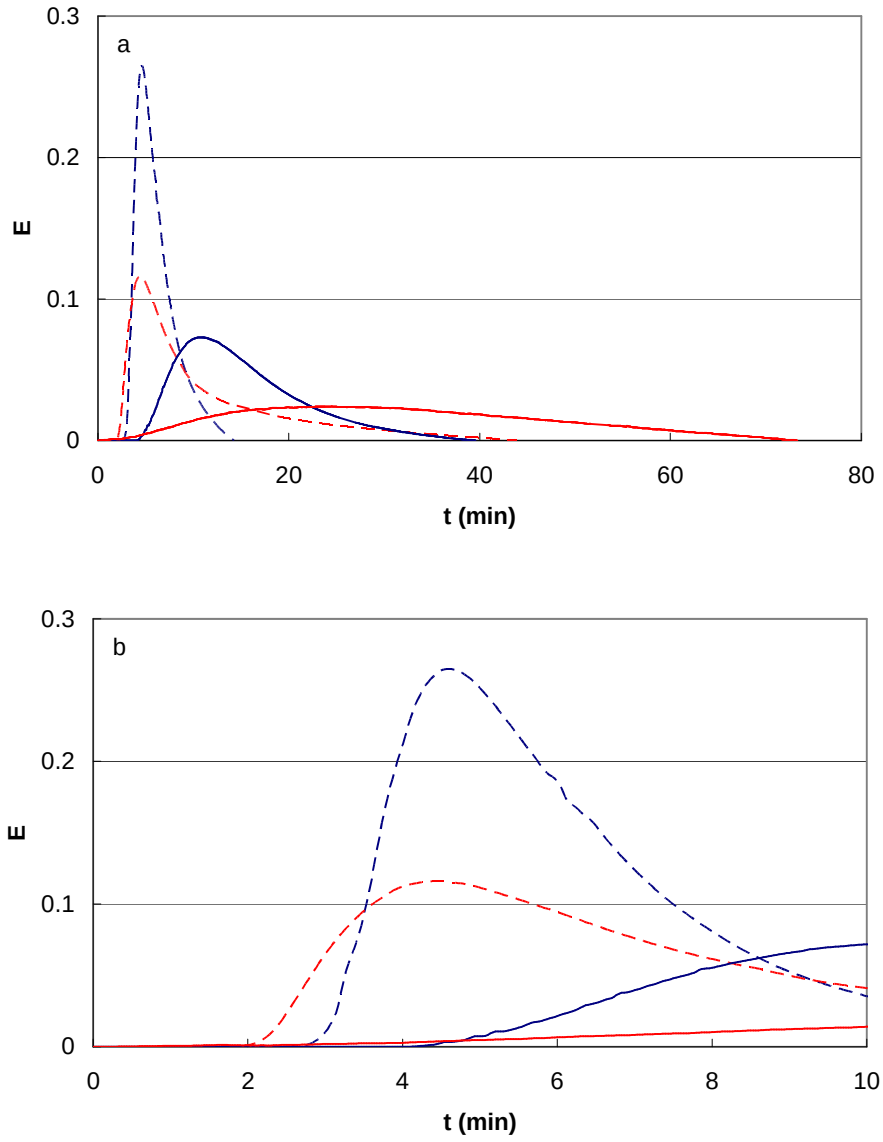

Figure 4.17. (a) RTD data obtained during the extraction of trilaurin (—) compared with the data of pure CO_2 (---) at flow rate of 1 ml/min under downflow (blue) and upflow (red) mode. Extractor of 8 mm in diameter and 15 cm in length filled with glass beads. (b) Detailed picture.

4.2.6 Perspectives

– Rate of saturation of the fluid with tracer can be another factor affecting the reproducibility. In this work, closed sample loop was used, i.e. it is connected to the fluid stream just at the moment of injection. Generally, imperfect tightness of the installation, which is totally negligible when the fluid is continuously fed into the installation by a pump, can be of importance if the fluid of high pressure stagnates in the loop for a long time, such as in our case of one-hour long runs. By opening the valve, pressure is balanced, but the concentration in capillaries connecting the valve to the column with tracer does not change as quickly and

can vary from one experiment to another. Hence, a loop with the fluid flowing continuously at low flow rate will be used in the future work to assure constant concentration at the injection.

- Effect of tracer on the flow pattern could be eliminated by decreasing the concentration in the injected pulse. It could be done by a split of the injection.
- Any possible interaction of tracer with the solute should be checked out. Possibility of experimental error in this case has to be verified as well. High pressure cell can be used to observe the behaviour of all used compounds and their mixtures with tracer under supercritical conditions in order to determine their state and possible interactions.
- Homogeneous distribution of the solute along the extractor during the extraction is another goal. It might be achieved finding a porous inert material to trap the trilaurin and avoid the dribbling or a solute that stays solid at supercritical conditions. Contribution of the rest of the test section to the final response should not be neglected. Convolution of the data is a solution to better characterize the flow inside the extractor
- Appropriate model to describe experimental data is to be found. To start off, we propose a model with two ideal mixers and plug flow, which seems to describe well the form of measured RTD curves. If there are any interactions of tracer with the solute, the adsorption/desorption term should be incorporated into the model.

4.2.7 Conclusions

Based on preliminary data, rough conclusions can be made:

- As showed by experiments at different flow rates without extraction, the tracer itself can influence the flow pattern in the extractor by changing the density of the passing solvent. At subcritical conditions, the limiting flow rate when this effect of tracer occurs is lower then at supercritical conditions. This can be explained by the fact that due to lower kinematic viscosity, the supercritical fluid is more prone to natural convection.
- No significant effect of flow direction on flow pattern was observed in liquid CO_2 flowing at 1 ml/min. On the contrary, when supercritical conditions were applied, the mixing in the column related probably to the presence of tracer resulted in peak tailing under upflow mode.
- Flow pattern measured during the extraction carried out under supercritical conditions depends significantly on the flow direction. Peaks corresponding to upflow are more dispersed in comparison to the downflow mode which indicates natural convention occurring in the extractor. Besides the natural convection related to changes in density, increase in the mean residence time related probably to the tracer interaction with the solute was observed.

CONCLUSIONS AND FUTURE WORK

The presented work deals with two problems connected to the efficiency of supercritical extraction processes.

Impact of structure modification on SCO_2 extraction

The objective was to test the ability of the process of Instantaneous Controlled Pressure-Drop (DIC) applied as pretreatment technique to enhance the supercritical extraction by structure modification of extracted material.

Three types of seeds were tested: amaranth seeds, soybeans and green coffee beans. The most important effect of the DIC treatment was observed in the case of soybeans.

Beans were treated by the DIC process and samples of milled and whole beans were extracted with supercritical CO_2. Structure of beans was determined using scanning electron microscopy, mercury porosimetry and helium pycnometry.

Soybeans were decorticated, treated by the DIC process (soaking in hot water, then treatment for 1 minute at 0.3 MPa followed by 2 minutes at 0.7 MPa) and extracted with supercritical CO_2 at 28 MPa and 40°C. In comparison to non-treated material which is rather compact and homogeneous, the internal structure of DIC-treated soybeans was substantially destroyed by the bursting moisture evaporation during the DIC treatment. The porosity was increased considerably: pores of order of magnitude from 1 mm to 0.01 mm represent about 19 % of the seed cross-section area, the increase of about tenfold for 100 nm pores and even thirtyfold for 10 μm pores. The smallest pores of radius less than 10 nm were not influenced by the DIC treatment. Also, DIC-treated beans are much more brittle which results in finer milling and consequently, in increased extraction yield.

Extraction of milled soybeans was well described by the BIC model. The external mass transfer coefficient does not change substantially by the DIC treatment. On the other hand, the internal mass transfer coefficient is about six times higher than in the case of non-treated material.

Extraction of whole beans was better described by the modified hot ball model. An increase in value of internal diffusion coefficient for DIC-treated beans of about one order of magnitude was observed, which proves again, that the DIC pretreatment is able to enhance the rate of slow extraction controlled by diffusion.

Green coffee beans were treated by the DIC process (moisturizing, then treatment for 45 s at 0.5 MPa) and extracted with supercritical CO_2 at 24 MPa and 50°C. Number of pores large enough to have an influence on the extraction rate in coffee beans did not change after the DIC treatment. Extraction data of milled beans were described by the BIC model. Comparing mass transfer coefficients, we can conclude that the DIC process does not influence significantly the mass transfer in the material during the extraction, which corresponds with porosimetry results.

Character of extract is different when milled beans and whole beans are extracted. Extract from milled beans consists of vegetable oil; on the other hand, when whole beans are extracted, the extraction of oil becomes impossible due to the presence of water in bean tissue and the extraction is highly selective for caffeine. We could not compare mass transfer coefficients for caffeine in whole and milled beans, because the extraction of caffeine in our experiments was limited by low solubility of caffeine in SCO_2. So even if there were any changes in the internal structure of beans, their influence could not appear in this case. Future work would include measurements at higher flow rates so that the solvent could not reach the point of saturation with caffeine.

Amaranth seeds are protected by a rigid hull difficult to remove, and negligible extraction yield is observed when whole seeds are treated. The DIC treatment had no effect on compactness of the hull. Very fine grinding had to be applied to disintegrate the rigid seeds and it seems to be a method effective enough to liberate most of the oil from seeds which, indeed, does not require any other pretreatment.

The effect of changes in conditions of the DIC process on the extraction yield could not be evaluated due to experimental error. However, for all applied conditions of the DIC process, the extraction was enhanced in comparison with the raw material.

We can conclude that the DIC process can be applied as a pretreatment technique to enhance extraction controlled by internal diffusion. This is for example the case of vegetable materials which cannot be, for various reasons, mechanically disintegrated before the extraction. Hence, the enhancement of extraction kinetics will result in increase of effectivity of the process making this one cheaper and thus more interesting for large scale applications.

The success of the technique depends on the nature of extracted material. Unfortunately, we did not obtain good results with green coffee beans, which is just the case of material extracted in large scale and without mechanical pretreatment. Nevertheless, supercritical extraction has been already applied in laboratory scale on wide range of materials of different character, and although extracts obtained this way may be of better quality than those extracted by conventional methods, the larger scale applications of these results are often inhibited just by process costs. Thus, from this point of view, the DIC process as a promising technique of pretreatment may help to introduce some laboratory results to practice.

Impact of natural convection on SCO_2 extraction

The objective was to introduce the method of measurement of RTD characteristic into the laboratory of supercritical extraction in order to follow the effect of flow direction on flow pattern in a supercritical extractor.

Experimental apparatus was assembled. Benzoic acid was used as tracer. Preliminary extractions of real vegetable material (milled soybeans) showed to be inapplicable for further studies, because the tracer was completely adsorbed on the matrix. Therefore, the idea of solvent deposited on an inert support was adopted. Glass beads were chosen as the support. Tetracosane was chosen as solute and applied in experiments at subcritical conditions. Later, in experiments at supercritical conditions, it was replaced by trilaurin due to frequent blockages of capillaries.

RTD measurements carried out in the extractor at subcritical conditions showed that the tracer itself can influence the flow pattern in the extractor by changing the density of the solvent. Hence, at flow rate of 0.5 ml/min (of compressed CO_2) and under upflow mode, a mixing in the extractor probably occurs. At higher flow rate (1 ml/min), the effect was not observed. Extraction of tetracosane at 12 MPa and room temperature (~25°C) was carried out in both upflow and downflow mode, but no effect on the flow pattern was observed.

A strong influence of flow direction during extraction was observed under supercritical conditions (trilaurin was extracted at 12 MPa and 40°C). Peaks corresponding to upflow are more dispersed in comparison to the downflow mode which indicates natural convention occurring in the extractor. Beside natural convection related to changes in density due to the dissolution of the solute, other phenomena may interconnect:

- flow pattern may be affected by the presence of the tracer itself that causes differences in density;
- an interaction of the tracer with the solute resulting in retardation of peak elution;
- trilaurin used as solute melts under high pressure and it probably partially dribbles from through the layer of glass beads in the direction of gravity. This would accelerate downflow extractions and inhibit, on the other hand, upflow extractions.

We conclude that the method of RTD measurement in supercritical extractor was applied and tested. Preliminary results show strong effect of flow direction on flow pattern during supercritical extraction. Future work will be oriented to verify presented hypothesis.

NOMENCLATURE

Latin letters

a	orifice area (m^2) (chapter 1.6); dimension of hemi-ellipsoid (m) (eq.(4.3)); roots of eq.(3.17)
a_0	specific surface (particle surface area per unit volume of extraction bed) (1/m)
B	adjustable constant of Langmuir-like equation (-)
c	solid phase concentration (kg/m^3); dimension of hemi-ellipsoid (m) (eq.(4.3))
c_i	concentration of solute in pores of a leaf (kg/m^3)
d_{32}	Sauter mean diameter (m)
D_{12}	binary diffusion coefficient (m^2/s)
D_i	internal (effective) diffusion coefficient (m^2/s)
D_{ax}	dispersion coefficient (m^2/s)
e	dimensionless extraction yield, $e=E/N$ (-); excentricity of hemi-ellipsoid (m) (eq.(4.3))
E	amount of extract (kg)
h	axial coordinate of an extraction column (m)
hr	parameter of modified hot ball model
k_c	kinetic constant of eq. (1.2)
k_f	external (solvent phase) mass transfer coefficient (m/s)
k_s	internal (solid phase) mass transfer coefficient (m/s)
k_{teor}	time constant in eq.(1.21) (1/s)
K	mass partition coefficient of the solute between the solid phase and the fluid phase at equilibrium (-)
$k_f a_0$	volumetric external mass transfer coefficient (1/s)
$k_s a_0$	volumetric internal mass transfer coefficient (1/s)
l	particle volume-to-surface ratio (m)
M_W	molar mass of gas (kg/mol)
N	solid feed (kg)
p_A , p_I	pressure and initial pressure in the autoclave (DIC installation) (Pa)
p_V	pressure in the vacuum tank (DIC installation) (Pa)
P	absolute pressure (Pa)
q	dimensionless amount of solvent, $q=Q/N$ (-)
q'	specific solvent flow rate, $q'= Q'/N$ (1/s)
Q	amount of solvent (kg)
Q'	solvent flow rate (kg/s)
r	radius of a spherical particle (m); radial coordinate in eq.(1.12)

r_b volumetric fraction of broken cells in disintegrated particles (-)

R gas constant (J/mol.K)

t extraction time (s)

t_i characteristic time (s)

T absolute temperature (K)

U superficial solvent velocity (m/s)

V volume of the autoclave (DIC installation) (m^3)

V_{total} volume of graduated cylinder (void fraction measurements) (m^3)

w leaf coordinate (m)

W parameter of slow extraction period in BIC model (-)

x solute concentration in the solid phase (kg/kg raw material)

x_0 initial solute content in the material (kg/kg raw material)

x_k initial content of solute in intact cells (kg/kg raw material)

x* concentration at the solid-fluid interface which is assumed to be in equilibrium with the fluid phase (kg/kg of raw material)

y solute concentration in the solvent phase (kg/kg solvent)

y_r oil solubility in supercritical CO_2 at given conditions (kg of oil/kg CO_2)

y^* equilibrium concentration of the solute in the solvent (kg /kg of solvent)

Y extraction yield (kg); dimensionless variable of BIC model (-) (chapter 3.2)

Y_∞ asymptotic extraction yield (kg)

z dimensionless variable of BIC model (-)

Z parameter of fast extraction period (-)

Greek letters

γ ratio of the specific heat at constant pressure and constant volume, $\gamma = C_p/C_v$ (-)

ε void fraction of the extracted material in extraction columns (-)

ε_p particle porosity (-)

ρ solvent density (kg/m^3)

ρ_s solid density (bulk density measured by Hg porosimetry) (kg/m^3)

ρ_{sk} skeletal density (measured by He pycnometry) (kg/m^3)

μ constant depending on the shape of extracted particles (-)

τ tortuosity of the interconnected pore network in the particle (-)

Abbreviations

BIC (model of) Broken and Intact Cells

DIC Détente Instantannée Contrôlée (Instantaneous Controlled Pressure-Drop)

ICPF AS CR	Institute of Chemical Process Fundamentals, Academy of Science of the Czech Republic
LEPTIAB	Laboratoire d'Étude des Phénomènes de Transfert et de l'Instantanéité: Agro-industrie et Bâtiment
LMTAI	Laboratire Maîtrise des Technologies Agro-Industrielles
RTD	Residence Time Distribution
SCO_2	Supercritical Carbon Dioxide
SFE	Supercritical Fluid Extraction

REFERENCES

[1] Taylor, L. T. "Supercritical Fluid Extraction." 1st ed., Techniques in Analytical Chemistry, John Wiley and Sons, Inc., **1996**.

[2] Brunner, G. "Gas Extraction." Springer-Verlag New York, Inc. **1994**.

[3] Sandler, S. I. Equations of state for phase equilibrium computations. *In* "Supercritical Fluids - Fundamentals for Application" E. Kiran and J. M. H. Levelt-Sengers (Eds.). NATO ASI, Kluwer. **1994.**

[4] Kikic, I., De Loos, T. W. Thermodynamic properties at high pressure. *In* "High Pressure Process Technology: Fundamentals and Applications" A. Bertucco and G. Vetter (Eds.), Industrial Chemistry Library Vol. 9, p. 659. Elsevier Science B. V. **2001.**

[5] Hougen, O. A., Watson, K. M. "Chemical Process Principles, Part III: Kinetics & Catalysis." Wiley, New York. **1947**.

[6] Lee, H., Thodos, G. Generalized viscosity behavior of fluids over the complete gaseous and liquid states. *Industrial and Engineering Chemistry Research*, **1990**, vol.29 (7)**,** p.1404-1412.

[7] Vesovic, V., Assael, M. J., Gallis, Z. A. Prediction of the Viscosity of Supercritical Fluid Mixtures. *International Journal of Thermophysics*, **2004**, vol.19 (5)**,** p.1297-1313.

[8] Luft, G., Recasens, F., Velo, E. Kinetic properties at high pressure. *In* "High Pressure Process Technology: Fundamentals and Applications" A. Bertucco and G. Vetter (Eds.), Industrial Chemistry Library Vol. 9, p. 659. Elsevier Science B. V. **2001.**

[9] Andrews, T. The Bakerian Lecture: On the Gaseous State of Matter. *Proceedings of the Royal Society of London*, **1875**, vol.24**,** p.455-463.

[10] Hannay, J. B., Hogarth, J. On the Solubility of Solids in Gases. *Proceedings of the Royal Society of London*, **1879**, vol.29 (324-326).

[11] Supercritical fluids: realising potential. *Chemistry world*, **2005**, vol. 2, no. 2.

[12] Zosel, K. Process for the separation of mixtures of substances. U. S. P. a. T. Office. Patent no. 3,969,196. **1969**.

[13] Pekhov, A. V., Goncharenko, G. K. Ekstakeija prjanogo rastitelnogo syrja szhizhennymi gazami. *Maslozhirovaja Promyshlennostj*, **1968**, vol.34 (10)**,** p.26-29.

[14] Hubert, P., Vitzthum, O. G. Fluid extraction of hops, spices, and tobacco with supercritical gases. *Angewandte Chemie (Int. Ed. Engl.)*, **1978**, vol.17 (10)**,** p.710-715.

[15] Luque de Castro, M. D., Jimenez-Carmona, M. M., V., F.-P. Towards more rational techniques for the isolation of valuable essential oils from plants. *Trends in Analytical Chemistry*, **1999**, vol.18 (11)**,** p.708-716.

[16] Székely, E. Supercritical Fluid Extraction. http://sunny.vemt.bme.hu/sfe/angol/supercritical.html. Accessed 21.9.2008.

[17] Vandana, V., Teja, A. S., Zalkow, L. H. Supercritical extraction and HPLC analysis of taxol from Taxus brevifolia using nitrous oxide and nitrous oxide + ethanol mixtures. *Fluid Phase Equilibria (Proceedings of the Seventh International Conference on Fluid Properties and Phase Equilibria for Chemical Process Design)*, **1996**, vol.116 (1-2)**,** p.162-169.

[18] Klink, G., Buchs, A., Gulacar, F. O. Supercritical fluid extraction of fatty acids and sterols from plant tissues and sediments. *Organic Geochemistry*, **1994**, vol.21 (5)**,** p.437-441.

[19] Smith, R. M. Supercritical fluids in separation science - the dreams, the reality and the future. *Journal of Chromatography A*, **1999**, vol.856 (1-2)**,** p.83-115.

[20] Lang, Q., Wai, C. M. Supercritical fluid extraction in herbal and natural product studies - a practical review. *Talanta*, **2001**, vol.53**,** p.771-782.

[21] Reverchon, E., De Marco, I. Supercritical fluid extraction and fractionation of natural matter. *Journal of Supercritical Fluids*, **2006**, vol.38 (2)**,** p.146-166.

[22] Montañés, F., Corzo, N., Olano, A., Reglero, G., Ibáñes, E., Fornari, T. Selective fractionation of carbohydrate complex mixtures by supercritical extraction with CO_2 and different co-solvents. *Journal of Supercritical Fluids (Selected contributions from 1st Iberoamerican Conference on Supercritical Fluids)*, **2008**, vol.45 (2)**,** p.189-194.

[23] Modey, W. K., Mulholland, D. A., Raynor, M. W. Analytical supercritical fluid extraction of natural products. *Phytochemical Analysis*, **1996**, vol.7 (1)**,** p.1-15.

[24] Francis, A. W. Ternary systems of liquid carbon dioxide. *Journal of Physical Chemistry*, **1954**, vol.58 (12)**,** p.1099-1114.

[25] Bartle, K. D., Clifford, A. A., Jafar, S. A., Shilstone, G. F. Solubilities of solids and liquids of low volatility in supercritical carbon-dioxide. *Journal of Physical and Chemical Reference Data*, **1991**, vol.20 (4)**,** p.713-756.

[26] Lucien, F. P., Foster, N. R. Solubilities of solid mixtures in supercritical carbon dioxide: a review. *Journal of Supercritical Fluids*, **2000**, vol.17 (2)**,** p.111-134.

[27] Reverchon, E. Supercritical fluid extraction and fractionation of essential oils and related products. *Journal of Supercritical Fluids*, **1997**, vol.10**,** p.1-37.

[28] Dean, J. R., Khundker, S. Extraction of pharmaceuticals using pressurised carbon dioxide. *Journal of Pharmaceutical and Biomedical Analysis*, **1997**, vol.15 (7)**,** p.875-886.

[29] Anitescu, G., Tavlarides, L. L. Supercritical extraction of contaminants from soils and sediments. *Journal of Supercritical Fluids*, **2006**, vol.38**,** p.167-180.

[30] Pourmortazavi, S. M., Hajimirsadeghi, S. S. Supercritical fluid extraction in plant essential and volatile oil analysis. *Journal of Chromatography A*, **2007**, vol.1163 (1-2)**,** p.2-24.

[31] Yin, J.-Z., Wang, A.-Q., Wei, W., Liu, Y., Shi, W.-H. Analysis of the operation conditions for supercritical fluid extraction of seed oil. *Separation and Purification Technology*, **2005**, vol.43**,** p.163-167.

[32] Brunner, G. Supercritical fluids: Technology and application to food processing. *Journal of Food Engineering*, **2005**, vol.67 (1-2)**,** p.21- 33.

[33] Zosel, K. Process for recovering caffeine. U. S. P. a. T. Office. Patent no. 3,806,619. **1974**.

[34] Gardner, D. S. Industrial scale hop extraction with liquid CO_2. *Chemistry and Industry*, **1982,** p.402-405.

[35] Zekovic, Z., Pfaf-Šovljanski, I., Grujic, O. Supercritical fluid extraction of hops. *Journal of the Serbian Chemical Society*, **2007**, vol.72 (1)**,** p.81-87.

[36] Eggers, R. Supercritical fluid extraction (SFE) of oilseeds/lipids in natural products. *In* "Supercritical fluid technology in oil and lipid chemistry" J. W. King and G. R. List (Eds.), p. 35-64. AOCS Press, Champaign, Illinois. **1996.**

[37] Perrut, M. Supercritical fluid applications: Industrial Developments and Economic Issues. *Industrial Engineering Chemical Research*, **2000**, vol. 39**,** p.4531-4535.

[38] Fahn, A. "Secretory tissues in plants." Academic Press, London. **1979**.

[39] Tzen, J. T. C., Cao, Y.-Z., Laurent, P., Ratnayake, C., Huang, A. H. C. Lipids, proteins, and structure of seed oil bodies from diverse species. *Plant Physiology*, **1993**, vol.101 (1)**,** p.267-276.

[40] Reverchon, E., Marrone, C. Modeling and simulation of the supercritical CO_2 extraction of vegetable oils. *Journal of Supercritical Fluids*, **2001**, vol.19 (2)**,** p.161-175.

[41] Reverchon, E., Kaziunas, A., Marrone, C. Supercritical CO_2 extraction of hiprose seed oil: experiments and mathematical modelling. *Chemical Engineering Science*, **2000**, vol. 55**,** p.2195-2201.

[42] del Valle, J. M., Uquiche, E. L. Particle size effects on supercritical CO_2 extraction of oil-containing seeds. *Journal of the American Oil Chemists' Society*, **2002**, vol.79 (12)**,** p.1261-1266.

[43] Seville, J. P. K., Santos, R. C. D., Al-Duri, B., Lu, T., Gaspar, F., Marriott, R., Mellor, S., Watkinson, C. *Process Engineering in Non-Food Crops LINK Seminar*.**2005**.

[44] Sovova, H., Komers, R., Kučera, J., Jež, J. Supercritical carbon dioxide extraction of caraway essential oil. *Chemical Engineering Science*, **1994**, vol.49 (15)**,** p.2499-2505.

[45] del Valle, J. M., Germain, J. C., Uquiche, E., Zetzl, C., Brunner, G. Microstructural effects on internal mass transfer of lipids in prepressed and flaked vegetable substrates. *Journal of Supercritical Fluids*, **2006**, vol.37 (2)**,** p.178-190.

[46] Catchpole, O. J., King, M. B. Measurement and correlation of binary diffusion coefficients in near critical fluids. *Industrial Engineering Chemical Research*, **1994**, vol.33**,** p.1828.

[47] Uquiche, E., del Valle, J. M., Ortiz, J. Supercritical carbon dioxide extraction of red pepper (*Capsicum annuum* L.) oleoresin. *Journal of Food Engineering*, **2004**, vol.65**,** p.55-66.

[48] Simeonov, E., Tsibranska, I., Minchev, A. Solid-liquid extraction from plants - experimental kinetics and modelling. *Chemical Engineering Journal*, **1999**, vol.73 (3)**,** p.255-259.

[49] McHugh, M., Krukonis, V. "Supercritical fluid extraction: principles and practice." 2. ed., Butterworth-Heinemann. **1994**.

[50] Femenia, A., Garcıa-Marın, M., Simal, S., Rossello, C., Blasco, M. Effects of supercritical carbon dioxide (SC-CO_2) oil extraction on the cell wall composition of almond fruits. *Journal of Agricultural and Food Chemistry*, **2001**, vol.49**,** p.5828-5834.

[51] Fraser, D. Bursting bacteria by release of gas pressure. *Nature*, **1951**, vol.167 (4236)**,** p.33-34.

[52] Lin, H.-M. Disintegration of yeast cells by pressurized carbon dioxide. *Biotechnology Progress*, **1991**, vol.7 (3)**,** p.201-204.

[53] Gaspar, F., Santos, R., King, M. B. Disruption of glandular trichomes with compressed CO_2: Alternative matrix pre-treatment for CO_2 extraction of essential oils. *Journal of Supercritical Fluids*, **2001**, vol.21 (1)**,** p.11-22.

[54] Bocevska, M., Karlović, D., Turkulov, J., Pericin, D. Quality of corn germ oil obtained by aqueous enzymatic extraction. *Journal of the American Oil Chemists' Society*, **1993**, vol.70 (12)**,** p.1273-1277.

[55] Concha, J., Soto, C., Chamy, R., Zúñiga, M. Enzymatic pretreatment on rose-hip oil extraction: Hydrolysis and pressing conditions. *Journal of the American Oil Chemists' Society*, **2004**, vol.81 (6)**,** p.549-552(4).

[56] Debenedetti, P. G., Reid, R. C. Diffusion and mass transfer in supercritical fluids. *AIChe Journal*, **1986**, vol.32 (12)**,** p.2034-2046.

[57] Beutler, H.-J., Gährs, H. J., Lenhard, U., Lürken, F. Einfluß der Lösungsmittelführung auf den Hochdruck-Extraktions-Prozeß. *Chemie-Ingenieur-Technik*, **1988a**, vol.60**,** p.773.

[58] Barton, P., Hughes, R. E. J., Hussein, M. M. Supercritical carbon dioxide extraction of peppermint and spearmint. *Journal of Supercritical Fluids*, **1992**, vol.5**,** p.157-162.

[59] Sovova, H., Kučera, J., Jež, J. Rate of the vegetable oil extraction with supercritical CO_2 - II. Extraction of grape oil. *Chemical Engineering Science*, **1994**, vol.49 (3)**,** p.415-420.

[60] Stüber, F., Vázquez, A. M., Larrayoz, M. A., Recasens, F. Supercritical fluid extraction of packed beds: External mass transfer in upflow and downflow operation. *Industrial Engineering Chemical Research*, **1996**, vol.35**,** p.3618.

[61] Reverchon, E., Marrone, C. Supercritical extraction of clove bud essential oil: isolation and mathematical modeling. *Chemical Engineering Science*, **1997**, vol.52 (20)**,** p.3421-3428.

[62] Wakao, N., Kaguei, S. "Heat and Mass Transfer in Packed Beds." Gordon and Breach Sci., New York, U.S.A., **1982**.

[63] Jones, M. C. Mass Transfer in SCFE from Solid Matrices. *In* "Supercritical Fluid Technology" T. J. Bruno and J. F. Ely (Eds.). CRC Press, Boca Raton, FL. **1991.**

[64] Puiggené, J., Larrayoz, M. A., Recasens, F. Free liquid-to-supercritical fluid mass transfer in packed beds. *Chemical Engineering Science*, **1997**, vol.52 (2)**,** p.195-212.

[65] Guardo, A., Coussirat, M., Recasens, F., Larrayoz, M. A., Escaler, X. CFD studies on particle-to-fluid mass and heat transfer in packed beds: Free convection effects in supercritical fluids. *Chemical Engineering Science*, **2007**, vol.62**,** p.5503-5511.

[66] Lim, G. B., Holder, G. D., Shah, Y. T. Mass transfer in gas-solid systems at supercritical conditions. *Journal of Supercritical Fluids*, **1990**, vol.3 (4)**,** p.186-197.

[67] Lim, G. B., Shin, H. Y., Noh, M. J., Yoo, K. P., Lee, H. Subcritical to supercritical mass transfer in gas-solid system. *Brunner, G., Perrut, M., Eds.; Proceed. 3rd. Intl. Symp. Supercrit. fluids. ISASF: Strasbourg*, **1994**.

[68] Lee, C. H., Holder, G. D. Use of supercritical fluid chromatography for obtaining mass transfer coefficients in fluid-solid systems at supercritical conditions. *Industrial Engineering Chemical Research*, **1995**, vol.34 (3)**,** p.906-914.

[69] Churchill, S. W. Comprehensive correlating equation for laminar, assisting, forced and free convection. *AIChE Journal*, **1977**, vol.23 (1)**,** p.10-16.

[70] Knaff, G., Schlünder, E. U. Mass Transfer for Dissolving Solids in Supercritical Carbon Dioxide. Part I: Resistance of the Boundary Layer. *Chemical engineering and processing*, **1987**, vol.21 (3)**,** p.151-162.

[71] Dams, A. Stoffübergang bei der überkritichen Extraktion im Festbett. *Chemie-Ingenieur-Technik*, **1989**, vol.61**,** p.712-715.

[72] Tan, C.-S., Liou, D.-C. Axial Dispersion of Supercritical Carbon Dioxide in Packed Beds. *Industrial Engineering Chemical Research*, **1989**, vol.28**,** p.1246-1250.

[73] Catchpole, O. J., Bernig, R., King, M. B. Measurement and Correlation of Packed-Bed Axial Dispersion Coefficients in Supercritical Carbon Dioxide. *Industrial Engineering Chemical Research*, **1996**, vol.35**,** p.824-828.

[74] Ghoreishi, S. M., Akgerman, A. Dispersion coefficients of supercritical fluid in fixed beds. *Separation and Purification Technology*, **2004**, vol.39 (1-2)**,** p.39-50.

[75] Funazukuri, T., Kong, C., Kagei, S. Effective axial dispersion coefficients in packed beds under supercritical conditions. *Journal of Supercritical Fluids*, **1998**, vol.13 (1-3)**,** p.169-175.

[76] Yu, D., Jackson, K., Harmon, T. C. Dispersion and diffusion in porous media under supercritical conditions. *Chemical Engineering Science*, **1999**, vol.54 (3)**,** p.357-367.

[77] Levenspiel, O. "Chemical reaction engineering." 3rd ed., John Wiley & Sons, Incorporated. **1999**.

[78] Brachet, A., Christen, P., Gauvrit, J.-Y., Longeray, R., Lantéri, P., Veuthey, J.-L. Experimental design in supercritical fluid extraction of cocaine from coca leaves. *Journal of Biochemical and Biophysical Methods*, **2000**, vol.43**,** p.353-366.

[79] Esquivel, M. M., Bernardo-Gil, M. G., King, M. B. Mathematical models for supercritical extraction of olive husk oil. *Journal of Supercritical Fluids*, **1999**, vol.16 (1)**,** p.43-58.

[80] Grosso, C., Ferraro, V., Figueiredo, A. C., Barroso, J. G., Coelho, J. A., Palavra, A. M. Supercritical carbon dioxide extraction of volatile oil from Italian coriander seeds. *Food Chemistry*, **2008**, vol.111**,** p.197-203.

[81] Naik, S. N., H., L., Maheshwari, R. C. Extraction of perfumes and flavours from plant materials with liquid carbon dioxide under liquid-vapor equilibrium conditions. *Fluid Phase Equilibria*, **1989**, vol.49**,** p.115-126.

[82] Nguyen, K., Barton, P., Spencer, J. S. Supercritical carbon dioxide extraction of vanilla. *Journal of Supercritical Fluids*, **1991**, vol.4 (1)**,** p.40-46.

[83] So, G. C., MacDonald, D. G. Kinetics of oil extraction from canola (rapeseed). *The Canadian Journal of Chemical Engineering*, **1986**, vol.64**,** p.80-86.

[84] Kandiah, M., Spiro, M. Extraction of ginger rhizome: kinetic studies with supercritical carbon dioxide. *International Journal of Food Science and Technology*, **1990**, vol.25**,** p.328-338.

[85] Crank, J. "The Mathematics of Diffusion." Clarendon Press, Oxford. **1975**.

[86] Bartle, K. D., Clifford, A. A., Hawthorne, S. B., Langenfeld, J. J., Miller, D. J., Robinson, R. A model for dynamic extraction using a supercritical fluid. *Journal of Supercritical Fluids*, **1990**, vol.3**,** p.143-149.

[87] Bartle, K. D., Boddington, T., Clifford, A. A., Hawthorne, S. B. The effect of the solubility on the kinetics of dynamic supercritical-fluid extraction. *Journal of Supercritical Fluids*, **1992**, vol.5 (3)**,** p.207-212.

[88] Reverchon, E., Donsi, G., Osseo, L. S. Modeling of supercritical fluid extraction from herbaceous matrices. *Industrial Engineering Chemical Research*, **1993**, vol.32 (11)**,** p.2721-2726.

[89] Goto, M., Roy, B. C., Hirose, T. Shrinking-core leaching model for supercritical-fluid extraction. *Journal of Supercritical Fluids*, **1996**, vol.9**,** p.128-133.

[90] Goto, M., Sato, M., Hirose, T. Extraction of peppermint oil by supercritical carbon dioxide. *Journal of Chemical Engineering of Japan*, **1993**, vol.26**,** p.401-407.

[91] Villermaux, J. Chemical engineering approach to dynamic modelling of linear chromatography. Flexible method for representing complex phenomena from simple concepts. *Journal of Chromatography*, **1987**, vol.406**,** p.11-26.

[92] Lack, E. A. Kriterien zur Auslegung von Anlagen für die Hochdruckextraktion von Naturstoffen. *Ph.D.Thesis*. TU Gratz, **1985**.

[93] Sovova, H. Rate of the vegetable oil extraction with supercritical CO_2 - I. Modelling of extraction curves. *Chemical Engineering Science*, **1994**, vol.49 (3)**,** p.409-414.

[94] Sovova, H. Mathematical model for supercritical fluid extraction of natural products and extraction curve evaluation. *Journal of Supercritical Fluids*, **2005**, vol.33**,** p.35-52.

[95] Zizovic, I., Stamenic, M., Orlovic, A., Skala, D. Supercritical carbon dioxide extraction of essential oils from plants with secretory ducts: Mathematical modelling on the micro-scale. *Journal of Supercritical Fluids*, **2007**, vol.39 (3)**,** p.338-346.

[96] Bertucco, A., Vetter, G., Eds. (2001). High Pressure Process Technology: Fundamentals and Applications. Vol. 9. Industrial Chemistry Library: Elsevier Science B. V.

[97] Allaf, K., Louka, N., Bouvier, J. M., Parent, M., Forget, M. Procédé de traitement de produits biologiques et installation pour la mise en œuvre d'un tel procédé., F. patent. Patent no. 9309726. **1993**.

[98] Allaf, K. Approche à l'analyse fondamentale de l'expansion par alvéolation selon différents procédés (puffing, cuisson-extrusion…). *Report DTAI.* Université de Technologie de Compiègne, **1988**.

[99] Overend, R. P., Chornet, E. Fractionation of lignocellulosics by steam-aqueous pretreatments. *Philosophical Transactions of the Royal Society of London, A*, **1987**, vol.321**,** p.523-536.

[100] Allaf, K. (2002). Analyse de l' instantanéité dans les Processus Thermodynamiques; Lois Fondamentales de la Thermodynamique de l' instantanéité. *In* "1er Symposium Franco-Libanais sur les technologies et études en Génie des Procédés et Biochimie", Beyrouth.

[101] Al Haddad, M. Contribution théorique et modélisation des phénomènes instantanés dans les opérations d' autovaporisation et de déshydratation. *PhD. Thesis*. Université de La Rochelle. La Rochelle, **2007**.

[102] Kristiawan, M., Sobolik, V., Al-Haddad, M., Allaf, K. Effect of pressure-drop rate on the isolation of cananga oil using instantaneous controlled pressure-drop process. *Chemical Engineering and Processing*, **2008**, vol.47 (1)**,** p.66-75.

[103] Sahyoun, W. Maîtrise de l'aptitude de matériaux agro-alimentaires aux procédés de séchage. Etude de l'adéquation entre les états structuraux, biochimiques, physiques et comportementaux sur les processus de déshydratation. *PhD. Thesis*. Université de Technologie de Compiègne. Compiègne, **1996**.

[104] Haddad, J., Louka, N., Gadouleau, M., Juhel, F., Allaf, K. Application du nouveau procédé de séchage/ texturation par détente Instantanée Contrôlée (DIC) aux poissons: impact sur les caractéristiques physicochimiques du produit fini. *Sciences des aliments*, **2001**, vol.21 (5)**,** p.481-498.

[105] Rakatozafy, H. D. Application du nouveau procédé de Deshydratation par Détentes Successives (DDS), dans le séchage des produits biologiques a haute valeur ajoutée. *PhD. Thesis*. Université de La Rochelle. La Rochelle, **2001**.

[106] Louka, N., Allaf, K. New process for texturing partially dehydrated biological products using Controlled Sudden Decompression to the vacuum. Application on potatoes. *Journal of Food Science*, **2002**, vol.67**,** p.3033-3038.

[107] Sanya, E. A., Rezzoug, S. A., Allaf, K. The conservation of achaeological waterlogged wood by using starch impregnation coupled with thermal treatment process. *Science and Technology for Cultural Heritage*, **2005**, vol.14**,** p.37-51.

[108] Klima, L. Chauffage des matériaux par micro-ondes. Application à la technologie DIC. *PhD. Thesis*. Université de La Rochelle. La Rochelle, **2006**.

[109] Rezzoug, S. A., Baghdadi, M. W., Louka, N., C., B., Allaf, K. Study of a new extraction process: controlled instantaneous decompression. Application to the extraction of essential oil from rosemary leaves. *Flavour and Fragrance Journal*, **1998**, vol.13**,** p.251-258.

[110] Kristiawan, M., Sobolík, V., Allaf, K. Isolation of Indonesian cananga oil by instantaneous controlled pressure drop. *Journal of Essential Oil Research*, **2008**, vol.20 (2)**,** p.135-146.

[111] Allaf, K., Cioffi, F., Rezzoug, S., Contento, M. P., Louka, N., Sanya, E. Procédé de traitement en vue de sécher, conserver, préserver, restaurer ou consolider le bois naturel, détérioré ou gorgé d'eau, et installation pour la mise en œuvre d'un tel procédé., Patent no. 97/14513. **1997**.

[112] Westerman, D., Santos, R. C. D., Bosley, J. A., Rogers, J. S., Al-Duri, B. Extraction of Amaranth seed oil by supercritical carbon dioxide. *Journal of Supercritical Fluids*, **2006**, vol.37**,** p.38-52.

[113] Kopcak, U., Mohamed, R. S. Caffeine solubility in supercritical carbon dioxide/co-solvent mixtures. *Journal of Supercritical Fluids*, **2005**, vol.34**,** p.209-214.

[114] Kurnik, R. T., Holla, S. J., Reid, R. C. Solubility of solids in supercritical carbon dioxide and ethylene. *Journal of Chemical and Engineering Data*, **1981**, vol.26 (1)**,** p.47-51.

[115] Liang-sun, L., Jin-feng, H., Oy-xing, Z. Solubilities of solid benzoic acid, phenanthrene, and 2,3-dimethylhexane in supercritical carbon dioxide. *Journal of Chemical Engineering Data*, **2001**, vol.46 (5)**,** p.1156 -1159.

[116] Newman, M. S., Deno, N. C. Behavior of organic compounds in 100% sulfuric acid. *Journal of the American Chemical Society*, **1951**, vol.73**,** p.3651-3653.

[117] Furuya, T., Teja, A. S. The solubility of high molecular weight *n*-alkanes in supercritical carbon dioxide at pressures up to 50 MPa. *Journal of Supercritical Fluids*, **2004**, vol.29**,** p.231-236.

[118] Bamberger, T., Erickson, J. C., Cooney, C. L. Measurement and Model Prediction of Solubilities of Pure Fatty Acids, Pure Triglycerides, and Mixtures of Triglycerides in Supercritical Carbon Dioxide. *Journal of Chemical and Engineering Data*, **1988**, vol.33**,** p.327-333.

[119] Soares, B. M. C., Gamarra, F. M. C., Paviani, L. C., Gonçalves, L. A. G., Cabral, F. A. Solubility of triacylglycerols in supercritical carbon dioxide. *Journal of Supercritical Fluids*, **2007**, vol.43**,** p.25-31.

[120] del Valle, J. M., Aguilera, J. M. An improved equation for predicting the solubility of vegetable oils in supercritical CO2. *Industrial and Engineering Chemistry Research*, **1988**, vol.27 (8)**,** p.1551-1553.

[121] Angus, S., Armstrong, B., de Reuck, K. M. *In* "International thermodynamic tables of the fluid state carbon dioxide ", p. 37-47. Oxford: Pergamon Press. **1976.**

[122] Leybros, J., Frémeaux, P. Extraction solide-liquide. Aspects théoriques. *In* "Techniques de l'Ingénieur", J2780. **1990**.

[123] Rezzoug, S. A., Boutekedjiret, C., Allaf, K. Optimization of operating conditions of rosemary essential oil extraction by a fast controlled pressure drop process using response surface methodology. *Journal of Food Engineering*, **2005**, vol.71**,** p.9-17.

[124] Peker, H., Srinivasan, M. P., Smith, J. M., McCoy, B. J. Caffeine Extraction Rates from Coffee Beans with Supercritical Carbon Dioxide. *AICHe Journal*, **1992**, vol.38 (5)**,** p.761-770.

[125] Reverchon, E., Taddeo, R. Extraction of Sage Oil by Supercritical CO_2: Influence of Some Process Parameters. *The Journal of Supercritical Fluids*, **1995**, vol.8**,** p.302-309.

[126] Roethe, A., Rosahl, B., Sockow, M., Roethe, K.-P. Physikalish-chemish begründete Beschreibung von Hochdruck-Extraktionsvorgängen. *Chem. Technik*, **1992**, vol.44**,** p.243-249.

STRUČNÉ SHRNUTÍ

1. Teoretická část

Látka se nachází v superkritickém stavu tehdy, je-li její teplota vyšší než kritická teplota a tlak vyšší než kritický tlak. V oblasti nad kritickým bodem existuje látka pouze v jedné fázi a označuje se jako superkritická tekutina. Hustota a rozpouštěcí schopnost superkritických tekutin je blízká kapalinám, ale zároveň se vyznačují nízkou kinematickou viskozitou, což jim umožňuje snadněji proniknout porézní strukturou. Lze je tedy dobře využít mimo jiné pro extrakci látek z rostlinných materiálů.

Ve srovnání s klasickými metodami získávání rostlinných extraktů, jimiž jsou destilace vodní parou a extrakce organickými rozpouštědly, je použití superkritického CO_2 jako rozpouštědla šetrnější k termolabilním látkám (kritická teplota CO_2 je 31,1°C). Je to levné a netoxické rozpouštědlo, které lze od výsledného extraktu oddělit prostým snížením tlaku pod kritickou hodnotu (kritický tlak CO_2 je 7,38 MPa). Čistým CO_2 lze extrahovat nepolární a slabě polární látky, pro extrakci polárních složek je nutné přidat v malé koncentraci polární modifikátor (nejčastěji etanol).

V laboratorním měřítku byla studována rozpustnost a optimální extrakční podmínky u široké škály nutričně a farmaceuticky významných složek, např. tokoferolů, karotenoidů, alkaloidů a nenasycených mastných kyselin. V průmyslovém měřítku je nejvýznamnější odstraňování kofeinu z kávových bobů a čajových listů a příprava extraktů z chmele pro pivovarnictví. Objem zpracovávané suroviny je v těchto případech vysoký a vysoké pořizovací náklady na extrakční zařízení jsou pak kompenzovány poměrně nízkými provozními náklady procesu. V mnohem menším měřítku jsou v průmyslu zastoupeny extrakce silic a látek významných pro farmaceutický průmysl, neboť zde je objem zpracovávané suroviny menší.

Zefektivnění samotného procesu extrakce by vedlo ke snížení celkových nákladů, a tím k jeho lepšímu využití v průmyslovém měřítku. Základními parametry při optimalizaci procesu jsou tlak a teplota, při které extrakce probíhá, délka extrakce a v neposlední řadě úprava materiálu před extrakcí. Nejčastější metodou přípravy materiálu je mechanické rozmělnění, tj. mletí, krájení, drcení či vločkování. Dochází při něm ke zmenšení velikosti částic, a tudíž ke zkrácení difúzní dráhy rozpouštědla v částici a ke zvýšení mezifázového rozhranní. Navíc se při mechanickém rozmělnění naruší buňky na povrchu částic, čímž dojde k uvolnění části extrahované složky, která byla původně v těchto buňkách uzavřena. Je ovšem mít na paměti, že je-li velikost částic příliš malá, může docházet ke ztrátě těkavých složek extraktu (zvláště při extrakcích silic) a dále ke kanálkování v prostoru extraktoru, tedy ke snížení efektivity a celkového výtěžku procesu.

Dalšími metodami úpravy materiálu jsou například vlhčení, způsobující nabobtnání materiálu a zvýšení prostupnosti buněčných stěn, nebo enzymatická hydrolýza, při které dochází k rozkladu hemicelulózy buněčné stěny. Na tento rozklad může mít vliv i samotný vysoký tlak aplikovaný

na materiál. Rovněž rychlé uvolnění tlaku CO_2 při odtlakování extraktoru se ukázalo jako způsob narušení struktur obsahujících olej.

První část této práce se zabývá právě otázkou vlivu předzpracování materiálu na výtěžek a kinetiku extrakce. Pro úpravu materiálu byl použit proces okamžité řízené expanze - DIC (z francouzského Détente Instantannée Contrôlée). Technika je založena na termomechanickém efektu vyvolaném tím, že produkt přechází velmi rychle z tlaku vodní páry několika barů do vakua. Tento přechod je termodynamicky nerovnovážným dějem, který má dva efekty. Na jedné straně je to zvýšené mechanické napětí, které vede k destrukci buněčných struktur a uvolnění těkavých látek, na straně druhé dochází k ochlazení produktu tím, že jde o adiabatickou expanzi. Toto ochlazení může zastavit degradaci termicky nestabilních látek v materiálu. Průběh zpracování je následující : materiál je vložen do autoklávu, počáteční ustavení vakua zaručuje lepší kontakt materiálu a vodní páry, která je do autoklávu následně vpuštěna; po určitou dobu probíhá ohřev za zvýšeného tlaku a poté je velmi rychle otevřen ventil spojující autokláv s rezervoárem vakua a v autoklávu prudce poklesne tlak na hodnotu kolem 5 kPa; ventil je poté opět uzavřen a následuje návrat na atmosférický tlak.

Cílem práce bylo zhodnotit strukturní změny v takto upraveném materiálu a jejich vliv na přestup hmoty během superkritické extrakce za použití matematického modelování extrakce.

Druhá část práce se věnuje vlivu směru toku na přirozenou konvekci v superkritickém extraktoru. Na rozdíl od kapalných systémů mají superkritické tekutiny větší sklon k přirozené konvekci, neboť jejich hustota je blízká kapalinám a zároveň jejich dynamická viskozita je nízká, vyznačují se tedy extrémně nízkou kinematickou viskozitou v porovnání s kapalinami i plyny (~10^{-9} m^2/s). Grashofovo číslo, charakterizující stupeň přirozené konvekce, je pro superkritické tekutiny velmi vysoké. Řada studií týkajících se extrakce z rostlin poukazuje na rozdíly ve výtěžku mezi pokusy prováděnými při toku ve směru a proti směru gravitace.

Stupeň přirozené konvekce lze vyhodnotit z měření axiální disperze v extraktoru metodou odezvy na stopovací látku. V literatuře existují studie zabývající se měřením axiální disperze v superkritickém extraktoru při toku rozpouštědla ve směru či proti směru gravitace. Autoři se shodují v tom, že směr toku rozpouštědla nemá vliv na míru axiální disperze v extraktoru, nicméně je třeba brát v úvahu fakt, že tato měření byla prováděna v čistém CO_2, nikoli při současně probíhající extrakci, a přirozená konvekce způsobená rozdílnou hustotou tekuté fáze se tedy nemohla projevit. Cílem této práce bylo sestavení experimentální aparatury a vypracování metodiky na měření odezvy v superkritickém extraktoru pro účely laboratoře, které umožní vyhodnotit axiální disperzi při současně probíhající extrakci.

2. Popis experimentální práce

Vliv modifikace struktury rostlinného materiálu na extrakci superkritickým CO_2

Jako modelové materiály byly použity sójové boby, zelené kávové boby a semena amarantu.

Část semen byla před extrakcí upravena procesem DIC, zbytek byl použit jako srovnávací vzorek. Byly připraveny dva typy vzorků – celá a mletá semena. Vzorky byly extrahovány superkrtickým CO_2 a zároveň byla provedena analýza jejich struktury metodou elektronové mikroskopie, rtuťové porosimetrie a heliové pyknometrie. U mletých vzorků bylo měřeno rozdělení velikosti částic metodou sítové analýzy. Extrakty z kávových bobů byly navíc analyzovány vysokotlakou kapalinovou chromatografií pro zjištění obsahu kofeinu. Pro stanovení celkového obsahu oleje v semenech byla použita extrakce organickým rozpouštědlem Randallovou metodou. Extrakční data byla proložena dvěma matematickými modely, pomocí nichž byly vyhodnoceny a porovnány koeficienty přestupu hmoty během extrakce.

Zpracování procesem DIC

Materiál je vložen do koše z perforované oceli a umístěn do autoklávu (1) o objemu 18 litrů. Autokláv je křídlovým ventilem (V2) oddělen od vakuové nádrže (2). Nasycená vodní pára (S1) je přiváděna do autoklávu tak, aby byl dosažen požadovaný tlak; autokláv samotný je rovněž ohříván nasycenou parou (S2). K nastolení atmosférického tlaku v autoklávu slouží ventil V3. Vakuum v nádrži je zajišťováno vývěvou (3), nádrž je chlazena vodou (W1). Kondenzát z nádrže lze odstranit otevřením ventilu V4. Pomocí manometrů a termočlánků je možno sledovat tlak a teplotu v autoklávu i v nádrži vakua.

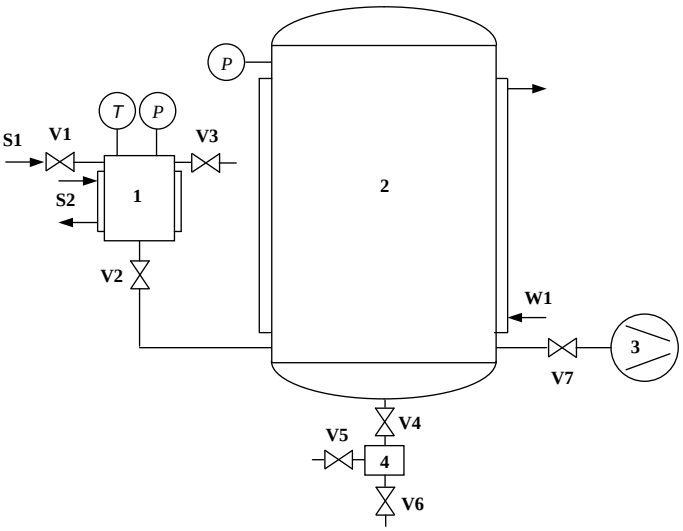

Obr. 1. Schéma aparatury procesu DIC.

Superkritická extrakce

Oxid uhličitý z tlakové lahve je čerpán vysokotlakým čerpadlem (1) do zásobníku (2), ve kterém je udržován požadovaný tlak, a dále přes uzavírací ventil (3) veden do extraktoru (4) uloženého ve vodní

lázni (5) vyhřáté na žádanou teplotu. K předehřátí CO_2 dochází již ve vstupní kapiláře ponořené rovněž do lázně. Tekutá fáze (CO_2 + extrakt) je z extraktoru odváděna do expanzního ventilu (6), kde dochází k uvolnění tlaku, CO_2 uniká jako plyn a extrakt je zachytáván ve U-trubici (7). Pravidelně během extrakce je U-trubice vážena, aby bylo možné sledovat přírůstek extraktu. Průtok rozpouštědla je nastaven ručně mikrometrickým expanzním ventilem a je odečítán na průtokoměru (8).

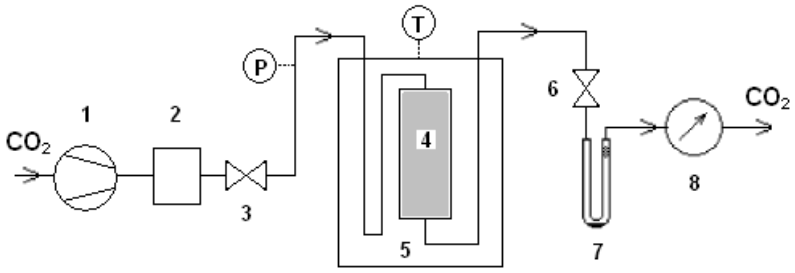

Obr. 2. Schéma aparatury superkritické extrakce.

Vzorky semen amarantu a sójových bobů byly extrahovány při tlaku 28 MPa a teplotě 40°C, vzorky kávy při tlaku 24 MPa a 50°C. U všech pokusů byl nastaven průtok 0.5 l/min (objem plynného CO_2 při laboratorní teplotě ~25°C). Mleté vzorky a vzorky amarantu byly extrahovány v extraktoru o objemu 12 ml a vnitřním průměru 8 mm, na celé boby pak byl použit extraktor o objemu 150 ml a vnitřním průměru 33 mm.

Vliv přirozené konvekce rozpouštědla na extrakci superkritickým CO_2

Pro účely studia axiální disperze v superkritickém extraktoru byla sestavena aparatura pro měření odezvy na stopovací látku. Pokusy byly prováděny při podkritických podmínkách (12 MPa, laboratorní teplota ~25°C) a při superkritických podmínkách (12 MPa, 40°C). Jako stopovací látka byla použita kyselina benzoová.

Popis aparatury

Oxid uhličitý z tlakové lahve je čerpán vysokotlakým čerpadlem (1) odděleným od zbytku aparatury uzavíracím ventilem (2). Samotná testovací jednotka se skládá z dávkovacího ventilu (3), kolonky, ve které je uložena stopovací látka (4), a extraktoru (5). Stálá požadovaná teplota je zajištěna uložením v boxu vyhřívaném horkým vzduchem. Nástřik stopovací látky (roztok kyseliny benzoové v superkritickém CO_2) se provádí přepnutím dávkovacího ventilu; odezva je sledována UV/VIS detektorem vybaveným vysokotlakou mikrokyvetou (7) při vlnové délce 230 nm. Extraktor je naplněn skleněnými kuličkami nebo rostlinným materiálem. Za detektorem je umístěn vyhřívaný expanzní ventil (8), kde dochází k poklesu tlaku na atmosférický tlak. Extrakt a stopovací látka jsou zachytávány v U-trubici, průtok plynného CO_2 je odečítán na průtokoměru.

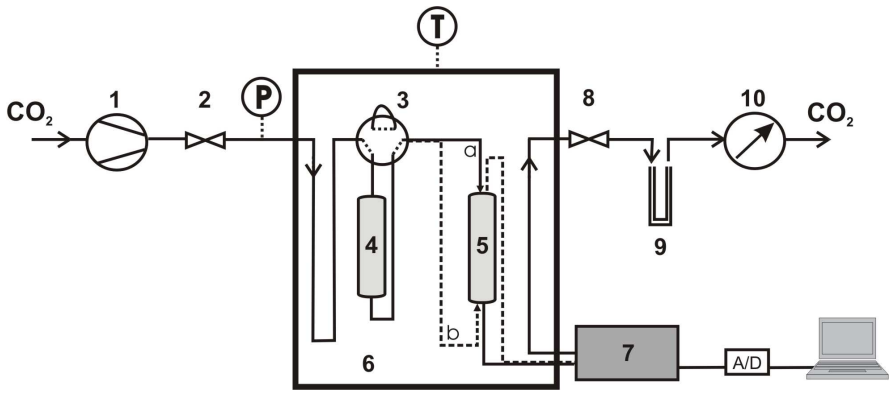

Obr. 3. Schéma aparatury pro měření odezvy na stopovací látku.

3. Přehled použitých modelů extrakce

K popisu extrakčních dat byly použity dva modely – model extrakce z celých a rozbitých buněk (model BIC, Broken and Intact Cells) a model „hot ball“ založený na difúzi z koule.

Model BIC vychází z předpokladu, že na povrchu částic, které vznikly mechanickým rozmělněním surového materiálu před extrakcí, se nachází vrstva buněk, jejichž stěny byly mechanickou úpravou poškozeny. Extrakce látek z této vrstvy je rychlá a závisí pouze na rozpustnosti extrahovaných složek v rozpouštědle. Naopak extrakce z nepoškozených buněk v jádru částice je brzděna velkým odporem buněčných struktur proti přestupu hmoty, je tedy řízena difúzí a je velmi pomalá. Model BIC popisuje tři periody extrakce: rychlou počáteční, přechodovou a pomalou fázi. Pomocí modelu lze vyhodnotit koeficienty přestupu hmoty při rychlé a pomalé extrakci. Z koeficientu přestupu hmoty lze zhruba odhadnout difúzní koeficient.

Model „hot ball“ vychází z popisu difúze z koule. V této práci je použita jeho modifikace, která zohledňuje možnost nenulové koncentrace na povrchu extrahovaných částic, tedy faktor omezení extrakce rozpustností dané složky v rozpouštědle. Z modelu lze vyhodnotit difúzní koeficient.

4. Výsledky a diskuse

Vliv modifikace struktury rostlin na superkritickou extrakci

Experimenty byly prováděny na třech typech semen – na semenech amarantu, na sójových bobech a zelených kávových bobech. Nejlepších výsledků bylo dosaženo v případě sójových bobů.

Semena amarantu jsou malá a jsou chráněna velmi odolnou slupkou. Úprava procesem DIC tuto slupku nenarušila, a extrakční výtěžek byl téměř zanedbatelný. Jedinou účinnou metoda se ukázalo být velmi jemné mletí; v tom případě ovšem dojde k uvolnění téměř veškerého oleje už při mletí, a jakékoli další zpracování semen amarantu před extrakcí je tedy zbytečné.

Sójové boby byly upraveny procesem DIC (vlhčení ve vodě, ohřev 1min při tlaku 0.3 MPa, poté 2 min při tlaku 0.7 MPa) a extrahovány superkritickým CO_2 při tlaku 28 MPa a teplotě 40°C.

Z výsledků získaných pomocí elektronového mikroskopu, Hg-porozimetrie a He-pyknometrie plyne, že úpravou bobů procesem DIC došlo k výrazným změnám v jejich struktuře. Původně kompaktní materiál se po úpravě stal velmi porézním, vzniklé póry o velikosti 1-0.01mm tvoří 19 % průřezu bobu, zastoupení pórů o velikosti kolem 100 nm vzrostlo asi desetkrát, u pórů velikosti okolo 10 μm to bylo až třicetkrát. Se zvýšenou porozitou souvisí i větší křehkost materiálu, která se projevila při mletí, kdy za stejných podmínek mletí byla v případě upravených bobů dosažena menší průměrná velikost částic.

Celkový obsah extraktu v bobech byl zjištěn Randallovou extrakcí hexanem. Průměrný obsah pro neupravený materiál byl zjištěn 0,193 kg/kg materiálu a pro upravený materiál 0,222 kg/kg materiálu. Tento nárůst extrakčního výtěžku je v souladu se zvýšenou porozitou, a byl pozorován i u následujících pokusů se superkritickým CO_2.

Data získaná z extrakce SCO_2 byla vynesena ve tvaru závislosti množství extraktu na proteklém množství rozpouštědla, hodnoty na osách v obr. 4 jsou převedeny na bezrozměrný tvar vydělením hmotností navážky materiálu v extraktoru. Extraktem je rostlinný olej.

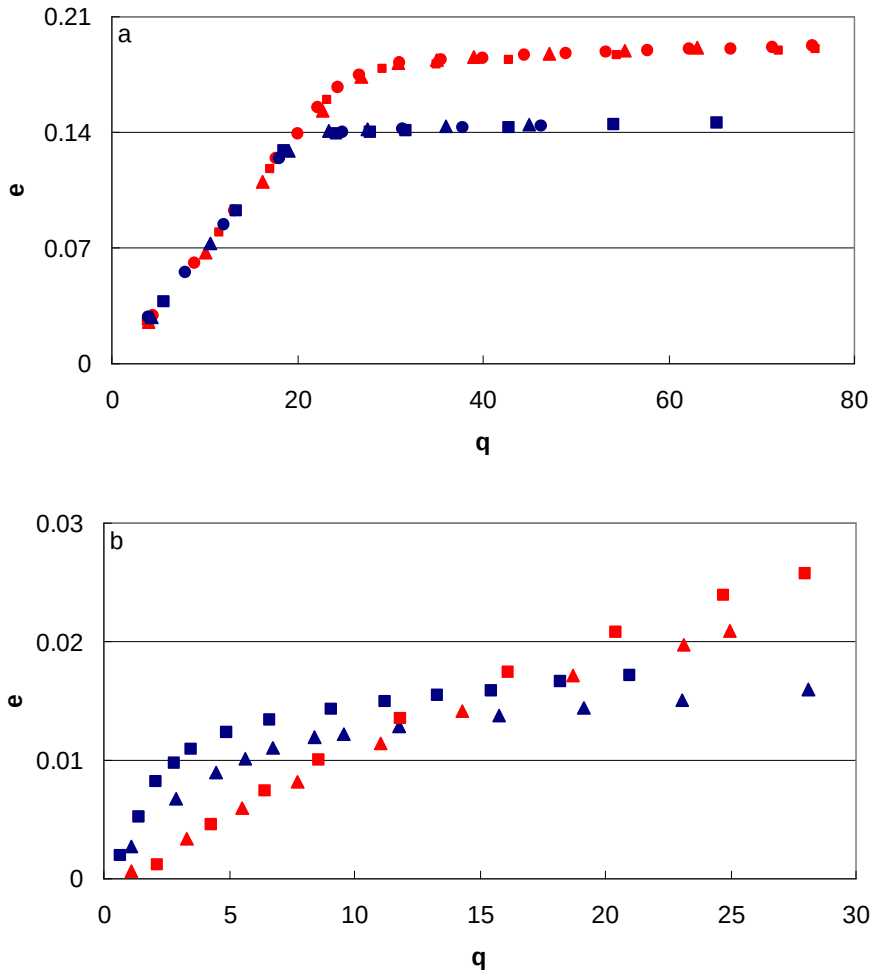

Obr. 4. Extrakční křivky mletých (a) a celých (b) sójových bobů. Modře – neupravené boby, červeně – boby upravené procesem DIC.

Extrakční data mletých bobů (Obr. 4a) vykazují standardní tvar, tedy rychlou počáteční periodu popisující extrakci dobře přístupného oleje a následnou pomalou periodou popisující extrakci z vnitřku částic. V případě celých bobů se výskyt vrstvy dobře přístupného oleje na povrchu nepředpokládá, nicméně z obr. 4b je vidět, že určité malé množství oleje na povrchu přeci jen bylo. Vysvětlením je, že povrch byl poškrábán při mechanickém odstraňování slupky bobu. Při procesu DIC, kde dochází ke kontaktu s vodní parou, byl tento olej smyt, proto extrakční křivky upravených bobů vykazují už jen pomalou periodu řízenou difúzí z částic.

Extrakce z mletých sójových bobů byla popsána modelem BIC, z něhož byly vyhodnoceny dva koeficienty přestupu hmoty – objemový koeficient přestupu hmoty v tekuté fázi, charakterizující přestup hmoty na rozhraní rozpouštěná látka/rozpouštědlo a související s rozpustností látky v rozpouštědle, a objemový koeficient přestupu hmoty v tuhé fázi, související s difúzním přestupem hmoty uvnitř částice. Z výsledků plyne, že rychlost přestupu hmoty v tekuté fázi se úpravou procesem DIC nezmění, zatímco rychlost přestupu hmoty uvnitř částic vzrostla u upravených bobů šestkrát. Toto zjištění je v souladu s výsledky pozorování strukturních změn bobů vlivem úpravy procesem DIC.

Extrakce z celých sójových bobů byla popsána modelem „hot ball“, z něhož byl vyhodnocen difúzní koeficient. Stejně jako u mletých bobů došlo po úpravě procesem DIC ke zrychlení přestupu hmoty v extrahovaných částicích; difúzní koeficient pro upravené boby je o řád vyšší něž pro boby neupravené.

Na sójových bobech byl dále testován vliv různých podmínek DIC na supekritickou extrakci. Rozdíly mezi naměřenými daty byly bohužel stejného řádu jako experimentální chyba, proto nemohl být vyhodnocen požadovaný závěr. Nicméně lze konstatovat, že jakkoli byly nastaveny podmínky procesu DIC, extrakční data vždy ukazovala zrychlení pomalé části v porovnání s daty pro neupravené boby.

Zelené kávové boby byly upraveny procesem DIC (vlhčení vodou, ohřev 45 s při tlaku 0.5 MPa) a extrahovány superkritickým CO_2 při tlaku 24 MPa a teplotě 50°C.

U zelených kávových bobů se vliv úpravy DIC na strukturu materiálu neprojevil. Porozita se zvýšila pouze na úrovni velmi malých pórů o velikosti kolem 10 nm, které nemají významný vliv na zvýšení rychlosti extrakce.

Na rozdíl od sójových bobů, kdy v případě mletých i celých bobů byl extraktem rostlinný olej, u kávových bobů se charakter extraktů lišil. Extrakt z mletých bobů je stejně jako u sójových bobů tvořen olejem, z celých bobů se však již olej neextrahuje a extrakt má charakter bílého prášku, jehož podstatnou část tvoří kofein. Stejně jako u průmyslových extrakcí, i v našich laboratorních pokusech byly boby před extrakcí navlhčeny vodou. Kofein je totiž polární látka, která se ve slabě nepolárním CO_2 nerozpouští, a je tedy nutno do systému přidat polární složku. Navíc se pravděpodobně voda podílí na narušení chemických vazeb, kterými je kofein zachycen v rostlinné matrici. Vysvětlením, proč se z celých bobů neextrahuje olej, může být právě přítomnost vody, která brání hydrofobnímu oleji pronikat extrahovanou částicí. U získaných extraktů jsme provedli analýzu vysokotlakou kapalinovou chromatografií za účelem stanovení obsahu kofeinu. Výsledky ukazují, že v extraktech

z mletých bobů tvoří kofein asi 8%, zatímco extrakty z celých bobů obsahují více než 60% kofeinu. Extrakční data a vyhodnocené koeficienty přestupu hmoty v extrahovaných částicích ukazují, že úpravou materiálu procesem DIC nedošlo ke zrychlení extrakce. Tento výsledek je ve shodě s tím, že struktura bobů se po úpravě nijak výrazně nezměnila. Navíc se v literatuře uvádí, že při extrakci z kávových bobů probíhá přenos hmoty v částici z převážné části přestupem přes buněčné stěny a jen malá část připadá na přestup póry. Extrakce je tedy usnadněna už samotným namáčením bobů, které způsobí, že rostlinné struktury nabobtnají a stanou se propustnější, bez ohledu na to, zda byl materiál ošetřen procesem DIC nebo ne. Koeficienty přestupu hmoty samotného kofeinu jsme bohužel nemohli ze získaných extrakčních dat vyhodnotit, neboť díky nízké rozpustnosti kofeinu v rozpouštědle byla jeho extrakce řízena právě rozpustností. Vliv úpravy materiálu před extrakcí by se tudíž nemohl nijak projevit, ani v případě, že by nějaký byl.

Vliv přirozené konvekce rozpouštědla na superkritickou extrakci

Odezva na stopovací látku byla sledována při toku rozpouštědla extraktorem ve směru a proti směru gravitace. Data v podobě napětí (mV) získaná z UV/VIS detektoru byla přepočtena na absorbanci a pomocí Lambert-Beerova zákona převedena na koncentraci stopovací látky. Odtud byla vypočtena střední doba prodlení a rozptyl píku a vyhodnocena distribuce dob prodlení E(t) pro jednotlivé pokusy. Pokusy byly nejprve prováděny při podkritických podmínkách (12 MPa, ~25°C) s extraktorem naplněným pouze inertními skleněnými kuličkami. Porovnání výsledků pro dva různé průtoky ukazuje, že při nízkém průtoku (0,5 ml/min stlačeného CO_2) je charakter proudění ovlivněn přítomností stopovací látky. Při toku vzhůru byla totiž pozorována větší disperze píku, která ukazuje na promíchávání uvnitř extraktoru vlivem rozdílů hustoty rozpouštědla způsobených přítomností stopovací látky. Po zvýšení průtoku na 1ml/min se tento efekt již neprojevuje.

Dalším krokem byla volba extrahovaného systému. Při extrakci z přírodního materiálu (konkrétně šlo o extrakci oleje z mletých sójových bobů) se ukázalo, že stopovací látka je zcela adsorbována na materiál, proto byla pro další pokusy zvolena alternativní možnost – nanesení vybrané extrahované látky na inertní skleněné kuličky. Pro pokusy v podkritické oblasti byl vybrán tetrakosan, který pak byl v pokusech za superkritických podmínek nahrazen trilaurinem.

Měření odezvy na stopovací látku během extrakce za superkritických podmínek (12 MPa, 40°C) ukázalo výrazný rozdíl v disperzi píku ve srovnání s výsledky pro tok rozpouštědla přes čisté skleněné kuličky. Při toku proti směru gravitace navíc dochází k velkému rozmytí píku, což naznačuje, že charakter proudění je opravdu ovlivněn přirozenou konvekcí v extraktoru. U pokusů za podkritických podmínek se tento efekt neprojevil, což je vysvětlitelné tím, že při těchto podmínkách je CO_2 ještě kapalný a kapaliny nejsou tolik náchylné ke vzniku přirozené konvekce jako superkritické tekutiny. Dalším studiem je třeba ověřit, nakolik se na pozorovaném rozmytí píku projeví vedlejší jevy, tedy již zmíněný vliv přítomnosti samotné stopovací látky a dále možné stékání extrahované látky po náplni z kuliček (trilaurin je za použitých podmínek kapalný).

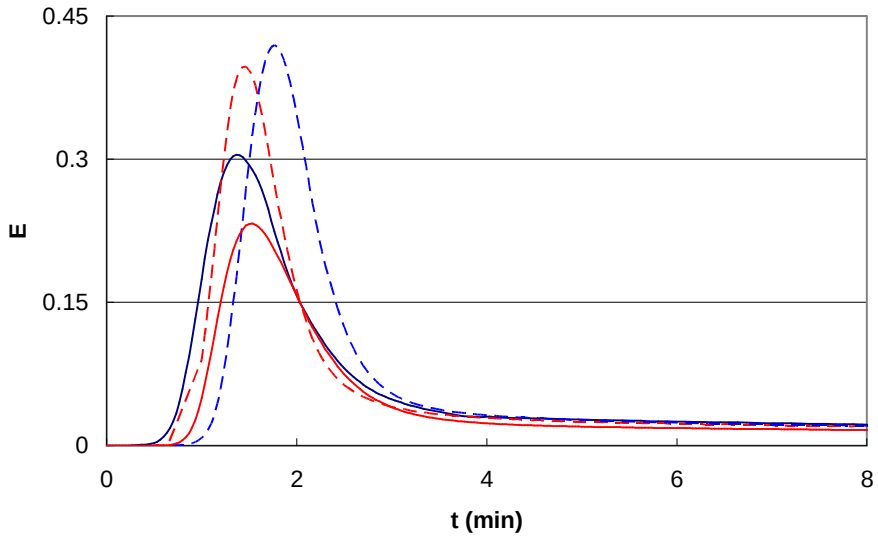

Obr. 5. Porovnání distribuce dob prodlení dat získaných během extrakce tetrakosanu podkritickým (kapalným) CO_2, (—) s daty odpovídajícími pokusům bez extrakce (---). Červeně – tok proti směru gravitace, modře – tok ve směru gravitace. Průtok stlačeného CO_2 (12 MPa, 25°C) je 1 ml/min. Extraktor o průměru 8 mm a délce 8 cm byl naplněn skleněnými kuličkami.

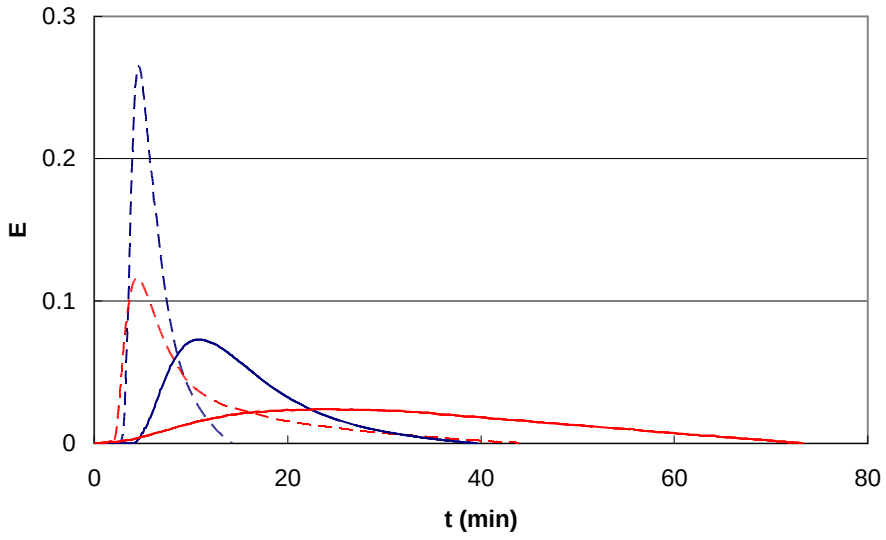

Obr. 6. Porovnání distribuce dob prodlení dat získaných během extrakce trilaurinu superkritickým CO_2, (—) s daty odpovídajícími pokusům bez extrakce (---). Červeně – tok proti směru gravitace, modře – tok ve směru gravitace. Průtok stlačeného CO_2 (12 MPa, 25°C) je 1 ml/min. Extraktor o průměru 8 mm a délce 15 cm byl naplněn skleněnými kuličkami.

5. Závěr

Tato práce se zabývá dvěma problémy souvisejícími s účinností procesu superkritické extrakce.
V první části byl studován vliv modifikace struktury rostlinného materiálu na superkritickou extrakci, konkrétně vliv úpravy materiálu procesem okamžité řízené expanze (DIC) na rychlost a výtěžek

extrakce superkritickým CO_2. Technika DIC byla aplikována na semena amarantu, sójové boby a zelené kávové boby.

Nejvýraznější změna struktury byla pozorována u sójových bobů. Vyhodnocením extrakčních dat bylo zjištěno, že extrakce z vnitřku extrahovaných částic (tedy řízená difúzí) byla výrazně urychlena v případě bobů předem zpracovaných technikou DIC. Naproti tomu struktura semen amarantu a zelených kávových bobů nebyla touto technikou ovlivněna, změny se neprojevily ani na rychlosti extrakce z částic. Vliv měnících se podmínek procesu DIC na průběh superkritické extrakce nemohl být vyhodnocen, jelikož rozdíly mezi naměřenými daty pro jednotlivé pokusy byly v řádu experimentální chyby.

Závěrem můžeme konstatovat, že technika DIC může být s výhodou použita pro úpravu materiálu před extrakcí v těch případech, kdy je průběh extrakce ovlivněn difúzí v extrahovaných částicích. V praxi to může být případ, kdy daný materiál nemůže být, z různých důvodů, upraven mletím a musí se extrahovat vcelku.

Druhá část práce shrnuje první výsledky měření odezvy na stopovací látku v superkritickém extraktoru za účelem určení stupně axiální disperze. V rámci této práce byla sestavena aparatura, vybrána stopovací látka a extrahovaný systém (extrahovaná látka nanesená na inertní skleněné kuličky) a provedena předběžná měření pro otestování funkčnosti metody.

Měření byla prováděna během extrakce při superkritických a podkritických podmínkách a odezva na stopovací látku byla porovnána pro tok rozpouštědla ve směru a proti směru gravitace. Bylo zjištěno, že při superkritických podmínkách je disperze píku odezvy mnohem výraznější při toku proti směru gravitace než při toku po směru gravitace. Dochází zde tedy pravděpodobně ke vzniku přirozené konvekce v důsledku rozdílů hustoty rozpouštědla podél extraktoru. U pokusů v podkritické oblasti jsme podobný jev nepozorovali.

Je nutno zdůraznit, že získané výsledky jsou pouze předběžné, v návaznosti na tuto práci bude probíhat další studium problematiky.

RESUME

1. État de l'art

On parle de fluide supercritique lorsqu'un fluide est chauffé au-delà de sa température critique et lorsqu'il est comprimé au-dessus de sa pression critique. Au-dessus de ces valeurs, le fluide n'existe que dans une seule phase. La densité et la capacité de dissolution des fluides supercritiques sont proches à celles des liquides, mais en même temps, ces fluides possèdent une viscosité cinématique très basse ce qui leur permet de pénétrer dans des structures poreuses plus facilement. Cette caractéristique, permet l'utilisation des fluides supercritiques lors des extractions des composés contenus dans les plantes.

En comparaison avec des méthodes classiques d'extraction (l'hydrodistillation et l'extraction par solvants organiques), l'extraction par CO_2 supercritique possède de plusieurs avantages. Entre autres, l'extraction se fait sans dégradation des composés (du fait que la température critique de CO_2 est de 31,1°C), par ailleurs, le CO_2 est d'une part pas trop couteux et d'autre part non-toxique car il peut être facilement séparé de l'extrait par une simple décompression. L'utilisation de CO_2 pur permet d'extraire les composés apolaires et légèrement polaires; pour obtenir des composées polaires, il est nécessaire d'ajouter un modificateur polaire (il s'agit le plus souvent de l'éthanol).

Au niveau de laboratoire, la solubilité et les conditions optimales ont été étudiées pour certains composés de haute valeur ajoutée en nutrition et en pharmacie, tels que les tocophérols, les caroténoïdes, les alcaloïdes et les acides gras insaturés. Parmi les applications industrielles de l'extraction supercritique, les plus importantes sont la production du café décaféiné et les extraits du houblon utilisés dans la brasserie. La quantité du matériel traitée est assez grande dans ces cas, les coûts d'investissement sont donc ainsi compensés par les frais de fonctionnement relativement bas. L'extraction des huiles essentielles et des composés pour l'industrie pharmaceutique n'est pas aussi représentée au niveau industriel, parce que la quantité du matériel traité est plus petite que dans des cas du café et du houblon.

Une augmentation de l'efficacité de l'extraction supercritique pourrait rendre le procédé moins cher et donc plus intéressant pour des applications industrielles. Les principaux paramètres d'optimisation du procédé sont les conditions d'extraction, c'est-à-dire la pression et la température, puis la durée d'extraction et non en dernier lieu le prétraitement de la matière primaire avant l'extraction. La technique de prétraitement la plus répandue est la désintégration mécanique représentée par le broyage, l'écrasement ou la floculation. Elle provoque une diminution de taille des particules, et par conséquent un raccourcissement du parcours de diffusion dans les particules et une augmentation de l'interface. De plus, pendent la désintégration, les cellules à la surface des particules sont écrasées et une partie du soluté, initialement enfermé dans ces cellules, est libérée. Néanmoins, il faut noter qu'avec des particules trop fines deux inconvénients apparaissent – une perte des composés les plus

volatiles (ce qui est important surtout pour l'extraction des huiles essentielles) et une création des canaux (chanelling) dans l'extracteurs qui baisse le rendement et l'efficacité du procédé.

Les méthodes alternatives de prétraitement sont par exemple l'humidification qui rend le matériel gonflé et les parois cellulaires plus perméables, ou l'hydrolyse enzymatique qui provoque une décomposition des parois cellulaires. La haute pression elle-même peut participer à la décomposition. La décompression rapide de l'extracteur a prouvé aussi une capacité de rompre des structures végétales contenant l'huile.

La première partie de la thèse concerne justement l'effet de prétraitement du matériel sur le rendement et la cinétique de l'extraction. Le procédé de Détente Instantanée Contrôlée (DIC) a été appliqué comme une technique de prétraitement. Le procédé est basé sur un effet thermomécanique induit lorsque le produit passe rapidement d'une pression de vapeur d'eau de quelques bars vers le vide. Ce passage qui met le système en déséquilibre thermodynamique a deux effets principaux, d'une part une contrainte mécanique élevée qui conduit à l'éclatement des cellules et la libération de molécules volatiles et d'autre part un refroidissement intense lié au fait que l'extrait soit libéré sous forme gazeuse dans un réservoir sous vide, ce qui permet de stopper toute réaction de dégradation thermique. La description du procédé est suivante : un échantillon est placé dans la chambre de traitement où le vide primaire est ensuite instauré par ouverture de la vanne de détente qui relie la chambre de traitement au réservoir à vide. Cette première mise sous vide permet d'assurer un meilleur contact du matériel avec la vapeur d'eau saturée qui est ensuite injectée dans la chambre de traitement. La pression de consigne est maintenue constante pendant la durée de traitement (fixée au départ) et puis, l'instauration de vide (~5kPa) par détente est établie d'une façon quasi-instantanée. Ensuite, la vanne de détente est fermée et la pression atmosphérique est rétablie dans la chambre de traitement.

La deuxième partie de la thèse concerne la convection naturelle dans un extracteur supercritique. A la différence des liquides, les fluides supercritiques inclinent plus à la développement de la convection naturelle, parce que leur densité est proche à celle des liquides, mais leur viscosité dynamique est basse, ce qui fait que leur viscosité cinématique est énormément basse en comparaison avec les liquides et les gaz (~10^{-9} m^2/s). Ainsi, le nombre de Grashof qui caractérise la convection naturelle est très grand pour les fluides supercritiques. Plusieurs études expérimentales montrent des différences en rendement trouvées pour les expériences réalisées avec l'écoulement du solvant dans le sens de la pesanteur et dans le sens opposite.

L'effet de la convection naturelle peut être évalué à partir de l'étude de la dispersion axiale mesurée par la méthode de réponse à l'injection du traceur dans l'extracteur. Les publications concernant l'étude de la dispersion axiale dans des conditions supercritiques ont examiné l'effet de la direction d'écoulement du solvant. Aucun effet n'a été constatée, cependant il faut noter que toutes les expériences ont été réalisées avec du CO_2 pure et aucune extraction n'a eu lieu pendant les expériences, donc la convection naturelle n'a pas pu se développer. Cette étude a pour le but de développer au sein de laboratoire une installation expérimentale pour mesurer la réponse

à l'injection du traceur qui permettra d'évaluer le degré de la dispersion axiale dans l'extracteur pendant l'extraction supercritique.

2. Matériel et Méthodes

L'effet de la modification de structure des végétaux sur l'extraction supercritique

Les tests ont portés sur trois grains différents: les grains d'amarante, de soja et les grains verts de café. Une partie des grains a été traitée par le procédé DIC, le reste a été gardé comme le témoin. Deux types d'échantillons ont été préparés – les grains broyés et les grains entiers. Les échantillons ont été extraits par le CO_2 supercritique, la structure interne des grains a été observée par la microscopie électronique à balayage, la porosimétrie à mercure et la pycnométrie à hélium. Pour le matériel broyé, l'analyse des tailles des particules a été faite. Les extraits des grains de café ont été analysés par la chromatographie en phase liquide à haute performance (HPLC) pour déterminer la concentration de caféine. Le contenu total en huile a été déterminé par extraction par solvant organique en utilisant la méthode d'extraction de Randall. Deux modèles mathématiques ont été appliqués pour traiter les données expérimentales ; les coefficients de transfert de masse pendant l'extraction ont été calculés à partir de ces modèles.

Traitement par le procédé DIC

Le matériel est placé dans un panier d'acier perforé et introduit dans la chambre de traitement de volume de 18 litres (1). La chambre de traitement est liée avec le réservoir à vide (2) par une vanne de détente (V2). La vapeur saturée sert premièrement à chauffer le matériel sous la pression demandée (S1), et en même temps la chambre de traitement elle-même est chauffée par la vapeur circulant dans sa double enveloppe (S2).

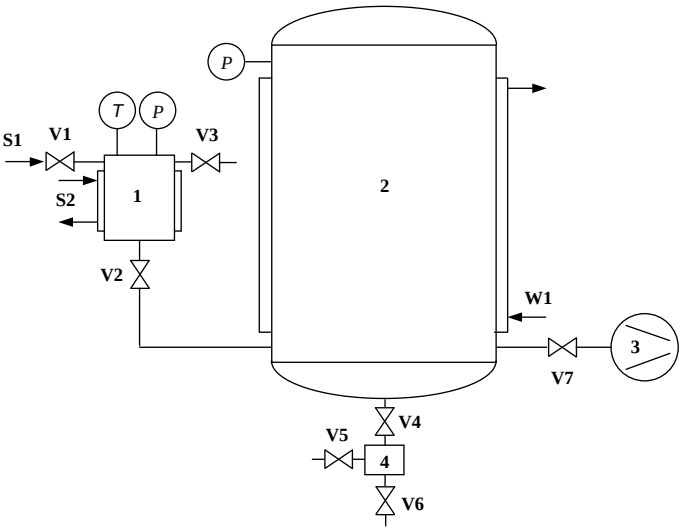

Figure 1. Le dispositif expérimental du procédé DIC.

La restauration de la pression atmosphérique dans la chambre de traitement est faite par la vanne V3. Le réservoir à vide est lié à une pompe à vide et il est refroidi par l'eau (W1). Le condensat est

récupéré par la vanne V4. La température et la pression dans la chambre de traitement sont suivies par le système des thermocouples et des manomètres.

Extraction supercritique

Le CO_2 sortant d'une bouteille à pression est comprimé par une pompe à haute pression (1). Un réservoir (2) sert à maintenir la pression constante. Puis le fluide est introduit dans l'extracteur (4) par une vanne d'arrêt (3). L'extracteur avec le capillaire d'entrée est placé dans un bain-marie (5) maintenu à la température d'extraction. Le CO_2 est donc préchauffé déjà dans le capillaire. Le fluide à la sortie de l'extracteur passe par un expandeur (6). La décompression vers la pression atmosphérique aboutit à la séparation de l'extrait dans un U-tube (7) et le CO_2 sous forme gazeuse s'échappe. Le poids de l'extrait est déterminé régulièrement pendant l'extraction; le débit de solvant est réglé par une vanne micrométrique et contrôlé par un débitmètre (8).

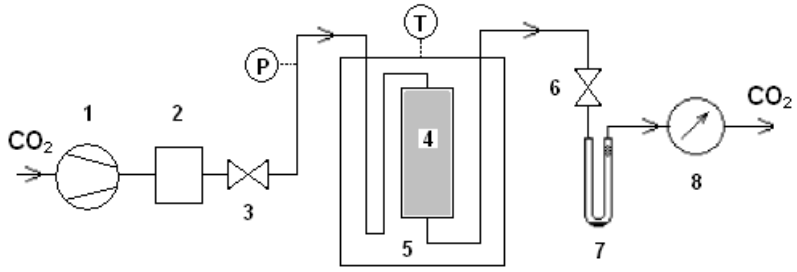

Figure 2. Le dispositif expérimental de l'extraction par CO_2 supercritique.

Les grains d'amarante et de soja ont été extraits à la pression de 28 MPa et 40ºC, ceux du café à 24 MPa et 50ºC. Le débit de solvant de 0,5 l/min (de CO_2 gazeux à la température de laboratoire ~25ºC, pression atmosphérique) a été fixé pour toutes les expériences. Les échantillons broyés ont été extraits dans un extracteur de 12 ml en volume et 8 mm en diamètre ; pour les grains entiers, un extracteur de 150 ml de 33 mm en diamètre a été utilisé.

L'effet de la convection naturelle dans le solvant sur l'extraction supercritique

Un dispositif expérimental construit pour l'étude de la dispersion axiale dans l'extracteur supercritique est schématisé sur la Figure 3. Les expériences ont été réalisées sous les conditions subcritiques (12 MPa, température de laboratoire ~25ºC) et supercritiques (12 MPa, 40ºC). L'acide benzoïque a été employé comme traceur.

Description du dispositif expérimental

Le CO_2 sortant d'une bouteille à pression est comprimé par une pompe à haute pression (1) qui peut être séparée du reste de l'installation par une vanne d'arrêt (2). La section de test est constituée de la vanne de commutation (3), la colonne avec le traceur (4) et l'extracteur (5). La température est maintenue constante par un box chauffé par l'air chaud (6). L'injection du traceur (solution de l'acide benzoïque dans le CO_2 supercritique) est réalisée par la vanne de commutation; la réponse est analysée

par le détecteur UV/VIS équipé d'une micro-cuvette résistante à haute pression. La longueur d'onde de 230 nm a été utilisée pour la détection. L'extracteur est rempli de billes en verre de 2 mm de diamètre ou de matériel végétal. La décompression vers la pression atmosphérique est réalisée par la vanne d'expansion (8). L'extrait et le traceur sont récupérés dans un U-tube, le débit du CO_2 gazeux est mesuré par un débitmètre.

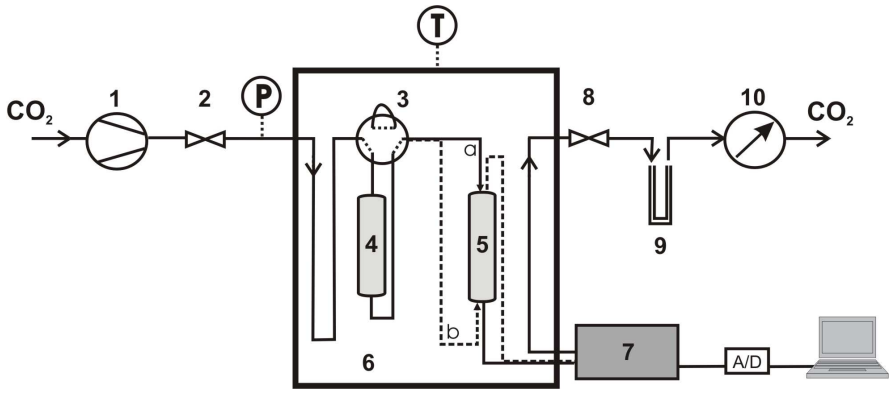

Figure 3. Le dispositif expérimental pour l'étude de dispersion axiale.

3. Modélisation de l'extraction

Deux modèles mathématiques ont été appliqués pour décrire les données expérimentales – modèle de l'extraction des cellules cassées et des cellules intactes (model BIC ; Broken and Intact Cells) et modèle « hot ball » basé sur la diffusion dans une sphère.

Modèle BIC présume qu'à la surface d'une particule d'un grain ayant subit une désintégration mécanique, il y a une région de cellules cassées par la désintégration. Extraction de la région des cellules cassées est rapide et sa vitesse ne dépend que de la solubilité du soluté dans le solvant. Par contre, l'extraction de la région des cellules intactes est très lente, elle est contrôlée par la diffusion de l'intérieur des cellules. Le modèle décrit trois périodes : une période rapide initiale, une période de transition et une période lente finale. Des coefficients de transfert de masse pour l'extraction rapide et lente peuvent être évalués à partir du modèle. Le coefficient de diffusion peut être estimé à partir du coefficient de transfert de masse.

Modèle « hot ball » décrit le transfert de masse dans une sphère. Dans cette thèse, une modification du modèle est utilisée – à la différence du modèle original, le modèle modifié tient compte de la limitation de l'extraction par la solubilité du soluté dans solvant. Ca se traduit par l'effet que la concentration du soluté à la surface des particules n'est pas forcément zéro. Le coefficient de diffusion est évalué à partir de ce modèle.

4. Résultats et Discussion

Trois grains différents ont été testés : les grains d'amarante, de soja et les grains verts de café. Les meilleurs résultats ont été obtenus pour le soja.extraits.

Les grains d'amarante sont petits et enveloppés dans une écorce rigide. Le traitement par le procédé DIC n'a pas désintégré l'écorce, et le rendement de l'extraction a été négligeable. Le broyage très fine paraît pouvoir être la seule méthode de prétraitement efficace; naturellement, à part de ce broyage qui libère la plupart d'huile, aucun autre prétraitement n'est nécessaire.

Les grains de soja ont été traités par DIC (humidification dans l'eau, traitement à 0,3 MPa pendant 1 minute suivi par 2 minutes à 0,7 MPa) et extraits par CO_2 supercritique à 28 MPa et 40ºC.

Les résultats obtenus par la microscopie électronique à balayage, la porosimétrie à mercure et la pycnométrie à hélium montrent que la structure des grains a été considérablement changée par le traitement par DIC. Le matériel initialement compact est devenu plus poreux. En effet, les pores de taille de 1-0,01 mm représentent environ 19% de la section du grain, le nombre des pores de diamètre d'environ 100 nm a augmenté dix fois, pour les pores de diamètre d'environ 10 µm, une augmentation allant jusqu'à trente fois a été notée. Une fragilité élevée liée à cette augmentation de porosité s'est manifestée pendant le broyage ; pour les mêmes conditions de broyage, les particules plus fines ont été obtenues dans le cas des grains traités par DIC.

Le contenu total de l'extrait a été déterminé par l'extraction de Randall par l'hexane. Les valeurs moyennes de 0,193 et 0,222 kg/kg de grains ont été trouvées respectivement pour les grains non-traités et traités par DIC. Cet accroissement correspond aux changements de structure des grains et il a été observé aussi pendant l'extraction supercritique.

Les données obtenues par l'extraction (les courbes d'extraction) sont présentées sur la figure 4, la masse d'extrait est tracée en fonction de masse de solvant. Les valeurs sont présentées sous forme non dimensionnelle (divisées par la masse de matériel chargé dans l'extracteur). L'extrait est une huile de soja.

Les courbes d'extraction des grains broyés (Figure 4a) ont une forme standard, c'est-à-dire il y a la période initiale rapide qui correspond à l'extraction de l'huile libérée des cellules cassées, suivie par la période lente décrivant l'extraction de l'intérieur des particules. Dans le cas des grains entiers, on ne suppose pas la présence de l'huile libre sur la surface des grains, mais on observe quand même une courte période rapide pendant l'extraction des grains non-traités (Figure 4b). Puisque les grains ont été décortiqués avant tout autre traitement, leurs surface a été rayée ce qui explique la présence d'une petite quantité d'huile. Par contre, pendant le traitement par DIC, cette huile a été probablement emportée par la vapeur ce qui fait que la période rapide n'existe pas dans le cas des grains traités par DIC.

L'extraction des grains broyés a été décrite par le modèle BIC, deux coefficients de transfert de masse ont été évalués – le coefficient volumétrique de transfert de masse en phase fluide qui caractérise

le transfert de masse des cellules cassée vers le solvant et se relie à la solubilité du soluté, et puis le coefficient volumétrique de transfert de masse en phase solide qui est en relation avec la diffusion au sein des particules. L'exploitation des résultats montre que la vitesse de transfert de masse en phase fluide ne change pas par le traitement par DIC, par contre la vitesse de transfert de masse dans les particules a augmenté de six fois après le traitement. Cette constatation est en accord avec les changements de structure des grains.

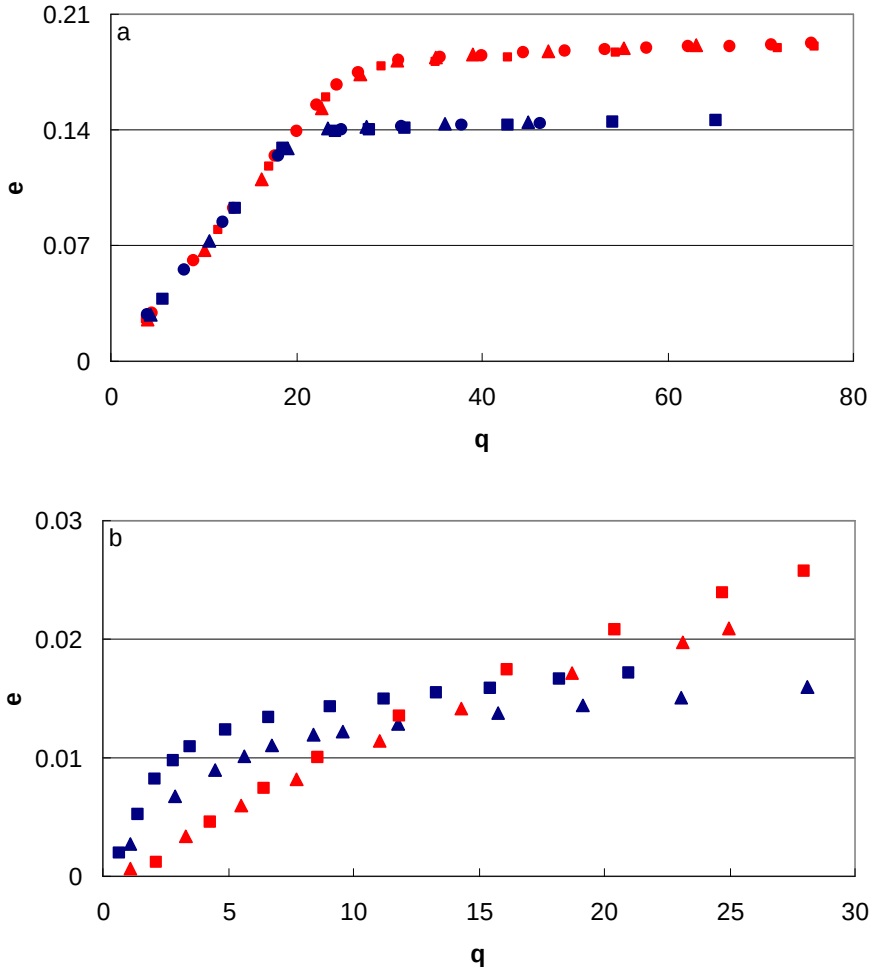

Figure 4. Les courbes d'extraction des grains broyés (a) et des grains entiers (b). Bleu – grains non-traités, rouge – grains traités par DIC.

L'extraction des grains entiers a été décrite par le model « hot ball », et le coefficient de diffusion a été évalué. De la même manière que dans le cas des grains broyés, le transfert de masse dans les particules a été accéléré après le traitement par DIC; le coefficient de diffusion a augmenté d'environ un ordre de magnitude.

Au-delà, l'effet des différentes conditions de traitement par DIC a été testé sur les grains de soja broyés. Malheureusement, les différences entres les séries des données expérimentales ont été de même grandeur que l'erreur expérimentale. Pour cette raison, l'effet n' pas pu être évalué, mais on

peut quand même constater que quoi qu'elles soient les conditions de traitement de DIC, une augmentation de la cinétique d'extraction pendant la période lente est observée.

Les grains de café ont été traités par DIC (humidification par eau, traitement à 0,7 MPa pendant 45 s) et extraits par CO_2 supercritique à 24 MPa et 50ºC.

Aucun effet significatif du traitement par le procédé DIC sur la structure du café n'a été constaté. La porosité a augmenté seulement au niveau des pores de très petite taille (environ 10 nm) qui ne sont pas significatifs pour l'augmentation de la cinétique d'extraction.

A la différence des grains de soja, où la même huile a été extraite à partir des grains broyés aussi bien que des grains entiers, la composition des extraits du café dépend de broyage. L'extrait des grains broyés est constitué de l'huile, par contre à partir des grains entiers, l'extrait est obtenu sous forme d'une poudre blanche, dans laquelle la caféine représente la majorité. Les grains ont été humidifié avant l'extraction, parce que la caféine est un composé polaire qui ne se dissout pas dans le CO_2 apolaire. L'adition d'un modificateur polaire, ce qui est l'eau dans ce cas, dans le système est nécessaire. De plus, l'eau aide probablement à rompre les valences chimiques existantes entre la caféine et la structure de la matrice végétale. L'absence d'huile, dans les extraits obtenus à partir des grains entiers, peut être expliquée justement la présence d'eau qui empêche l'huile (hydrophobe) de traverser la structure du grain. Les extraits obtenus ont été analysés par la chromatographie en phase liquide à haute performance (HPLC) pour déterminer le contenu de caféine. Dans les extraits des grains broyés la caféine représente environ 8%, par contre les extraits des grains entiers contiennent plus que 60% de caféine.

Les courbes expérimentales d'extraction et les coefficients de transfert de masse montrent que l'extraction du café n'a pas été affectée par le traitement par DIC, ce qui est en accord avec les résultats de porosimetrie. De plus, on peut trouver dans la littérature que le transfert de masse pendant l'extraction des grains de café s'effectue surtout à travers des parois cellulaires et seulement une petite partie correspond au transfert dans les pores. Alors, l'extraction est déjà facilitée par l'humidification qui provoque un gonflement du matériel et une perméabilité des parois cellulaires élevée, indépendamment du traitement par DIC. Malheureusement, les coefficients de transfert de masse correspondant à la caféine pure n'ont pas été déterminés car l'extraction de la caféine a été limitée par la faible solubilité de la caféine dans le CO_2 supercritique. De ce fait, on peut conclure que, même si il y avait un effet de la modification de structure par DIC sur l'extraction de la caféine, cet effet ne pourrait pas se manifester dans nos expériences.

L'effet de la convection naturelle dans le solvant sur l'extraction supercritique

La réponse à l'injection du traceur dans l'extracteur a été observée sous l'écoulement du solvant dans le sens de la pesanteur et dans le sens opposite. La réponse du détecteur sous forme de tension (mV) a été transformée à l'absorbance et la concentration a été calculée à partir de l'absorbance par la loi de Lambert-Beer. Puis, la distribution des temps de séjour E(t) a été déterminée, et deux moments ont

été calculés – la moyenne des temps de séjour et la variance. Tout d'abord, les expériences ont été réalisées sous conditions subcritiques (12 MPa, ~25ºC) dans l'extracteur rempli seulement par les billes en verre, sans le soluté. Les résultats obtenus pour deux différents débits de solvant montrent qu'avec le débit plus faible (0,5 ml/min de CO_2 compressé) le caractère d'écoulement est affecté par la présence du traceur. Le taux de dispersion plus important a été observé pour l'écoulement contre le sens de gravitation, ce qui signifie qu'il y a un mélange dans l'extracteur causé par des différences de densité provoquées par la présence du traceur. Le phénomène disparait lorsque le débit est plus élevé (1 ml/min). Ensuite, il a fallu choisir le système d'extraction. Tout d'abord, l'extracteur a été rempli par le matériel végétal (grains de soja broyés), mais tout le traceur injecté a été adsorbé sur la matrice, on a du donc choisir une solution alternative – un soluté déposé sur les billes en verre inertes. Tetracosane choisi pour les expériences en régime subcritique a été ensuite remplacé par trilaurine pour les essaies sous conditions supercritiques.

La mesure de réponse à l'injection du traceur pendant l'extraction sous conditions supercritiques (12MPa, 40ºC) a montré qu'il y avait une différence considérable de dispersion des pics en comparaison avec les pics correspondant au flux du solvant par les billes en verre pures. Quand le flux en contre sens de la pesanteur a été imposé, la dispersion du pic de réponse a été très large ce qui indique la présence de la convection naturelle dans l'extracteur. Cet effet n'a pas été observé sous conditions subcritiques ce qui peut être facilement expliqué, parce que le CO_2 est liquide sous ces conditions et les liquides n'inclinent pas autant à la convection naturelle que les fluides supercritiques.

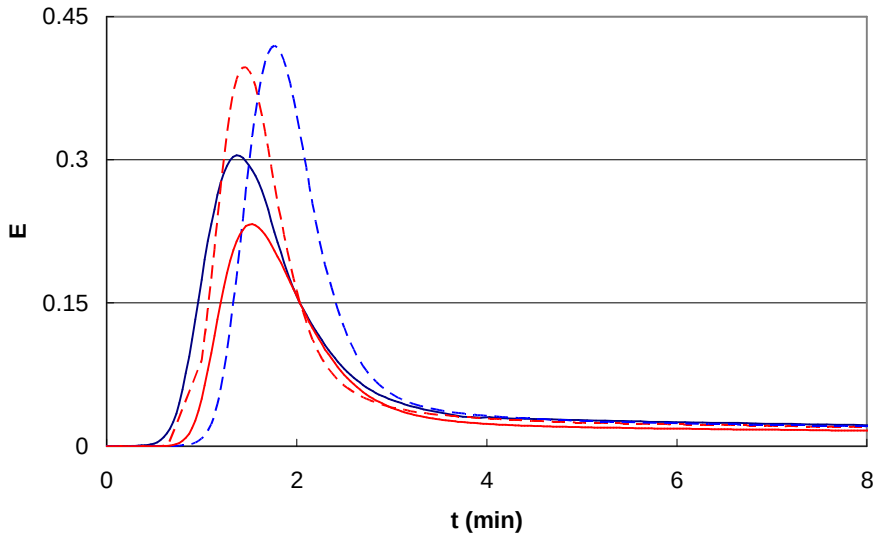

Figure 5. Distribution des temps de séjour sous conditions subcritiques : comparaison de l'écoulement pendant l'extraction de tetracosane (—) avec le flux par les billes en verre pures (---). Rouge – flux dans le sens de la pesanteur, bleu – flux dans le sens opposite à la pesanteur. Débit de CO_2 compressé (12 MPa, 25ºC) est 1 ml/min. Extracteur de diamètre de 8 mm et de longueur de 8 cm a été repli par les billes en verre.

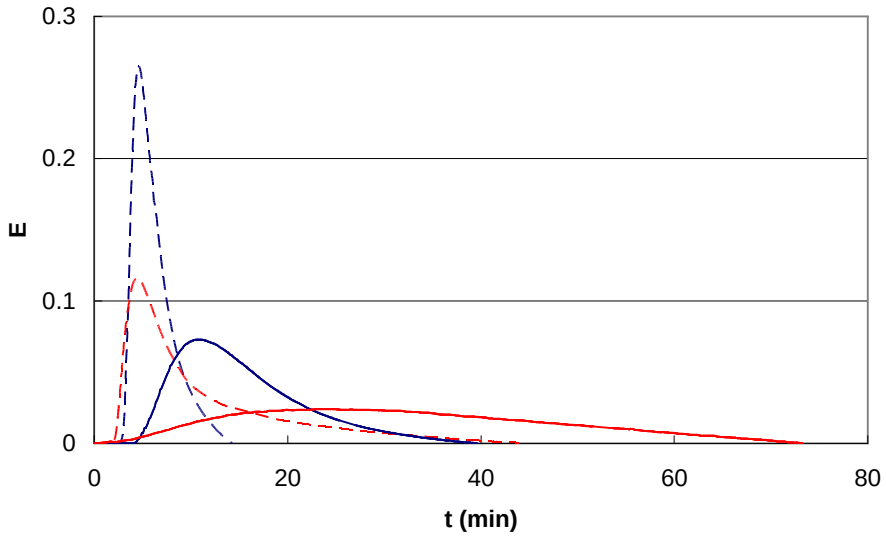

Figure 6. Distribution des temps de séjour sous conditions supercritiques : comparaison de l'écoulement pendant l'extraction de trilaurine (—) avec le flux par les billes en verre pures (---). Rouge – flux dans le sens de la pesanteur, bleu – flux dans le sens opposite à la pesanteur. Débit de CO_2 compressé (12 MPa, 25ºC) est 1 ml/min. Extracteur de diamètre de 8 mm et de longueur de 15 cm a été repli par les billes en verre.

Dans le travail à venir, il faut vérifier l'importance de l'effet des phénomènes secondaires sur la dispersion des pics. C'est premièrement l'effet du traceur et puis la possibilité que la trilaurine, qui d'ailleurs fond sur conditions imposées, déposée sur les billes, ruissèle doucement dans l'extracteur ce qui par conséquent influence le caractère d'écoulement.

Conclusions

Les travaux présentés concernent deux problèmes liés à l'efficacité de l'extraction supercritique.

La première partie est une étude de l'effet de la modification de structure des végétaux sur l'extraction supercritique, concrètement de l'effet du traitement par le procédé DIC sur la cinétique et le rendement de l'extraction par le CO_2 supercritique. La technique a été appliquée sur trois types de grains – grains d'amarante, de soja et de café.

Le changement le plus remarquable de la structure interne a été observé pour les grains de soja, et la cinétique d'extraction à partir de l'intérieur des particules (donc contrôlée par diffusion) a augmenté considérablement après le traitement par DIC. Par contre, aucun changement structural n'a été observé pour les grains d'amarante et de café, la vitesse d'extraction n'a pas changé non plus après le traitement par DIC. L'effet des conditions différentes de DIC sur le cours d'extraction n'a pas pu être évalué car les différences entres les séries des valeurs mesurées ont été de même grandeur que les erreurs expérimentales.

Pour conclure, on constate que le procédé DIC peut être appliqué en tant que technique de prétraitement du matériel avant l'extraction dans les cas où l'extraction est contrôlé par diffusion

au sein des particules. En pratique, il s'agit par exemple de l'extraction des matériaux qui, pour des raisons différentes, ne peuvent pas être broyés avant l'extraction et donc doivent être extraits en morceaux entiers.

La deuxième partie de la thèse résume les résultats de la mesure de réponse à l'injection du traceur dans un extracteur supercritique réalisée afin d'évaluer la dispersion axiale dans l'extracteur. Un dispositif expérimental a été construit, le système d'extraction (un soluté déposé sur les billes en verre inertes) a été choisi et les expériences préliminaires ont été réalisées pour tester la méthode.

Les mesures sous conditions subcritiques et supercritiques ont été effectuées pour la direction d'écoulement dans le sens de la pesanteur et dans le sens opposite. Sous les conditions supercritiques, le pic de réponse est beaucoup plus dispersé dans le cas d'écoulement contre le sens de gravitation qu'au sens de gravitation. Il est donc probable que la convection naturelle se développe, grâce aux différences de densité du fluide le long de l'extracteur. Ce phénomène n'a pas été observé sous conditions subcritiques. Néanmoins, il faut noter que les résultats présentés sont préliminaires. Une étude plus profonde de cette problématique est à réaliser.

PUBLICATION

Rochová, K. Sovová, H., Sobolík, V., Allaf, K. Impact of seed structure modification on the rate of supercritical CO_2 extraction. *Journal of Supercritical Fluids*, **2008**, vol. 44 (2), p. 211-218.